Modeling of Biological and Economical Phenomena Based on Analysis of Nonlinear Competitive Systems

非線形競合システム解析に基づく生命と経済現象のモデル化

Risa Uechi

上地 理沙

Abstract

The concept of stability is important in order to understand natural phenomena in physical systems and complex or nonlinear dynamical systems such as biological, environmental and social systems. Complex and nonlinear dynamical systems are characterized by self-interactions, self-organization, spontaneous emergence of order and dissipative structures. Complex and nonlinear dynamical systems are difficult to handle unlike linear dynamical systems since their complex interactions and structures make it difficult to understand a response of a system from external effects and perturbations, and there are no simple ways to extract conservation laws or orders. However, conservation laws, symmetries and orders in nonlinear dynamical systems are expected to exist in biology, ecology and economical system. In this thesis, we introduce our approach to find conservation laws and principal theories in complex systems and their applications based on methods for conservation law in physics. First, we discuss a conservation law of an interacting system by applying Lagrangian or Hamiltonian approaches in physics to the model of ordinary differential equations for Lotka-Volterra type of prey-predator competitive system. We show our investigation that it is possible to apply Lagrangian approach and Noether ' s theorem to symmetric 2n-dimensional nonlinear differential equations, and the system of 2n-dimensional equation has the conservation law derived from Noether ' s theorem. As an example of ecology, we applied our 2n-dimensional nonlinear differential equations for prey-predator system to the relation between Canadian Lynx and Snowshoe hare. We found a stable rhythm of change in the dynamics of Lynx and hare. Using the same approach, we also introduce the conservation law in Turing pattern. Second, we discuss the probability distribution of impact degree of metabolic network using generating function approach and data from Kyoto Encyclopedia of Genes and Genomes (KEGG) database to estimate damage expansion rate. We investigate the model of expected impact degree for multiple knockouts. In the last part of the thesis, we introduce the embedded information analysis in empirical correlation matrix using stock-market data. We present a new measure to investigate the functional structure of financial markets, the Sector Dominance Ratio (SDR). We investigate the information contained in raw and partial correlations using the sector dominance ratio and its variation over time. We find a characteristic change of the largest eigenvalue from raw and partial correlations and the SDR that coincides with sharp breaks in asset valuations. Finally, we conclude and discuss the topics of thesis and future works.

Publication Notes

Chapter 3 is based on the paper
L. Uechi and T. Akutsu, "Conservation Laws and Symmetries in Competitive Systems", *Progress of Theoretical Physics Supplement*, No. 195, (2012), 210.

Chapter 4 is based on the paper
L. Uechi and T. Akutsu, "Stability and Restoration phenomena in Competitive Systems", *Progress of Theoretical Experimental Physics*, (2013) 103J01.

Chapter 6 is based on the paper
L. Uechi, T. Akutsu, H. E. Stanley, A. J. Marcus and D. Y. Kenett, "Sector dominance ratio analysis of financial markets", *Physica A*, 412, 488-509, (2015).

Contents

Chapter 1

Introduction

1.1 Background

The system of life emerged about thirty four millions ago, and the origin of life has been considered since human obtained the intelligence to think about surrounding nature. It is referred that the system of life is not a miracle as if a clock is made naturally around a sand beach but necessary phenomena [47]. The emergences of life or living system are related to complexity and diversity of molecules which compose of its structure, and these complex interactions support the system of life. If we divide a living organism into a molecule, it would be no longer a living system. In addition to these complex phenomena and structure, the system of life has a property called dissipative structure (Figure 1.1). The lives take energies and materials from external world and also dissipate energy and materials to outside while remaining these structures. Besides dissipative structure, the phenomena of biology have many contradicted properties such as diversity, conservation, evolution and stability. Not only in biological phenomena, dissipative structure is observed in the field of economy [41, 132]. Our industrial society consume resources from nature and labor from minimum community defined as family, then dissipate exhaust gas to nature and retired people to family. Although living organism has dissipative structure by itself, it would be consumable supplies for maintaining industrial society. There may be some relations among dissipative structure, symmetry (extreme principle) and scalability.

It is known that nonlinear dynamical systems or non-equilibrium systems are difficult to handle unlike linear dynamical systems, their complex interactions and structures make it so difficult to understand a response of a system from perturbations or external effects. Therefore it seems that there exist no simple laws or orders in such nonlinear systems. However, from the perspective of natural sciences, conservation laws, symmetries and orders in nonlinear dynamical systems would exist even in nonlinear and non-equilibrium systems such as biology [96], ecology, and economical systems. Also, in the field of economy, a conserved quantity in the phenomena is studied [33]. The concept of symmetry provides us with quantitative formulation of conservation laws and enables us to find stable solutions of nonlinear differential equations and systems [44].

The researches on symmetries and the first integrals of systems attracted attention in the twenty century. The Lagrangian approach to equations of motion is known as an important method to analyze conservation laws in nonlinear dynamics [38] and generalized to space-time and multi-dimensional systems [42, 46]. The concept of symmetry provides us with quantitative formulation of conservation laws

and enables us to find stable solutions of nonlinear differential equations [44].

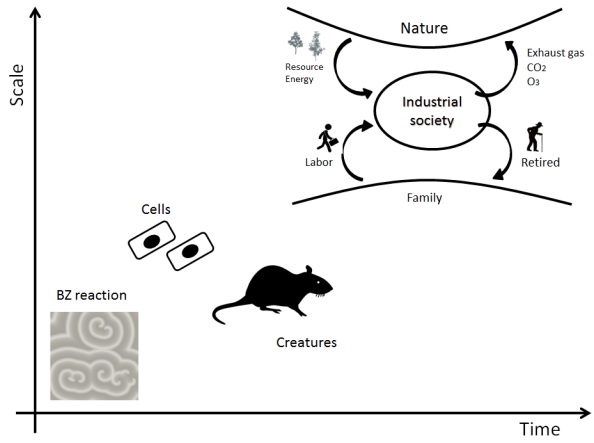

Figure 1.1: Examples of dissipative structures in the world.

The important models in the field of ecology or economy are that of Malthus for a population analysis, prey-predator nonlinear differential equations known as Lotka-Volterra equation. Also, in the field of economy, a conserved quantity in the phenomena of business cycle [125] is studied and this model of business cycle is regarded as a predator-prey type of competitive system, and also a mathematical model for Lanchester Strategic Management is known as a predator-prey type competitive system [32]. The classical predator-prey model is deterministic model described as nonlinear ordinary differential equations. In addition to these deterministic models, there are various prey-predator type competitive models with perturbations. However, most of them are with small and stochastic perturbations. The behaviors of conservation laws with external perturbations have been seldom considered.

In addition to the deterministic nonlinear dynamical model in biological system, it has been shown by many researchers that a relatively simple set of interactions can explain complex phenomena. For example, Turing suggested chemical molecular mechanism called the reaction-diffusion system which is defined as semi-linear parabolic partial differential equations. This reaction-diffusion system is well applied for explaining stripe patterns of the marine angelfish. It is also an interesting problem to investigate in ecological systems if a large complex system should be stable or not, and many researchers have discussed the criteria concerning the stability of a system for deterministic ordinary differential equations and statistical framework.

Beside analytical mechanics, the statistical mechanics and approaches are also important methods to analysis complex phenomena in our world since many phenomena show probabilistic behaviors. It is also known that economical and financial markets are highly complex adaptive systems, resulting from multi-scale interactions amongst individuals, institutions, companies and countries. To better understand the dynamics and structure of financial markets, one can draw on the tools developed in the discipline of complexity science, which has focused on the extraction of useful information for understanding and controlling dynamic interacting systems such as economic, biological, and other complex systems. Approaches of analytical and statistical mechanics also have been proposed for avoiding and controlling systemic risks and crises in financial markets, while complex phenomena such as chaos generally lead to

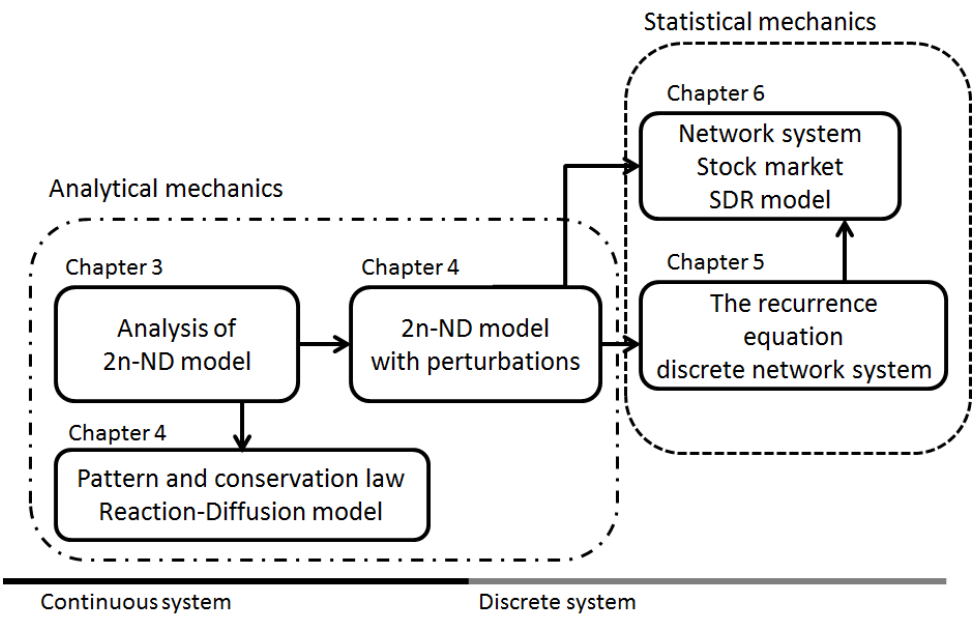

Figure 1.2: The flow of methods and discussion in this thesis.

unpredictability, classical dynamics and quantum statistical mechanics in physics have been applied to many fields of science. Such methods have been successful in analyzing information and conservation laws, and have contributed to the understanding of nonlinear and complex dynamical interacting systems that are not in a state of equilibrium.

The network approach also has been used to analyze metabolic network and connections between world financial markets and social network since many data are available because of advancement of technology such as DNA and RNA analysis in biological experiments and web system. Percolation theory for discrete network system has developed, and examining stability and robustness of network structure has become primary research subjects. For example, the robustness of metabolic network is measured using impact degree. These approaches are also important in the field of economy.

In this thesis, we will analyze these complex systems using analytical, statistical mechanics and the concept of conservation law in natural science (Figure 1.2). We will study whether there would be conservation laws or conserved quantities in complex or non-equilibrium systems which are used to be considered not having conservation law. We will explicitly discuss properties of the conserved, stable nonlinear interacting system with external perturbations and the conservation law, its indications and possible applications to nonlinear interacting system. We will reconstruct non-equilibrium phenomena from the perspective of conservation law in analytical mechanics, and try to handle these complex phenomena using extreme principles in Chapter 3. Based on the concept of conservation law in complex phenomena, we introduce external perturbations to the model with conservation law in order to investigate characteristic changes of a system with a conservation law. It would be possible to simulate realistic system by using external perturbations. We also apply the concept of conservation law and nonlinear system for reaction-diffusion system to examine relations between pattern and conservation law. Besides

these deterministic models, it is also primary subjects to analyze system from perspective of statistical mechanics. It is because complex systems have characteristic properties such as unpredictability and chaos. In addition, discrete network systems became novel and important subjects since advances of technology of web system and biological experiments. We combine both continuous and discrete methods to analyze complex systems such as ecology, metabolic network system using recurrence equations, and network system in stock markets.

1.2 Aim and scope

In this section, we briefly introduce aim and scope of this thesis.

In Chapter 3, we discuss the existence of conservation laws in a $2n$-dimensional Lotka-Volterra type of competitive system with general nonlinear interactions. Nonlinear competitive systems and nonlinear cooperative systems are well known in ecology and biology, as well as in the fields of information system and observed in complex system. We will employ the Lagrangian approach to examine a system of $2n$-dimensional nonlinear differential equations which contains linear interactions Lotka-Volterra type of nonlinear interactions, and self-interactions. We discuss that symmetries and conservation laws of nonlinear interactions are important in nature by analyzing a general nonlinear dynamical (ND) system using Noether's theorem. We show it is possible to derive the conservation law of classical Lotka-Volterra equation and the results are consistent to classical Lotka-Volterra system.

In Chapter 4, we will explain the properties of solutions with a conservation law and applications to biological systems. We extend the BCF model and $2n$-dimensional nonlinear dynamical model to simulate external perturbations numerically. We will explicitly discuss properties of the conserved, stable, 2-variable nonlinear interacting system with external perturbations and the conservation law, its indications and possible applications to nonlinear interacting system. We will show that 2-variable ND model has the properties of restoration and recovery from external perturbations. We also show it is possible to simulate realistic data of Canadian lynx and snowshoe hare population cycles and predict unknown population changes of snowshoe hare from Canadian lynx data and 2-variable ND model.

In Chapter 5, we develop a model of expected impact degree using recurrence and difference equation to estimate the impact degree with multiple knockouts and evaluate. We propose a model of discrete recurrence equations inspired by branching process and percolation. We propose the model of expected impact degree without size effects and the model of expected impact degree with finite size effects of metabolic network. We evaluate which model is suitable for simulating the expected impact degree for multiple knockouts and behaviors of metabolic network with multiple knockouts. We discuss the robustness and structural properties such as stability, symmetry and scalability using the model of expected impact degree. We show it is possible to simulate impact degree by simple nonlinear recurrence equation and importance of effects of network size.

In Chapter 6, we propose a new approach to uncover the functional dominance of economic sectors using RMT. We propose a new indicator, the Sector Dominance Ratio (SDR), to examine economic sectoral makeup at a certain reference time interval using both raw correlation and partial correlation matrices. We will introduce the SDR methodology and study the dynamic changes of SDR employing eigenvectors obtained from both raw and partial correlation matrices. The SDR uses RMT to identify the informative components of the empirical correlation matrices, and thus, unlike other factor models or principal components-based indicators, does not require making assumptions on where the meaningful

system information is embedded. We examine the SDR for both yearly and monthly bases for raw correlation and partial correlation matrices. We apply the SDR methodology to study the structure of four different stock markets, those of the U.S., U.K., Germany, and Japan, and investigate whether the economic sectoral makeup is indeed apparent in the observed prices and their evolution over time. The information obtained from the model of SDR provides important insights into the underlying driving forces in the dynamics of real stock markets: not only the importance of each sector, but also the state of the sector and whether its activity or growth rate is increasing or decreasing. Finally, we show the SDR is useful for predicting the behavior of VIX indexes using Granger causality and cross correlation tests for both raw and partial correlation. We show that the method of raw and partial correlations and the model of SDR provide important information on the underlying structure of financial markets and their dynamics.

1.3 Contribution

We have three contributions in this thesis.

The first one is proposing a novel method to derive conservation law from a system composed by nonlinear first-order differential equations, especially $2n$-dimensional differential equations.. Some methods such as Lie method [13, 85], Painlevé analysis [17] have been applied to search conservation laws or symmetries. For example, José Fernández-Núñez studied symmetries of two-dimensional Lotka-Volterra system [25] using Lagrangian structure. They discussed a Lagrangian structure in Lotka-Volterra system with Lagrangian linear in velocities. However, we expect a conservation law which is velocity-independent, and the symmetric nonlinear differential equations of $2n$-dimensional nonlinear dynamical system will be given from conservation laws by Noether's theorem [97]. In Chapter 3, we provide a model of $2n$ Nonlinear Dynamical model with conservation law to study the conservation law and symmetries in competitive systems using analytical mechanics such as Lagrangian approach and Noether's theorem which are not applied in prior research We investigate a system of $2n$ dimensional coupled first-order nonlinear differential equations which contains many complex nonlinear interactions. We show a system with symmetric nonlinear interaction has a conservation law and exists in the form of the $2n$ independent variables or $2n$ dimension. Using $2n$-nonlinear model, we can consider all quadratic nonlinear effects and examine dynamical changes with conserved quantity at arbitrary time point. We show that the possibility to have conservation law if a system is composed of even variables. We also find that there are many practical applications for the conservation law such as checking the accuracy of numerical solutions and state of a system.

In Chapter 4, we examine characteristic properties of ecological systems from the perspective of oscillation phenomena based on the $2n$ Nonlinear Dynamical model and conservation law. It has been shown that a relatively simple set of interactions can explain complex phenomena in biological systems [30, 86]. For example, Turing suggested chemical molecular mechanism called the reaction-diffusion system [129] which is defined as semi-linear parabolic partial differential equations. This reaction-diffusion system is well applied for explaining stripe patterns of the marine angelfish, *Pomacanthus*, and restoration phenomena in its stripe patterns from injuries was observed [62, 65, 71]. Prigogine also proposed Brusselator model with nonlinear ordinary differential equations to illustrate spatial oscillations and Turing patterns [5]. It is also an interesting problem to investigate in ecological systems if a large complex system should be stable or not, and many researchers have discussed the criteria con-

cerning the stability of a system for n dimensional ordinary differential equations and statistical framework [16, 19, 43, 83, 126]. We focus on the ten-year cycle of lynx and hare using the model based on 2-variable nonlinear dynamical model. Our research shows it is possible to simulate population data of lynx using only one parameter of external perturbation. We show the existence of the standard rhythm which is presented by the numerical simulations of 2-variable nonlinear dynamical model. The necessity of the standard rhythm of a system is explained from the perspective of the conservation law. We can assume by checking the changing of conservation law that there was some catastrophic external effects for considering prey-predator nonlinear competitive systems, which property is not observed in previous works. In addition to the example of 2-variable nonlinear dynamical system, we extend our approach to a system of partial differential equations such as a system described as Turing pattern. The conservation law of Turing pattern is proposed.

In Chapter 5, we try to construct the model of expected impact degree for multiple knockouts based on simple recurrence equations inspired by Branching Process and using data of Kyoto Encyclopedia of Genes and Genomes (KEGG) database. We introduce novel nonlinear effects of size of network to the model of expected impact degree, and it is found that the model of expected impact degree with effects of size well fits to observed data from KEGG database. The efficient method to calculate impact degree that of large scale metabolic network is recently proposed [93, 123] and investigated [124]. However, it takes much computational times and costs to find precise impact degree with multiple knockouts more than 3 because of computational complexity, therefore, it is impossible to find expected impact degree more than 3. In this study, we develop a model of expected impact degree using recurrence and difference equation to estimate the impact degree with multiple knockouts and evaluate which model is suitable for simulating the expected impact degree for multiple knockouts. The model of expected impact degree can predict the expected impact degree with arbitrary number of knockouts which were not proposed in prior research. It became possible to evaluate expected impact degree more than 3 with high speeds. We investigate other properties of metabolic network such as scalability and symmetry which support the stability in metabolic network.

In Chapter 6, we present a novel measure, Sector Dominance Ratio (SDR), to quantify the evolving of activity of economic sectors with respect to time in financial markets. Kinlaw *et al.* [60] introduced a method to measure systemic importance using the absorption ratio and variance of eigenvectors introduced by [64], which is equal to the fraction of a markets total variance explained by a subset of important factors. In addition, the network structure of markets and the interactions and dependencies among economic sectors within national markets also can be modeled using such a structure [18]. However, there are few researches focusing the relation between the direction of components of eigenvector and economic sector. We focused the direction of eigenvector assuming that it would be related to economic activity and investigated SDR for quantifying economic activity. Using SDR model, it becomes possible to extract information embedded in stock markets data and identify economic sectors with increasing dominance at certain time interval. The SDR model also provides us the information of systemic risk in stock market system. We also show it is possible to use the SDR model as an indicator of Volatility index especially in U.S. and U.K. stock markets, and Granger Causality Analysis supports that the SDR model can predict changes in the Volatility index.

1.4 Organization of the thesis

The rest of this thesis is organized as follows.

In Chapter 2, we briefly review fundamental knowledge for this study and introduce our study.

In Chapter 3, we introduce the concept of conservation laws and symmetries in competitive system using Lagrangian approach and Noether's theorem. We propose a model with conservation law as $2n$-ND model. The model is extended by adding external perturbation terms in Chapter 4, and we examine the realistic example in ecological system using $2n$-ND model. We also extend our methods to the system of partial differential equations such as Turing pattern,

In Chapter 5, we introduce the model for describing the expected impact degree for multiple knock-outs in metabolic network system.

In Chapter 6, we show it is possible to extract information from highly complex system such as financial stock market systems. We introduce the application of random matrix theory the model to predict state of interacting stock markets.

In Chapter 7, we provide concluding remarks of this thesis and show future directions.

Chapter 2

Preliminaries

2.1 Extreme principle in natural science

In natural science and informatics, extreme principle, maximum or minimum principle has played an important role. Isaac Newton discovered universal gravitation and the laws of motion which explain the relation between force and velocity. After investigation of the Newtonian mechanics, Joseph-Louis Lagrange succeeded to reformulate Newtonian mechanics to Lagrangian mechanics. In Lagrangian mechanics, the behavior of natural system follows to minimize physical quantity of energy. Based on the principle of least action, fundamental theories of physics have developed.

The concept of extreme principle had been applied for many fields of physics such as thermodynamics. In the field of thermodynamics, natural phenomena are divided into two states, that is reversible reaction and irreversible reaction. The concept of entropy divides reversible reaction and irreversible reaction. Arther Eddington express the concept of entropy as arrow of time. For example, if we take the video for the motion of pendulum, we won't distinguish between normal playback and reverse playback. As well, also if one puts milk into black coffee, the spreads and motion of molecules of milk can't be reversible.

The system of reversible reaction is also called as equilibrium system, and irreversible reaction is called as non-equilibrium system. In the case of equilibrium system, another property is extreme principle. In the case of isolated system, entropy will increase finitely and extreme value is achieved in equilibrium system. It is known that extreme principle does not form in the system of non-equilibrium far from equilibrium state. However, Las Onsager advocated that there exist extreme principles in non-equilibrium system which is close to equilibrium state in 1931. Onsager investigated linear relation in non-equilibrium systems which are close to equilibrium systems. It is possible to handle non-equilibrium systems which are close to equilibrium system as equilibrium system. Ilya Prigogine referred to concept of dissipative structure. Ilya Prigogine also hypothesize that the phenomena such as biology, ecology and social system are supported by dissipative structure and dissipative structure would be related to the concept of principle of minimum entropy production.

2.2 Variation of functionals

The calculus of variations deals with the problem of determining the extreme values of certain variable as functionals. Using functional, we can find a rule which associate a real number to each function. Let A be a set of functions, $f_1, f_2, \ldots$; then a functional J defined on A is a mapping $J{:}A \to R^1$ which associates to each $f \in A$ a real number $J(f)$. That is to say the fundamental problem of the calculus of variations is to determine which objects in A afford minimum value to J when a functional J and a set of admissible objects A are given.

2.3 Euler Lagrange equation from single integral problems

Lemma 2.3.1. *Let x_1 and $x_2(> x_1)$ be two constant values, and $F(x)$ be a continuous function among the range $x_1 \leq x \leq x_2$. If an arbitrary continuous function $\eta(x)$ which satisfies conditions*

$$\eta(x_1) = \eta(x_2) = 0, \tag{2.1}$$

and

$$\int_{x_1}^{x_2} \eta(x)F(x)dx = 0, \tag{2.2}$$

it is possible to proof that

$$F(x) \equiv 0, \tag{2.3}$$

where $x_1 \leq x \leq x_2$. If $F(x') \neq 0$ and $F(x') > 0$ when x' is in an interval (x_1, x_2), $F(x)$ is larger than 0 since $F(x)$ is continuous. Suppose that the continuous function η is chosen as follows

$$\eta(x) = \begin{cases} 0 & (x_1 \leq x \leq x_1'), \\ (x - x_1')^2(x - x_2')^2 & (x_1' \leq x \leq x_2'), \\ 0 & (x_2' \leq x \leq x_2). \end{cases} \tag{2.4}$$

Then following equation is given as

$$\int_{x_1}^{x_2} \eta(x)F(x)dx = \int_{x_1'}^{x_2'} (x - x_1')^2(x - x_2')^2 F(x)dx > 0. \tag{2.5}$$

It does not satisfy (2.2)*, therefore, $F(x) \equiv 0$.*

We consider a functional $J : A \to R$ called as fundamental or action integral:

$$J(x) \to \ min, \ on\ A. \tag{2.6}$$

Let $C^2[a, b]$ denote the set of all functions on the interval $[a, b]$ whose second derivatives are continuous, and $x(t)$ is the function which is included in $C^2[a, b]$. Functions $x(t)$ and $x^k(t)$ $(k = 1, \ldots, n)$ are defined as follows

$$x(t) = (x^1(t), ..., x^n(t)), t \in [a, b], \tag{2.7}$$

$$x^k(t) \in x(t), \dot{x}^k = \frac{dx^k}{dt}. \tag{2.8}$$

The boundary conditions of each function are given as follows

$$x^k(a) = \alpha^k, \tag{2.9}$$
$$x^k(b) = \beta^k, \tag{2.10}$$

where both α^k and β^k are defined as real numbers. The functional $J(x(t))$ is given as follows

$$J(x(t)) = \int_a^b \mathcal{L}(t, x^1(t) \cdots x^n(t), \dot{x}^1(t) \cdots \dot{x}(t)^k)dt. \tag{2.11}$$

Lemma 2.3.2. *If $x(t)$ is the minimum value of the functional J, it is obtained as*

$$\int_a^b \Big\{\frac{\partial \mathcal{L}}{\partial x^k} - \frac{d}{dt}\left(\frac{\partial \mathcal{L}}{\partial \dot{x}^k}\right)\Big\}\eta^k(t)dt = 0. \tag{2.12}$$

Note that $\eta(t) \in C_n^2$ and $\eta(a) = \eta(b) = 0$.

Proof of Lemma 2.3.2. The first variation of δJ is calculated as follows

$$\begin{aligned}\delta J(x(t), \eta^k(t)) &= \Big\{\frac{d}{dt}\int_a^b L(t, x^k(t) + \varepsilon\eta^k(t), \dot{x}^k(t) + \varepsilon\dot{\eta}^k(t))dt\Big\}_{\varepsilon=0} \\ &= \int_a^b \Big\{\frac{\partial \mathcal{L}}{\partial x^k}\frac{dx^k}{d\varepsilon} + \frac{\partial \mathcal{L}}{\partial \dot{x}^k}\frac{d\dot{x}^k}{d\varepsilon}\Big\}dt\end{aligned} \tag{2.13}$$

Using the condition that $x_\varepsilon = x + \varepsilon\eta^k$, we can obtain $\delta J(x(t), \eta^k(t))$ as follows

$$\begin{aligned}\delta J(x(t), \eta^k(t)) &= \int_a^b \Big\{\frac{\partial \mathcal{L}}{\partial x^k}\eta^k + \frac{\partial \mathcal{L}}{\partial \dot{x}^k}\dot{\eta}^k\Big\}dt \\ &= \int_a^b \frac{\partial \mathcal{L}}{\partial x^k}\eta^k dt + \Big[\frac{\partial \mathcal{L}}{\partial \dot{x}^k}\eta^k\Big]_a^b - \int_a^b \frac{d}{dt}\left(\frac{\partial \mathcal{L}}{\partial \dot{x}^k}\right)\eta^k dt \\ &= \int_a^b \Big\{\frac{\partial \mathcal{L}}{\partial x^k} - \frac{d}{dt}\left(\frac{\partial \mathcal{L}}{\partial \dot{x}^k}\right)\Big\}\eta^k dt.\end{aligned} \tag{2.14}$$

Considering the equation (2.2), the formal of Euler-Lagrange equation is derived as follows

$$\frac{\partial \mathcal{L}}{\partial x^k} - \frac{d}{dt}\left(\frac{\partial \mathcal{L}}{\partial \dot{x}^k}\right) = 0. \tag{2.15}$$

We can derive the law of energy conservation using Euler-Lagrange equation. □

2.4 The Noether's theorem and conservation laws

In this section, we show the classical theorem by Emmy Noether on invariant variational problems and conservation law which is derived using Lagrangian and the theorem by Emmy Noether [73].

We show that the classical theorem of Emmy Noether and conservation laws using Euler-Lagrange equation E_k,

$$E_k \equiv \frac{\partial \mathcal{L}}{\partial x^k} - \frac{d}{dt}\frac{\partial \mathcal{L}}{\partial \dot{x}^k} \quad (k = 1, \ldots, n). \tag{2.16}$$

Then we have:

Theorem 2.4.1. (Noether)

$$-E_k(\xi_s^k - \dot{x}^k \tau_s) = \frac{d}{dt}\Big(\Big(\mathcal{L} - \dot{x}^k \frac{\partial \mathcal{L}}{\partial \dot{x}^k}\Big)\tau_s + \frac{\partial \mathcal{L}}{\partial \dot{x}^k}\xi_s^k - \Phi_s\Big). \tag{2.17}$$

Proof of Theorem 2.4.1. Using (A.10), definition of basic derivations and chain rule of differentiation,

$$\frac{\partial \mathcal{L}}{\partial \dot{x}^k}\frac{d\xi_s^k}{dt} = \frac{d}{dt}\Big(\frac{\partial \mathcal{L}}{\partial \dot{x}^k}\xi_s^k\Big) - \Big\{\frac{d}{dt}\frac{\partial \mathcal{L}}{\partial \dot{x}^k}\Big\}\xi_s^k, \tag{2.18}$$

$$\frac{\partial \mathcal{L}}{\partial t}\tau_s = \frac{d\mathcal{L}}{dt}\tau_s - \frac{\partial \mathcal{L}}{\partial x^k}\dot{x}^k\tau_s - \frac{\partial \mathcal{L}}{\partial \dot{x}^k}\ddot{x}^k\tau_s, \tag{2.19}$$

$$\frac{\partial \mathcal{L}}{\partial \dot{x}^k}\dot{x}^k\frac{d\tau_s}{dt} + \frac{\partial \mathcal{L}}{\partial \dot{x}^k}\ddot{x}^k\tau_s = \frac{d}{dt}\Big(\frac{\partial \mathcal{L}}{\partial \dot{x}^k\tau_s}\Big) - \frac{d}{dt}\Big(\frac{\partial \mathcal{L}}{\partial \dot{x}^k}\Big)\dot{x}^k\tau_s. \tag{2.20}$$

Substituting these formulation into (A.10) and using Euler-Lagrange equation E_k, we can obtain the classical theorem by Emmy Noether. We shall apply deformation of formula (A.10) as follows

$$\frac{\partial \mathcal{L}}{\partial t}\tau_s + \frac{\partial \mathcal{L}}{\partial x^k}\xi_s^k + \frac{\partial \mathcal{L}}{\partial \dot{x}^k}\frac{d\xi_s^k}{dt} - \frac{\partial \mathcal{L}}{\partial \dot{x}^k}\dot{x}^k\frac{d\tau_s}{dt} + \mathcal{L}\frac{d\tau_s}{dt} = \frac{d\Phi_s}{dt}, \tag{2.21}$$

$$\begin{aligned}\frac{d\mathcal{L}}{dt}\tau_s - \frac{d\mathcal{L}}{dx^k}\dot{x}^k\tau_s - \frac{\partial \mathcal{L}}{\partial \dot{x}^k}\ddot{x}^k\tau_s + \frac{\partial \mathcal{L}}{\partial x^k}\xi_s^k\frac{\partial \mathcal{L}}{\partial \dot{x}^k}\frac{d\xi_s^k}{dt} - \frac{\partial \mathcal{L}}{\partial \dot{x}^k}\dot{x}^k\frac{d\tau_s}{dt} \\ + \mathcal{L}\frac{d\tau_s}{dt} = \frac{d\Phi_s}{dt},\end{aligned} \tag{2.22}$$

$$\begin{aligned}\frac{d\mathcal{L}}{dt}\tau_s - \Big\{\frac{\partial \mathcal{L}}{\partial x^k}\ddot{x}^k\tau_s + \frac{\partial \mathcal{L}}{\partial \dot{x}^k}\dot{x}^k\frac{d\tau_s}{dt}\Big\} - \frac{\partial \mathcal{L}}{\partial x^k}\dot{x}\tau_s + \frac{\partial \mathcal{L}}{\partial x^k}\xi_s^k + \frac{\partial \mathcal{L}}{\partial \dot{x}^k}\xi_s^k \\ + \mathcal{L}\frac{d\tau_s}{dt} = \frac{d\Phi_s}{dt},\end{aligned} \tag{2.23}$$

$$\begin{aligned}\frac{d\mathcal{L}}{dt}\tau_s - \Big\{\frac{d}{dt}\Big(\frac{\partial \mathcal{L}}{\partial \dot{x}^k}\dot{x}^k\tau_s\Big) - \frac{d}{dt}\Big(\frac{\partial \mathcal{L}}{\partial \dot{x}^k}\Big)\dot{x}^k\tau_s\Big\} - \frac{\partial \mathcal{L}}{\partial \dot{x}}\tau_s + \frac{\partial \mathcal{L}}{\partial x^k}\xi_s^k \\ + \frac{\partial \mathcal{L}}{\partial \dot{x}^k}\frac{d\xi_s^k}{dt} + \mathcal{L}\frac{d\tau_s}{dt} = \frac{d\Phi_s}{dt},\end{aligned} \tag{2.24}$$

$$\begin{aligned}\frac{d\mathcal{L}}{dt}\tau_s - \Big\{\frac{d}{dt}\Big(\frac{\partial\mathcal{L}}{\partial\dot{x}^k}\dot{x}^k\tau_s\Big) - \frac{d}{dt}\Big(\frac{\partial\mathcal{L}}{\partial\dot{x}^k}\Big)\dot{x}^k\tau_s\Big\} - \frac{\partial\mathcal{L}}{\partial x^k}\dot{x}^k\tau_s + \frac{\partial\mathcal{L}}{\partial x^k}\xi_s^k \\ + \frac{d}{dt}\Big(\frac{\partial\mathcal{L}}{\partial\dot{x}^k}\xi_s^k\Big) - \Big\{\frac{d}{dt}\frac{\partial\mathcal{L}}{\partial\dot{x}^k}\Big\}\xi_s^k + \mathcal{L}\frac{d\tau_s}{dt} = \frac{d\phi_s}{dt},\end{aligned} \tag{2.25}$$

$$\begin{aligned}\frac{d}{dt}\Big\{\mathcal{L}\tau_s\Big\} - \Big\{\frac{d}{dt}\Big(\frac{\partial\mathcal{L}}{\partial\dot{x}^k}\dot{x}^k\tau_s\Big)\dot{x}^k\tau_s\Big\} - \frac{\partial\mathcal{L}}{\partial x^k}\dot{x}^k\tau_s + \frac{\partial\mathcal{L}}{\partial x^k}\xi_s^k \\ + \frac{d}{dt}\Big(\frac{\partial\mathcal{L}}{\partial\dot{x}^k}\xi_s^k\Big) - \Big\{\frac{d}{dt}\frac{\partial\mathcal{L}}{\partial\dot{x}^k}\Big\}\xi_s^k = \frac{d\Phi_s}{dt},\end{aligned} \tag{2.26}$$

$$\begin{aligned}\frac{d}{dt}\Big\{\mathcal{L}\tau_s\Big\} - \Big\{\frac{d}{dt}\Big(\frac{\partial\mathcal{L}}{\partial\dot{x}^k}\dot{x}^k\tau_s\Big) - \frac{d}{dt}\Big(\frac{\partial\mathcal{L}}{\partial\dot{x}^k}\Big)\dot{x}^k\tau_s\Big\} - \frac{\partial\mathcal{L}}{\partial x^k}\dot{x}^k\tau_s \\ + \frac{\partial\mathcal{L}}{\partial x^k}\xi_s^k - \frac{d}{dt}\Big(\frac{\partial\mathcal{L}}{\partial\dot{x}^k}\xi_s^k\Big) - \Big\{\frac{d}{dt}\frac{\partial\mathcal{L}}{\partial\dot{x}^k}\Big\}\xi_s^k = \frac{d\phi_s}{dt},\end{aligned} \tag{2.27}$$

$$\begin{aligned}\frac{d}{dt}\Big\{\mathcal{L}\tau_s\Big\} - \frac{d}{dt}\Big(\frac{\partial\mathcal{L}}{\partial\dot{x}^k}\dot{x}^k\tau_s\Big) - \Big\{\frac{\partial\mathcal{L}}{\partial x^k} - \frac{d}{dt}\Big(\frac{\partial\mathcal{L}}{\partial\dot{x}^k}\Big)\Big\}\dot{x}^k\tau_s \\ + \frac{d}{dt}\Big(\frac{\partial\mathcal{L}}{\partial\dot{x}^k}\xi_s^k\Big) + \Big\{\frac{\partial\mathcal{L}}{\partial x^k} - \frac{d}{dt}\Big(\frac{\partial\mathcal{L}}{\partial\dot{x}^k}\Big)\Big\}\xi_s^k = \frac{d\Phi_s}{dt}.\end{aligned} \tag{2.28}$$

Then we can obtain following formulation using Euler-Lagrange equation,

$$-E_k\Big\{\dot{x}^k\tau_s - \xi_s^k\Big\} = \frac{d\Phi_s}{dt} - \frac{d}{dt}\Big\{\mathcal{L}\tau_s\Big\} + \frac{d}{dt}\Big(\frac{\partial\mathcal{L}}{\partial\dot{x}}\dot{x}^k\tau_s\Big) - \frac{d\Phi_s}{dt}. \tag{2.29}$$

The theorem of Emmy Noether is given as follows

$$-E_k\Big\{\xi_s^k - \dot{x}^k\tau_s\Big\} = \frac{d}{dt}\Big\{\Big(\mathcal{L} - \frac{\partial\mathcal{L}}{\partial\dot{x}^k}\dot{x}^k\Big) + \frac{\partial\mathcal{L}}{\partial\dot{x}^k}\xi_s^k - \Phi_s\Big\}, \tag{2.30}$$

where $s = 1, \ldots, r$, Φ_s is defined as a gauge function. □

Theorem 2.4.2. *By the definition of $E_k = 0$ and r-parameter transformations, we can obtain the conservation law Ψ_s as follows*

$$\Psi_s \equiv \Big(\mathcal{L} - \dot{x}^k\frac{\partial\mathcal{L}}{\partial\dot{x}^k}\Big)\tau_s + \frac{\partial\mathcal{L}}{\partial\dot{x}^k}\xi_s^k - \phi_s = constant \quad (s = 1, \ldots, r). \tag{2.31}$$

Since the expressions Ψ_s defined in theorem 2.4.2 are constant whenever $E_k = 0$ $(k = 1, \ldots, n)$. Therefore, equation (2.31) are interpreted as conservation laws of the system whose governing equations are $E_k = 0$.

2.4.1 An example of conservation law using Noether's theorem

Let us consider a particle of mass m moves in a plane, and it is attracted to the origin by a force inversely proportional to the square of its distance from the origin. In this case, the action integral is given as follows

$$J(r,\theta) = \int_{t_0}^{t_1}\Big\{\frac{1}{2}m(\dot{r}^2 + r^2\theta^2) + \frac{A}{r}\Big\}dt, \tag{2.32}$$

where A is constant and r and θ are the polar coordinates of the particle. We will consider the one-parameter family of rotations as

$$\bar{t} = t, \quad \bar{r} = r, \quad \bar{\theta} = \theta + \varepsilon, \tag{2.33}$$

Note that $d\bar{\theta}/dt = d\theta/dt$. By applying Noether's theorem, the conservation law is given as follows

$$\Big(\mathcal{L} - \dot{r}\frac{\partial \mathcal{L}}{\partial \dot{\theta}} - \dot{\theta}\frac{\partial \mathcal{L}}{\partial \dot{r}}\Big)\tau + \frac{\partial \mathcal{L}}{\partial \dot{r}}\rho + \frac{\partial \mathcal{L}}{\partial \dot{\theta}}\sigma = constant, \tag{2.34}$$

where τ, ρ, and σ are the generators given by

$$\tau \equiv \frac{\partial \bar{t}}{\partial \varepsilon}\Big|_0 = 0, \quad \rho \equiv \frac{\partial \bar{r}}{\partial \varepsilon}\Big|_0 = 0, \quad \sigma \equiv \frac{\partial \theta}{\partial \varepsilon}\Big|_0 = 1. \tag{2.35}$$

Consequently, we can obtain the law of conservation of angular momentum,

$$mr^2\theta = constant. \tag{2.36}$$

The action integral is also explicitly independent of time t, we can obtain the conservation law for time transformation as follows

$$\mathcal{L} - \dot{\theta}\mathcal{L}_{\dot{\theta}} - \dot{r}\mathcal{L}_r = constant, \tag{2.37}$$

or

$$\frac{1}{2}m(\dot{r}^2 + r^2\dot{\theta}^2) - \frac{A}{r} = constant. \tag{2.38}$$

This is a statement of conservation of energy for the system.

2.5 Overview of Random Matrix Theory (RMT)

Considering a portfolio of N stocks with time T records, the distribution of eigenvalue λ of random matrix $\rho(\lambda)$ is given as

$$\rho(\lambda) = \frac{Q}{2\pi\sigma^2}\frac{\sqrt{(\lambda_{max} - \lambda)(\lambda - \lambda_{min})}}{\lambda}, \tag{2.39}$$

where $\lambda_{max} \geq \lambda \geq \lambda_{min}$. The distribution is bounded with $n \to \infty$ and $T \to \infty$, and since the condition that $Q = T/n \geq 1$ is fixed, it holds that

$$\lambda_{min}^{max} = \sigma^2\Big(1 + \frac{1}{Q} \pm 2\sqrt{\frac{1}{Q}}\Big). \tag{2.40}$$

The value of σ^2 is equal to the variance of the elements and equal to one ($\sigma^2 = 1$) for stock correlation matrices Eq. (2.39). We examine whether there exist eigenvalues obtained from empirical correlation matrices that deviate from the range of the distribution of eigenvalues, λ_{max}, corresponding to random matrices using Eq. (2.39) and Eq. (2.40). The eigenvalues of the random matrix represent zero-embedded information; therefore, the deviation from the range, λ_{max}, defined by (2.40) provides a measure for non-spurious information about behaviors of stock markets that are embedded in the correlation matrices.

Chapter 3

Conservation laws and symmetries in competitive systems

3.1 Background

In this chapter, we will introduce the conservation laws and symmetries in competitive systems using analytical mechanics. It is known that nonlinear dynamical systems and non-eqilibrium systems which are characterized by complex interactions, self organizations, spontaneous emergence of order [47], dissipative structure [104] and nonlinear cooperative phenomena have shown essential roles in natural sciences, as well as financial system, ecological system, and life science. [26, 115].

Since nonlinear dynamical systems or non-equilibrium systems are difficult to handle unlike linear dynamical systems, their complex interactions and structures make it so difficult to understand a response of a system from perturbations or external effects. Therefore it seems that there exist no simple laws or orders in such nonlinear systems.

However, from the perspective of natural sciences, conservation laws, symmetries and orders in nonlinear dynamical systems would exist even in nonlinear and non-equilibrium systems such as biology [96], ecology, and economical systems.

The important models in the field of ecology or economy are that of Malthus (1959) for a population analysis, Alfred Lotka (1925) [74] and Vito Volterra (1926) [134] for prey-predator nonlinear differential equations known as Lotka-Volterra (LV) equation. Also, in the field of economy, a conserved quantity in the phenomena of business cycle [125] is studied and this model of business cycle is regarded as a predator-prey type of competitive system, and also a mathematical model for Lanchester Strategic Management is known as a predator-prey type competitive system [32].

The researches on symmetries and the first integrals of the LV system attracted attention in the 20th century. The Lagrangian approach to equations of motion is known as an important method to analyze conservation laws in nonlinear dynamics [38] and generalized to space-time and multi-dimensional systems [42, 46]. The concept of symmetry provides us with quantitative formulation of conservation laws and enables us to find stable solutions of nonlinear differential equations [44].

In addition, several methods such as the Lie method [13, 85], Painlevé analysis [17], have been applied to search conservation laws or symmetries. For example, José Fernández-Núñez studied symmetries of two-dimensional LV system [25] using Lagrangian approach. They discussed a Lagrangian

structure in LV system with Lagrangian linear in velocities. However, we expect a conservation law which is velocity-independent, and the symmetric nonlinear differential equations of $2n$-dimensional nonlinear dynamical system will be given from conservation laws by Noether's theorem [97].

The symmetry and conservation law in the $2n$-dimensional first-order nonlinear differential equations need a binary coupled form, therefore, the system of the nonlinear differential equations becomes the even dimensions $(2, 4, 6, \ldots, 2n)$. We denote the requirement of the symmetric form as the binary-coupled form (BCF).

In this chapter, we discuss the existence of conservation laws in a $2n$-dimensional Lotka-Volterra type of competitive system with general nonlinear interactions. Competitive systems are well known in ecology and biology, as well as in the fields of information system [105]. We will employ the Lagrangian approach to examine a system of $2n$-dimensional nonlinear differential equations which contains linear interactions Lotka-Volterra type of nonlinear interactions, and self interactions. We discuss that symmetries and conservation laws of nonlinear interactions are important in nature by analyzing a general nonlinear dynamical (ND) system using Noether's theorem.

In section 3.2, we refer to notations of Euler-Lagrange equation and Noether's theorem to define conservation laws. In section 3.3, we introduce Lagrangian and conservation laws of a general competitive system for the $2n$-dimensional ND system. Then we discuss that a symmetric and nonlinear dynamical system should exist in a form of $2n$-dimensional nonlinear differential equations when conservation law exists. In section 3.4, we will illustrate examples of conservation laws in two variables to explain the results discussed in section 3.3. In section 3.5, we will discuss our results.

3.2 Noether's theorem and conservation laws

The general formulation of necessary condition for extrema in Lagrangian formulation, $\mathcal{L}(t, x^k(t), \dot{x}^k(t))$, is given by

$$\delta J = \delta \int \mathcal{L}(t, x^k(t), \dot{x}^k(t))dt = 0 \qquad (k = 1, \ldots, n), \tag{3.1}$$

and all functions, $x(t) = (x^1(t), \ldots, x^n(t)), t \in [a, b]$, belong to $C^2[a, b]$, which denotes the set of all continuous functions on the interval $[a, b]$ and the second derivatives of all functions are continuous.

If $x(t)$ is a relative minimum of the functional J, the condition (3.1) generates,

$$E_k \equiv \frac{\partial \mathcal{L}}{\partial x^k} - \frac{d}{dt}\left(\frac{\partial \mathcal{L}}{\partial \dot{x}^k}\right) = 0. \tag{3.2}$$

This is the Euler-Lagrange equation which determines equations of motion of a system.

Noether's theorem describes that the Lagrangian with Euler-Lagrange equation is invariant under certain space-time transformations, and invariances of Lagrangian generate respective conservation laws. For example, the time-translation invariance of Lagrangian corresponds to the conservation of energy of a system. Let us consider r-parameter transformations in general that will be regarded as transformations of configuration space, $(t, x^1, \ldots, x^n)$-space, depending upon r real, independent parameters $\varepsilon^1, \ldots, \varepsilon^r$. The transformations are defined by

$$\begin{aligned} \bar{t} &= t + \tau_s(t, x)\varepsilon^s + o(\varepsilon), \\ \bar{x}^k &= x^k + \xi^k_s(t, x)\varepsilon^s + o(\varepsilon), \end{aligned} \tag{3.3}$$

where s ranges over $1, \ldots, r$, and $o(\varepsilon)$ denotes the terms which go to zero faster than $|\varepsilon|$, $\lim_{|\varepsilon|\to 0} o(\varepsilon)/|\varepsilon| = 0$. The functions $\tau_s(t, x)$ and $\xi_s^k(t, x)$ for linear parts of $\bar{t}$ and $\bar{x}^k$ with respect to ε are commonly called the infinitesimal generators of the transformations. Classical theorem of Emmy Noether on invariant variational problems can be derived under the hypotheses of extrema (3.1), and transformation (3.3) [73]. The result is the r identities produced by the transformation (3.3),

$$-E_k(\xi_s^k - \dot{x}^k\tau_s) = \frac{d}{dt}\left(\left(\mathcal{L} - \dot{x}^k\frac{\partial\mathcal{L}}{\partial\dot{x}^k}\right)\tau_s + \frac{\partial\mathcal{L}}{\partial\dot{x}^k}\xi_s^k - \Phi_s\right), \tag{3.4}$$

where $k = 1, \ldots, n$ is summed, and Φ_s is an arbitrary function defined as a gauge function of the transformation. Note that the arbitrary choice of a gauge function will not change equations of motion of a system, which can be usually used for a convenient expression of conservation laws. If the fundamental integral (3.1) is divergence-invariant under the r parameter group of transformation (3.3), and if $E_k = 0$ for $k = 1, \ldots, n$, then following r expressions are obtained:

$$\Psi_s \equiv \left(\mathcal{L} - \dot{x}^k\frac{\partial\mathcal{L}}{\partial\dot{x}^k}\right)\tau_s + \frac{\partial\mathcal{L}}{\partial\dot{x}^k}\xi_s^k - \Phi_s = constant. \tag{3.5}$$

This defines the conserved quantities of a system. Since the expressions Ψ defined in (3.5) are constant with the condition: $E_k = 0 (k = 1, \ldots, n)$, they are the first integrals of the differential equations of motion, that is, the conserved quantities. In physical applications, the first integral (3.5) is interpreted as the energy of the system, whose governing equations are $E_k = 0$. In general, the expressions Ψ is constant with respect to time and along any extremal solutions of a system. By employing the formalism, the conservation law and symmetry of nonlinear dynamical differential equations are discussed in the section 3.3, and we will show the first integrals, the symmetry of Ψ and its solutions in an explicit coupled two-variables system in section 3.4, as an example for the current approach.

3.3 Conserved quantities and symmetric BCF in $2n$-dimensional nonlinear dynamical (ND) systems

Nonlinear dynamical systems are well known in feed-back systems, such as biology, environmental sciences and computer systems, and they are important to understand many complicated interactive structures. Consider a nonlinear dynamical system that has $2n$ variables. The system has self-interactions, mixing interactions of quadratic forms of all combinations, such as

$x_1^2, x_2^2, \ldots, x_1x_2, x_3x_4, \ldots$. In this section, we will show the following. (1) We begin to examine a nonlinear dynamical system of $2n$ variables in symmetric form. The variables $(x_1, x_2, x_3, \ldots, x_{2n})$ are, for example, $2n$ species of competing creatures in LV system [115], or a cell-structured organism which cooperates together [96]. We will write down a quadratically interacting system as general as possible and investigate the properties of nonlinear interactions as a whole. (2) We will discuss that the solution of the $2n$-dimensional ND differential system with respect to the conservation law and Noether's theorem by calculating Ψ explicitly. (3) We will show that a coupled nonlinear dynamical system in BCF has a conserved quantity, or Hamiltonian of the BCF, which is velocity-independent.

The $2n$-dimensional ND system in BCF having $2n$ variables $(x_1, \ldots, x_{2n})$ is generally described as,

$$\begin{aligned}
\dot{x}_{2k-1} &= \sum_{i=1}^{n}(a_{2k-1,2i-1}x_{2i-1} + a_{2k-1,2i}x_{2i}) + \sum_{j=1}^{2n} a_{2k-1,2n+j}x_j x_{2k-1} \\
&\quad + \sum_{i=1}^{n}{}' a_{2k-1,4n+i}x_{2i-1}x_{2i}, \\
\dot{x}_{2k} &= \sum_{i=1}^{n}(a_{2k,2i-1}x_{2i-1} + a_{2k,2i}x_{2i}) + \sum_{j=1}^{2n} a_{2k,2n+j}x_j x_{2k} \\
&\quad + \sum_{i=1}^{n}{}' a_{2k,4n+i}x_{2i-1}x_{2i},
\end{aligned} \tag{3.6}$$

where $k = 1, 2, \ldots, n$. The first summation expresses the linear part of interaction which contains all variables $x_1, \ldots, x_{2n}$. The second term is the competitive interaction expressed by coupled two variables, $x_k x_1, \ldots, x_k x_{2n}$. This term is typical in classical LV equations. The third term with prime, $\sum_{i=1}^{n}{}' x_{2i-1}x_{2i}$, expresses all the mixing interactions other than $i = k$.

The Lagrangian of (3.6) is given by the following form,

$$\begin{aligned}
\mathcal{L} &= \sum_{i=1}^{n}(\alpha_{2i-1}\dot{x}_{2i-1}x_{2i} + \alpha_{2i}x_{2i-1}\dot{x}_{2i}) \\
&\quad + \sum_{i=1}^{n}\sum_{j=1}^{2n} \alpha_{\{2n+2n(i-1)+j\}}x_{2i-1}x_j \\
&\quad + \sum_{i=1}^{n}\sum_{j=1}^{2n} \alpha_{\{2n^2+2n+2n(i-1)+j\}}x_{2i}x_j \\
&\quad + \sum_{i=1}^{n}\sum_{j=1}^{2n} \alpha_{\{4n^2+2n+2n(i-1)+j\}}x_{2i-1}x_{2i}x_j.
\end{aligned} \tag{3.7}$$

Applying Euler-Lagrange equation (3.2) to Eq. (3.7), we can get ordinary differential equations; the ordinary differential equation for $\dot{x}_{2k-1}$ is derived as

$$\begin{aligned}
d_{2k,2k-1}\dot{x}_{2k-1} &= \sum_{i=1}^{n}(\alpha_{2n+2n(i-1)+2k} + \alpha_{2n^2+2n+2n(k-1)+2i-1})x_{2i-1} \\
&\quad + \sum_{i=1}^{n}(\alpha_{2n^2+2n+2n(i-1)+2k} + \alpha_{2n^2+2n+2n(k-1)+2i})x_{2i} \\
&\quad + \sum_{j=1}^{2n} \alpha_{4n^2+2n+2n(k-1)+j}x_j x_{2k-1} \\
&\quad + \sum_{i=1}^{n} \alpha_{4n^2+2n+2n(i-1)+2k}x_{2i-1}x_{2i},
\end{aligned} \tag{3.8}$$

and the ordinary differential equation for $\dot{x}_{2k}$ is derived as

$$\begin{aligned} d_{2k-1,2k}\dot{x}_{2k} = & \sum_{i=1}^{n}(\alpha_{2n+2n(i-1)+2k-1} + \alpha_{2n+2n(k-1)+2i-1})x_{2i-1} \\ & + \sum_{i=1}^{n}(\alpha_{2n^2+2n+2n(i-1)+2k-1} + \alpha_{2n+2n(k-1)+2i})x_{2i} \\ & + \sum_{j=1}^{2n}\alpha_{4n^2+2n+2n(k-1)+j}x_j x_{2k} \\ & + \sum_{i=1}^{n}\alpha_{4n^2+2n+2n(i-1)+2k-1}x_{2i-1}x_{2i}, \end{aligned} \tag{3.9}$$

where $d_{2k,2k-1} = \alpha_{2k} - \alpha_{2k-1}$ and $d_{2k,2k-1} = -d_{2k-1,2k}$ for all k. The conditions of parameters can be obtained by comparing (3.6) and (3.8) when the coupled ND differential equations have a conserved quantity. The conditions of coefficients for $\dot{x}_{2k-1}$ are given by,

$$\begin{aligned} a_{2k-1,2i-1} &= \frac{1}{d_{2k,2k-1}}(\alpha_{2n+2n(i-1)+2k} + \alpha_{2n^2+2n+2n(k-1)+2i-1}), \\ a_{2k-1,2i} &= \frac{1}{d_{2k,2k-1}}(\alpha_{2n^2+2n+2n(i-1)+2k} + \alpha_{2n^2+2n+2n(k-1)+2i}), \\ a_{2k-1,2n+j} &= \begin{cases} \dfrac{2}{d_{2k,2k-1}}\alpha_{4n^2+2n+2n(k-1)+2k} & (j = 2k), \\ \dfrac{1}{d_{2k,2k-1}}\alpha_{4n^2+2n+2n(k-1)+j} & (j \neq 2k), \end{cases} \\ a_{2k-1,4n+i} &= \frac{1}{d_{2k,2k-1}}\alpha_{4n^2+2n+2n(i-1)+2k} \quad (i \neq k), \end{aligned} \tag{3.10}$$

and also by comparing (3.6), (3.9), we get conditions of parameters for $\dot{x}_{2k}$ ND differential equations,

$$\begin{aligned} a_{2k,2i-1} &= \frac{1}{d_{2k-1,2k}}(\alpha_{2n+2n(i-1)+2k-1} + \alpha_{2n+2n(k-1)+2i-1}), \\ a_{2k,2i} &= \frac{1}{d_{2k-1,2k}}(\alpha_{2n^2+2n+2n(i-1)+2k-1} + \alpha_{2n+2n(k-1)+2i}), \\ a_{2k,2n+j} &= \begin{cases} \dfrac{2}{d_{2k-1,2k}}\alpha_{4n^2+2n+2n(k-1)+2k} & (j = 2k-1), \\ \dfrac{1}{d_{2k-1,2k}}\alpha_{4n^2+2n+2n(k-1)+j} & (j \neq 2k-1), \end{cases} \\ a_{2k,4n+i} &= \frac{1}{d_{2k-1,2k}}\alpha_{4n^2+2n+2n(i-1)+2k-1} \quad (i \neq k). \end{aligned} \tag{3.11}$$

One should note that if the parameters satisfy these conditions, then the ND differential equations have a conserved quantity. The conserved quantity for time transformation for the coupled ND equations is

given by,

$$\begin{aligned}\Psi \equiv & \sum_{i=1}^{n}\sum_{j=1}^{2n} \alpha_{\{2n+2n(i-1)+j\}} x_{2i-1} x_j \\ & + \sum_{i=1}^{n}\sum_{j=1}^{2n} \alpha_{\{2n^2+2n+2n(i-1)+j\}} x_{2i} x_j \\ & + \sum_{i=1}^{n}\sum_{j=1}^{2n} \alpha_{\{4n^2+2n+2n(i-1)+j\}} x_{2i-1} x_{2i} x_j.\end{aligned} \tag{3.12}$$

The conserved quantity, $\Psi(x_1, x_2, \ldots, x_{2n})$, that produces the first order coupled nonlinear differential equations in BCF is conserved and constant with respect to time.

In this ND system, we define the stable solutions as follows. When one substitutes the solutions $(x_1, x_2, \ldots, x_{2n})$ into $\Psi(x_1, x_2, \ldots, x_{2n})$ obtained in certain time range and Ψ becomes strictly constant, we say that the solutions are stable in the time range. If Ψ is not constant, solutions are unstable or may not exist. In addition, one can conclude that the coefficients of the ND system are strictly constrained by the conservation law. This is also one of the important results of the conserved ND system. When the coefficients satisfy the relations (3.10) and (3.11), the ND differential equations have solutions that maintain the conserved quantity $\Psi(x_1, x_2, \ldots, x_{2n})$. If the ND system do not meet conditions (3.10) and (3.11), Ψ may not be constant with respect to time. It will be shown explicitly in examples in the section 3.4.

However, because nonlinear coefficients can be assumed to take any values although they are restricted by some conditions, there exist cases that the general nonlinear dynamical system does not have solutions despite the fact that it has formally the conserved quantity Ψ. For this reason, we mainly concern ourselves to analyze cases in our BCF competitive system which has converged solutions and a conserved quantity Ψ.

The conserved quantity Ψ is invariant under exchanges of any variables $x_i \leftrightarrow x_j$;

$$\Psi(x_1, \ldots, x_i, \ldots, x_j, \ldots, x_{2n}) = \Psi'(x_1, \ldots, x_j, \ldots, x_i, \ldots, x_{2n}), \tag{3.13}$$

where $\Psi'(x_1, \ldots, x_j, \ldots, x_i, \ldots, x_{2n})$ is obtained from Ψ by renaming of coefficients. Because of the symmetry, the addition of other BCF, for example, $\Psi(x_{2n+1}, x_{2n+2})$ assuming the similar nonlinear interaction to the whole system, changes only $n \to n+1$ in (3.12), which means the conservation law of the system is unchanged. It indicates that the property of ND system may be kept unchanged even when the nonlinear differential equations are changed to as $n \to n+1$; $\Psi(x_1, \ldots, x_{2n}) = constant$ can be maintained as $\Psi(x_1, \ldots, x_{2n}, x_{2n+1}, x_{2n+2}) = constant$, if the coefficients of nonlinear interactions of $\Psi(x_{2n+1}, x_{2n+2})$ with others are not extremely different. The condition (3.13) could be interpreted in terms of conservation law to maintain stability, homeostasis of a biological system.

The conserved quantity $\Psi(x_1, \ldots, x_{2n}) = constant$, can be used to check the accuracy of numerical solutions to the $2n$ differential equations. Let us suppose that solutions to (3.6), $x_1, \ldots, x_{2n}$ are obtained. Then, one should substitute all solutions to (3.12) to check if Ψ becomes constant or not. In the Figure 3.1 and Figure 3.2, the solutions to classical LV equation in the example of the section 3.4.2 are shown. The parameters of solution 1 and solution 2 are $\alpha_1 = -0.02$, $\alpha_2 = -0.02$, $\alpha_3 = 50.0$, $\alpha_4 = 100.0$,

$\alpha_5 = 1.0$, and initial values of solution 1 and solution 2 are $x_1 = 10.0$, $x_2 = 10.0$ (see (3.25)). The size of interval ΔH in Runge-Kutta methods of solution 1 is $\Delta H = 0.01$, and solution 2 is $\Delta H = 0.5$.

If Ψ is exactly constant in the assumed interval $t \in [a, b]$, the solutions, $x_1, \ldots, x_{2n}$, are expected to be exact. If $\Psi \approx constant$, $x_1, \ldots, x_{2n}$ are approximate solutions that depend on the accuracy of $\Psi = constant$.

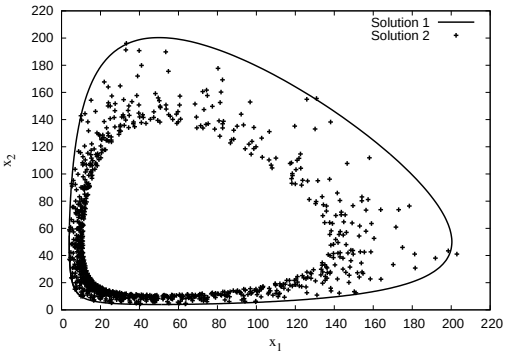

Figure 3.1: Numerical simulations of classical LV equation. Solution 1 and Solution 2 have different increment.

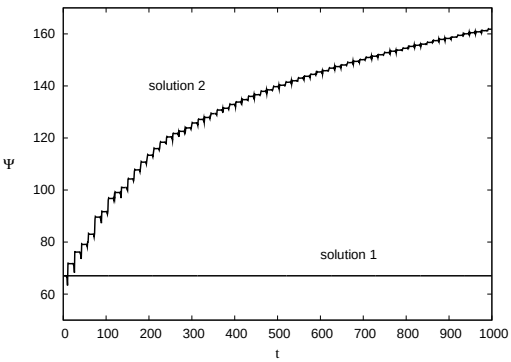

Figure 3.2: Numerical simulation of conserved quantity Ψ. Solution 1 are constant but Solution 2 oscillate and increase with respect to time.

3.4 Examples

The conservation law (3.12) in the BCF is a velocity-independent form. In the work of J. Fernández-Núñez, some functions are velocity-dependent and coupled with derivative terms such as $\dot{x}_{2i}\log x_{2i-1}/x_{2i}$ and $\dot{x}_{2i-1}\log x_{2i}/x_{2i-1}$ to obtain the classical LV system, and we also found a velocity-independent form of the exponential type, $\exp\{f(x_1, x_2, \ldots)\}$, shown in the example in section 3.4.2.

3.4.1 2-variable system

Here, we show an example of $2n$-dimensional ND system in the case of $n = 1$ in (3.6). The ND system of (3.6) is defined by

$$\begin{aligned} \dot{x}_1 &= a_{11}x_1 + a_{12}x_2 + a_{13}x_1^2 + a_{14}x_1x_2, \\ \dot{x}_2 &= a_{21}x_1 + a_{22}x_2 + a_{23}x_1x_2 + a_{24}x_2^2. \end{aligned} \tag{3.14}$$

The mixing interactions and self-interactions are expressed as x_1x_2, x_1^2 and x_2^2. Since this system has two variables, we have only x_1x_2 mixing interaction. The Lagrangian of this system is described from (3.7) as

$$\begin{aligned} \mathcal{L} = \alpha_1\dot{x}_1x_2 + \alpha_2x_1\dot{x}_2 + \alpha_3x_1^2 + (\alpha_4 + \alpha_5)x_1x_2 \\ +\alpha_6x_2^2 + \alpha_7x_1^2x_2 + \alpha_8x_1x_2^2. \end{aligned} \tag{3.15}$$

From (3.15), we get the following nonlinear differential equation,

$$\dot{x}_1 = \frac{1}{d_{21}}\{(\alpha_4 + \alpha_5)x_1 + 2\alpha_6 x_2 + 2\alpha_8 x_1 x_2 + \alpha_7 x_1^2\}, \tag{3.16}$$

$$\dot{x}_2 = \frac{1}{d_{12}}\{2\alpha_3 x_1 + (\alpha_4 + \alpha_5)x_2 + 2\alpha_7 x_1 x_2 + \alpha_8 x_2^2\}. \tag{3.17}$$

The parameter d_{21} is given by $d_{21} = \alpha_2 - \alpha_1 = -d_{12}$. The conserved quantity Ψ of this system is obtained as follows

$$\Psi \equiv \alpha_3 x_1^2 + (\alpha_4 + \alpha_5)x_1 x_2 + \alpha_6 x_2^2 + \alpha_7 x_1^2 x_2 + \alpha_8 x_1 x_2^2. \tag{3.18}$$

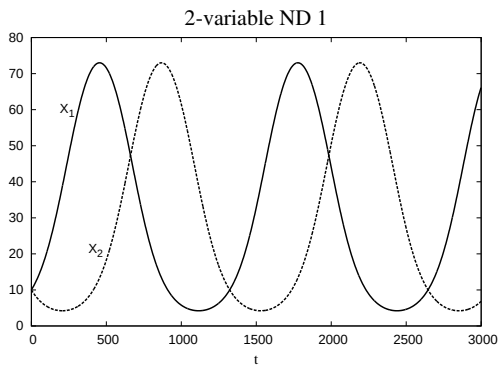

Figure 3.3: Numerical simulation of 2-variable ND 1. The parameters of 2-variable ND 1: $\alpha_1 = 1.0$, $\alpha_2 = 2.0$, $\alpha_3 = -0.01$, $\alpha_4 = 0.5$, $\alpha_5 = 0.5$, $\alpha_6 = -0.01$, $\alpha_7 = -0.01$, $\alpha_8 = -0.01$, initial values are $x_1 = 10.0$, $x_2 = 10.0$.

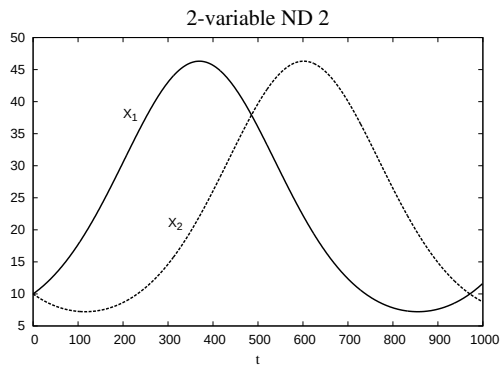

Figure 3.4: Numerical simulation of 2-variable ND 1. The parameters of 2-variable ND 2: $\alpha_1 = 1.0$, $\alpha_2 = 2.0$, $\alpha_3 = -0.1$, $\alpha_4 = 0.5$, $\alpha_5 = 0.5$, $\alpha_6 = -0.1$, $\alpha_7 = -0.01$, $\alpha_8 = -0.01$, initial values are $x_1 = 10.0$, $x_2 = 10.0$.

We show numerical simulations of 2-variable ND system in Figures 3.3, 3.4, 3.5, and 3.6. Note that 2-variable ND 1 in Figure 3.3 and 2-variable ND 2 in Figure 3.4 with different parameters are periodically stable and have the same conserved quantity Ψ defined as (3.18). The parameters of both 2-variable ND 1 and ND 2 are given in caption Figure 3.3 and Figure 3.4. The solutions of 2-variable ND 1 and ND 2 are periodic and steady state in Figure 3.5, and the conserved quantity defined in (3.18) is given in Figure 3.6. The conserved quantity of 2-variable ND 1 and ND 2 is strictly constant with respect to time.

In Figure 3.7 and Figure 3.8, we show an example in the case that parameters of $2n$-ND system (3.6) do not satisfy the condition (3.10) and (3.11). The conserved quantity Ψ is not equal to a constant in time. In the simulation of 2-variable ND 3* in Figure 3.7, the coefficient of x_1^2 in (3.16) changed from α_7 to $-\alpha_7$, and the coefficient d_{12} in (3.17) changed from d_{12} to d_{21} and the coefficient x_2^2 in (3.17) also changed α_8 to $-\alpha_8$ so that the system of differential equations does not satisfy the condition (3.10), (3.11) and the conservation law (3.18). The parameters are determined as $\alpha_1 = 1.0$, $\alpha_2 = 2.0$, $\alpha_3 = 0.5$, $\alpha_4 = 0.5$, $\alpha_5 = 0.5$, $\alpha_6 = 0.1$, $\alpha_7 = 0.01$, $\alpha_8 = 0.01$, and initial values are $x_1 = 10.0$, $x_2 = 10.0$. In the simulation 3.8, quantity Ψ increased exponentially and diverged. Ψ is not constant with respect to time in this case. It indicates that Ψ is not constant when the coefficients do not meet the condition (3.10) and (3.11), and Ψ diverged when the solutions of the system diverged with respect to time.

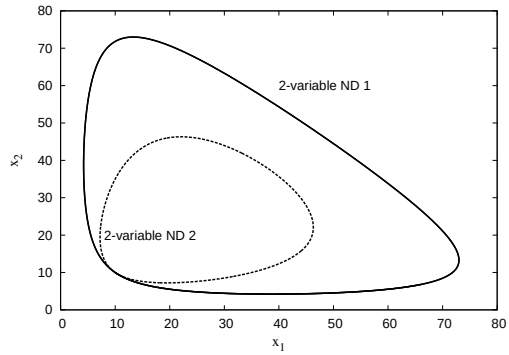

Figure 3.5: Numerical solutions of 2-variable ND 1 and ND 2.

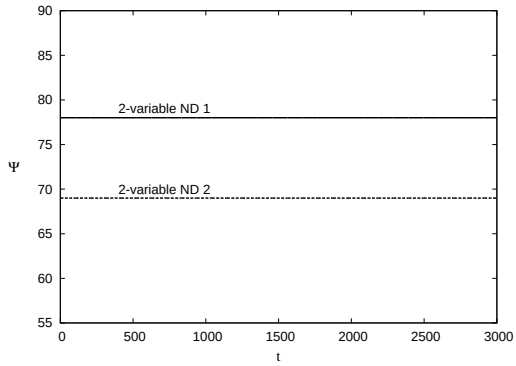

Figure 3.6: Numerical solutions of conserved quantity Ψ of 2-variable ND 1 and ND 2. Note that Ψ is constant in both cases.

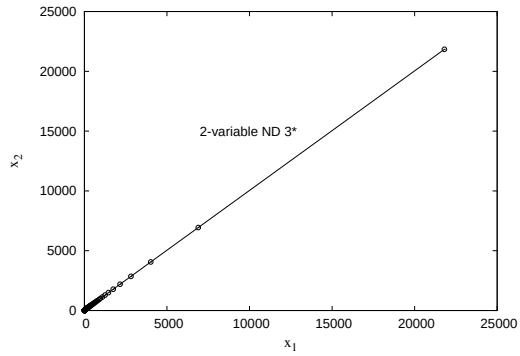

Figure 3.7: Numerical solutions of 2-variable ND 3* system with parameters which do not satisfy conditions.

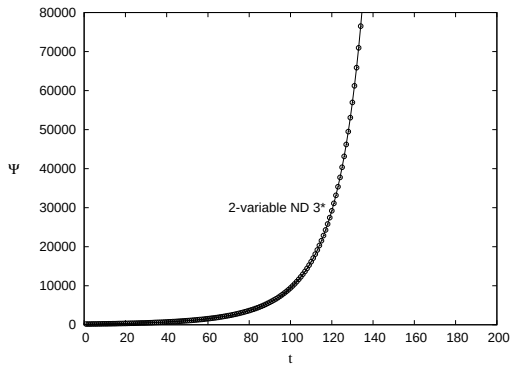

Figure 3.8: Numerical solutions of Ψ of 2-variable ND 3*. Note that the solutions are not constant and diverge with respect to time.

Next, let us assume that the 3-variable system has a similar conservation law as (3.18), and we obtain the Lagrangian of the following type,

$$\begin{aligned}\mathcal{L} = {} & \alpha_1\dot{x}_1x_2 + \alpha_2\dot{x}_2x_3 + \alpha_3\dot{x}_3x_1 + \alpha_4x_1x_2 + \alpha_5x_1x_3 \\ & + \alpha_6x_2x_3 + \alpha_7x_1^2 + \alpha_8x_2^2 + \alpha_9x_3^2 + \alpha_{10}x_1^2x_2 \\ & + \alpha_{11}x_1x_2^2 + \alpha_{12}x_1^2x_3 + \alpha_{13}x_1x_3^2 + \alpha_{14}x_2^2x_3 + \alpha_{15}x_2x_3^2\end{aligned} \tag{3.19}$$

The conserved quantity of (3.19) is given by

$$\begin{aligned}\Psi = {} & \alpha_4x_1x_2 + \alpha_5x_1x_3 + \alpha_6x_2x_3 + \alpha_7x_1^2 + \alpha_8x_2^2 + \alpha_9x_3^2 \\ & + \alpha_{10}x_1^2x_2 + \alpha_{11}x_1x_2^2 + \alpha_{12}x_1^2x_3 + \alpha_{13}x_1x_3^2 \\ & + \alpha_{14}x_2^2x_3 + \alpha_{15}x_2x_3^2\end{aligned} \tag{3.20}$$

The Lagrangian (3.19) produces, the following ordinary differential equations,

$$\begin{aligned}
\alpha_1\dot{x}_2 - \alpha_3\dot{x}_3 =& 2\alpha_7 x_1 + \alpha_4 x_2 + \alpha_5 x_3 + 2\alpha_{10}x_1x_2 + \alpha_{11}x_2^2 \\
&+ 2\alpha_{12}x_1x_3 + \alpha_{13}x_3^2, \\
\alpha_2\dot{x}_3 - \alpha_1\dot{x}_1 =& \alpha_4 x_1 + 2\alpha_8 x_2 + \alpha_6 x_3 + 2\alpha_{11}x_1x_2 \\
&+ 2\alpha_{14}x_2x_3 + \alpha_{10}x_1^2 + \alpha_{15}x_3^2, \\
\alpha_3\dot{x}_1 - \alpha_2\dot{x}_2 =& \alpha_5 x_1 + \alpha_6 x_2 + 2\alpha_9 x_3 + \alpha_{12}x_1^2 + 2\alpha_{13}x_1x_3 \\
&+ \alpha_{14}x_2^2 + 2\alpha_{15}x_2x_3.
\end{aligned} \tag{3.21}$$

The type of differential equations is a little different from that of the $2n$ variables. The coupled linear equation (3.21) can be solved for x_3, resulting in

$$\begin{aligned}
&(\alpha_2\alpha_{13} + \alpha_3\alpha_{15})x_3^2 + \{(2\alpha_1\alpha_{15} + 2\alpha_3\alpha_{14})x_2 + (2\alpha_1\alpha_{13} + 2\alpha_2\alpha_{12})x_1 \\
&+ (2\alpha_1\alpha_9 + \alpha_2\alpha_5 + \alpha_3\alpha_6)\}x_3 + (\alpha_1\alpha_5 + 2\alpha_2\alpha_7 + \alpha_3\alpha_4)x_1 \\
&+ (\alpha_1\alpha_6 + \alpha_2\alpha_4 + 2\alpha_3\alpha_8)x_2 + (\alpha_1\alpha_{12} + \alpha_3\alpha_{10})x_1^2 \\
&+ (2\alpha_3\alpha_{11} + 2\alpha_2\alpha_{10})x_1x_2 + (\alpha_1\alpha_{14} + \alpha_2\alpha_{11})x_2^2 = 0.
\end{aligned} \tag{3.22}$$

This is another time-independent relation of the 3-variable ND system. However, the time-independent relation is obtained from the differential equations, not from the conservation law Ψ. Hence, it indicates that there are two types of time-independent relations: (1) the time-independent relation that is strictly determined by Lagrangian or Noether's theorem; (2) the time-independent relation that is derived from a particular structure of differential equations, but is not necessarily related to the conservation law. The conserved quantity, Ψ, is strictly constant with respect to time, which is more general than the relation (3.22).

3.4.2 Exponential types of 2 variable coupled LV system

We show another type of conserved quantity of 2 variables which is similar to Lyapunov function.The classical type of LV equation is defined as

$$\begin{aligned}
\dot{x}_1 &= a_{11}x_1 + a_{12}x_1x_2, \\
\dot{x}_2 &= a_{21}x_2 + a_{22}x_1x_2.
\end{aligned} \tag{3.23}$$

x_1 and x_2 are interpreted as a prey and a predator, respectively. The Lagrangian of (3.23) is described as follows

$$\mathcal{L} = \exp\{\alpha_1 x_1 + \alpha_2 x_2\}\{\alpha_3\dot{x}_1 + \alpha_4\dot{x}_2 + \alpha_5 x_1x_2\}. \tag{3.24}$$

We can get the conditions of parameter from (3.23) and (3.24),

$$\begin{aligned}
\dot{x}_1 &= \frac{1}{d_{12}}\alpha_5\{\alpha_2 x_1x_2 + x_1\}, \\
\dot{x}_2 &= \frac{1}{d_{21}}\alpha_5\{\alpha_1 x_1x_2 + x_2\},
\end{aligned} \tag{3.25}$$

where $d_{12} = \alpha_1\alpha_4 - \alpha_2\alpha_3 = -d_{21}$ This is the condition for parameters to have a conserved quantity. The conserved quantity Ψ is obtained as

$$\Psi \equiv \alpha_5 \exp\{\alpha_1 x_1 + \alpha_2 x_2\} x_1 x_2. \tag{3.26}$$

The logarithm of (3.26) is similar to a well known Lyapunov function $V(x_1, x_2)$ which has the property $dV(x_1, x_2)/dt = 0$. It can be directly explained that the time derivative of conserved quantity should vanish, $d\Psi/dt = 0$, and therefore, Lyapunov function has a strong relation with Noether's theorem.

One can see that the conservation law and Lyapunov function are explicitly related to each other in the case of this simple example. However, it is not clear whether the connections between the $2n$-dimensional ND system and Lyapunov function are directly related to each other. Let us assume 3-variable type of differential equations of exponential type. The Lagrangian of linear 3-variable first-order equation is assumed as

$$\begin{aligned}\mathcal{L} = &\exp\{\alpha_1 x_1 + \alpha_2 x_2 + \alpha_3 x_3\}\{\alpha_4 \dot{x}_1 + \alpha_5 \dot{x}_2 + \alpha_6 \dot{x}_3 + \\ &\alpha_7 x_1 + \alpha_8 x_2 + \alpha_9 x_3 + \alpha_{10} x_1 x_2 + \alpha_{11} x_1 x_3 + \alpha_{12} x_2 x_3\}.\end{aligned} \tag{3.27}$$

Applying Eq. (3.2) to Eq. (3.29), we get three equations as

$$\begin{aligned}&(\alpha_1\alpha_5 - \alpha_2\alpha_4)\dot{x}_2 + (\alpha_1\alpha_6 - \alpha_3\alpha_4)\dot{x}_3 + \alpha_1\alpha_7 x_1 + (\alpha_1\alpha_8 + \alpha_{10})x_2 \\ &+ (\alpha_1\alpha_9 + \alpha_{11})x_3 + \alpha_1\alpha_{10}x_1x_2 + \alpha_1\alpha_{11}x_1x_3 + \alpha_1\alpha_{12}x_2x_3 + \alpha_7 = 0, \\ &(\alpha_2\alpha_4 - \alpha_1\alpha_5)\dot{x}_1 + (\alpha_2\alpha_6 - \alpha_3\alpha_5)\dot{x}_3 + (\alpha_2\alpha_7 + \alpha_{10})x_1 + \alpha_2\alpha_8 x_2 \\ &+ (\alpha_2\alpha_9 + \alpha_{12})x_3 + \alpha_2\alpha_{10}x_1x_2 + \alpha_2\alpha_{11}x_1x_3 + \alpha_2\alpha_{12}x_2x_3 + \alpha_8 = 0, \\ &(\alpha_3\alpha_4 - \alpha_1\alpha_6)\dot{x}_1 + (\alpha_3\alpha_5 - \alpha_2\alpha_6)\dot{x}_2 + (\alpha_3\alpha_7 + \alpha_{11})x_1 + (\alpha_3\alpha_8 + \alpha_{12})x_2 \\ &+ \alpha_3\alpha_9 x_3 + \alpha_3\alpha_{10}x_1x_2 + \alpha_3\alpha_{11}x_1x_3 + \alpha_3\alpha_{12}x_2x_3 + \alpha_9 = 0.\end{aligned} \tag{3.28}$$

The conserved quantity is velocity-independent and given by

$$\begin{aligned}\Psi = &\exp\{\alpha_1 x_1 + \alpha_2 x_2 + \alpha_3 x_3\}\{\alpha_7 x_1 + \alpha_8 x_2 + \alpha_9 x_3 \\ &+ \alpha_{10} x_1 x_2 + \alpha_{11} x_1 x_3 + \alpha_{12} x_2 x_3\}.\end{aligned} \tag{3.29}$$

The nonlinear equation (3.28) can be solved for x_3, resulting in

$$\begin{aligned}x_3 = &\frac{1}{\sigma_1 + \sigma_2 x_1 + \sigma_3 x_2}[\{\phi_3\alpha_1\alpha_7 + \phi_1(\alpha_2\alpha_7 + \alpha_{10}) + \phi_2(\alpha_3\alpha_7 + \alpha_{11})\}x_1 \\ &+ \{\phi_3(\alpha_1\alpha_8 + \alpha_{10}) + \phi_1\alpha_2\alpha_8 + \alpha_2(\alpha_3\alpha_8 + \alpha_{12})\}x_2 \\ &+ \{\phi_3\alpha_1\alpha_{10} + \phi_1\alpha_2\alpha_{10} + \phi_2\alpha_3\alpha_{10}\}x_1x_2 + \phi_3\alpha_7 + \phi_1\alpha_8 + \phi_2\alpha_9]\end{aligned} \tag{3.30}$$

where $\phi_1 = \alpha_3\alpha_4 - \alpha_1\alpha_6$, $\phi_2 = \alpha_1\alpha_5 - \alpha_2\alpha_4$, $\phi_3 = \alpha_2\alpha_6 - \alpha_3\alpha_5$, $\sigma_1 = -\phi_3(\alpha_1\alpha_9 + \alpha_{11}) - \phi_1(\alpha_2\alpha_9 + \alpha_{12}) - \phi_2\alpha_3\alpha_9$, $\sigma_2 = -\phi_3\alpha_1\alpha_{11} - \phi_1\alpha_2\alpha_{11} - \phi_2\alpha_3\alpha_{11}$, $\sigma_3 = -\phi_3\alpha_1\alpha_{12} - \phi_1\alpha_2\alpha_{11} - \phi_2\alpha_3\alpha_{12}$. As discussed in the example 3.4.1, the conserved quantity is strictly constant with respect to time, which is more general than equation (3.30).

3.5 Discussion

In this research project, we have investigated a system of $2n$ dimensional, coupled first order differential equations which contains self-interactions, and mixing interactions by using Noether's theorem. We discussed that the nonlinear differential equations with a conserved quantity, Ψ, calculated by Noether's theorem have converged stable solutions, and the coefficients of nonlinear interactions are strictly confined by the conservation law of the system. The conserving converged solutions are shown by a closed curve in (x_1, x_2)-coordinates for 2-dimensional case, and in general, it should be discussed by a closed hyper-surface in $(x_1, x_2, \ldots, x_{2n})$-coordinates for $2n$-dimensional case.

Conventionally, the analysis of conserved quantity of solutions to a system of coupled differential equations is discussed with Lyapunov function [84]. There are two main types of Lyapunov functions that are strict Lyapunov and non-strict Lyapunov functions. Our conserved quantity would correspond to the strict Lyapunov function, due to the global property of Lagrangian approach. The theorem relates stability and conserved quantity analogous to conservation laws of energy and momentum in physics, hence it is helpful to understand a system of nonlinear differential equations in view of scientific or physical terms.

A system of symmetric nonlinear coupled first order differential equations has a conservation law and exists in the form of the $2n$-independent variables $(x_1, x_2, \ldots, x_{2n})$. We termed the system of symmetric first-order differential equations composed of the $2n$-dimensional nonlinear interactions as the binary-coupled form (BCF). If a coupled nonlinear system exists in a form of symmetric first-order differential equations, which has a velocity-independent conserved quantity as discussed in this thesis, the system tends to be composed of the binary-coupled form $(2, 4, 6, \ldots, 2n)$. The predator-prey type system (2-coupled form), food-web system [40, 92], and gene regulation network system [39, 88] may be typical examples, and also the computer network seems to be expressed by $2n$-coupled form [105]. If a competitive system is the odd-variable type, the system of the first-order differential equations becomes little different as shown in the example in section 3.4.2.

When a binary-coupled system with a conservation law $\Psi(x_1, \ldots, x_{2n})$ and another system with $\Psi(x_{2n+1}, x_{2n+2})$ interact with each other and result in constructing a new binary-coupled system, the system should have the conservation law in the form of $\Psi(x_1, \ldots, x_{2n}) + \Psi(x_{2n+1}, x_{2n+2}) \to \Psi(x_1, \ldots, x_{2n+2})$ as in the form (3.12), even if they are nonlinearly interacting as (3.6). This may indicate an addition law for the same conserving ND systems. The addition law may be interpreted as the restoration or rehabilitation phenomena known in a large system of neural network or computer network when a small disordered device or part of a large network system is replaced by a normal device.

The conservation law is also used to check the accuracy of numerical solutions of nonlinear differential equations. The binary-coupled differential equations have interesting properties as shown in this chapter, and the system of BCF $(2, 4, 6, \ldots, 2n)$ seems to be found in social, natural and biological sciences. If a system of BCF is naturally discovered in nature, the consequences discussed in BCF system would help understand structures, interactions, evolution mechanism of biological systems as well as social, economic and environmental systems.

We have investigated and discussed the property of $2n$-dimensional ND system in general. Although $2n$-dimensional ND system is discussed as a continuous system by employing differential equations, it is useful to examine their qualitative character of the classical LV system. However, most of biological phenomena may be mesoscopic, and a discrete system would fit actual phenomena more than a continuous system.

Chapter 4

Stability and restoration phenomena in competitive systems

4.1 Background

In this chapter, we will introduce characteristic properties of ecological system using $2n$ Nonlinear Dynamical model. The concept of stability is important in order to understand natural phenomena in physical, biological and engineering systems. In our previous study, we studied the relation between a conservation law and stability of a $2n$-dimensional competitive system that contains competitive interactions, self-interactions and mixing interactions. The system consists of $2n$-dimensional nonlinear differential equations required from Noether's theorem [130]. The $2n$-dimensional nonlinear ordinary differential equations for a competitive system constructed to satisfy the conservation law have properties such as the addition law, which is empirically interpreted as recovery from injuries of skin and tissues in biological bodies.

It has been shown by many researchers that a relatively simple set of interactions can explain complex phenomena in biological systems [30, 86]. For example, in 1952, Turing suggested chemical molecular mechanism called the reaction-diffusion system [129] which is defined as semi-linear parabolic partial differential equations. This reaction-diffusion system is well applied for explaining stripe patterns of the marine angelfish, *Pomacanthus*, and restoration phenomena in its stripe patterns from injuries was observed [62, 65, 71]. Prigogine also proposed Brusselator model with nonlinear ordinary differential equations to illustrate spatial oscillations and Turing patterns [5]. It is also an interesting problem to investigate in ecological systems if a large complex system should be stable or not, and many researchers have discussed the criteria concerning the stability of a system for n dimensional ordinary differential equations and statistical framework [16, 19, 43, 83, 126]. What would be a reason why a simple set of interactions can explain complex phenomena? We discussed a system of interactions generalizing Lotka-Volterra type nonlinear competitive interactions and suggested that a conservation law could be a key to understand complex phenomena even in biological and ecological systems.

We investigated the system of $2n$-dimensional coupled first-order differential equations by using Noether's theorem, which led to the following results. (i) The form of differential equations and coefficients of nonlinear interactions are strictly confined when the system has a conservation law which is constructed by interacting species of a particular experimental system. (ii) The conserved quantity of a

system produces a Lyapunov function which is usually employed to study solutions of nonlinear differential equations. The conserved quantity is constructed by Noether's theorem, but the analysis of Lyapunov function would be used to check solutions to differential equations including those for non-conservative and dissipative systems. The system of differential equations with conservation law is different in this respect. (iii) A system of interactions could be analyzed as an assembly of a basic binary-coupled form (BCF). In other words, a complex interacting system can be decomposed into an assembly of binary-coupled systems. The BCF system is a simple basic set to explain complex phenomena defined by Noether's theorem. (iv) The BCF system with conservation law indicates an addition law which may be interpreted as the restoration or rehabilitation phenomena; those are known in a large system of neural network or computer network when a small disordered device or a part of network system is replaced by a normal device. These properties could be applied to stability and restoration phenomena of biological systems. (v) The conservation law is also useful to check accuracy of numerical solutions to nonlinear differential equations. As summarized above, we discussed that the basic nonlinear system in BCF is stable. The binary-coupled system and addition law supported by a conservation law can lead to a large, stable complex system. This is an important conclusion on the conserved binary-coupled model. Because the BCF system has such several interesting properties, we will apply the model in order to study stability and interaction mechanisms of biological systems.

In this chapter, we will explain the properties of solutions with a conservation law and applications to biological systems. In Section 4.2, we extend the BCF model to simulate external perturbations numerically. There are various prey-predator type competitive models with perturbations, however, most of them are with small, stochastic perturbations. The behaviors of conservation laws with external perturbations have been seldom considered. We will explicitly discuss properties of the conserved, stable, 2-variable nonlinear interacting system with external perturbations and the conservation law, its indications and possible applications to nonlinear interacting system. We will show that 2-variable ND model has the properties of restoration and recovery from external perturbations. In Section 4.3, stability and population cycles of biological systems are examined in terms of a conservation law of the system. We will also examine specific examples of the Canadian lynx and snowshoe hare [4, 7, 21, 63, 79, 121, 122] and the question of population cycles, and food chain of microbes in the lake [28, 111]. Discussion and summary of results are given in Section 4.5.

4.2 The model of binary-coupled form (BCF)

4.2.1 $2n$-ND system with perturbations

We discussed BCF system and the conservation law of $2n$-nonlinear dynamical ($2n$-ND) model in detail in the previous work [130]. In this study, we add external perturbations in $2n$-variable nonlinear differential equations in order to examine characteristic behaviors of conserved nonlinear interacting systems. It should be noticed that the $2n$-ND model is extended by adding external perturbation terms which maintain a conservation law given by Noether's theorem. The odd variable terms for x_i ($i = 1, \ldots, 2n$)

are

$$
\begin{aligned}
d_{2k,2k-1}\dot{x}_{2k-1} = \sum_{i=1}^{n}\Big\{&(\alpha_{\{2ni+2k\}} + \alpha_{\{2n^2+2nk+2i-1\}})x_{2i-1} \\
&+ (\alpha_{\{2n^2+2ni+2k\}} + \alpha_{\{2n^2+2nk+2i\}})x_{2i} \\
&+ \alpha_{\{4n^2+2ni+2k\}}x_{2i-1}x_{2i}\Big\} \\
&+ \sum_{j=1}^{2n}\alpha_{\{4n^2+2nk+j\}}x_j x_{2k-1} + c_{2k-1},
\end{aligned}
\tag{4.1}
$$

where $k = 1, \ldots, n$. The even variable terms for x_i $(i = 1, \ldots, 2n)$ are

$$
\begin{aligned}
d_{2k-1,2k}\dot{x}_{2k} = \sum_{i=1}^{n}\Big\{&(\alpha_{\{2ni+2k-1\}} + \alpha_{\{2nk+2i-1\}})x_{2i-1} \\
&+ (\alpha_{\{2n^2+2ni+2k-1\}} + \alpha_{\{2nk+2i\}})x_{2i} \\
&+ \alpha_{\{4n^2+2ni+2k-1\}}x_{2i-1}x_{2i}\Big\} \\
&+ \sum_{j=1}^{2n}\alpha_{\{4n^2+2nk+j\}}x_j x_{2k} + c_{2k},
\end{aligned}
\tag{4.2}
$$

where $\dot{x} = dx/dt$, coefficients, $d_{i,j}$ express $d_{2k,2k-1} = \alpha_{2k} - \alpha_{2k-1}$, $d_{2k-1,2k} = \alpha_{2k-1} - \alpha_{2k}$. The linear coefficients and nonlinear coefficients α_i, $(i = 1, \ldots, 8n^2 + 2n)$ are arbitrary constant values. The last terms c_{2k-1}, c_{2k}, $(k = 1, \ldots, n)$ of (4.1) and (4.2) are constants or piecewise continuous constants, which are interpreted as external perturbations (temperature, seasons and other temporal, external inputs). One should note that constant terms have dimension of velocity, so they are different from actual external perturbations which are considered to effectively express external perturbations. Because external perturbations (inputs) change population densities as $\dot{x} = dx/dt$, we simulate numerically those effects with c_{2k-1}, c_{2k} as external inputs. The system has a conservation law derived from Noether's theorem which is proved in the reference [130]:

$$
\begin{aligned}
\Psi \equiv \sum_{i=1}^{n}\sum_{j=1}^{2n}\Big\{&\alpha_{\{2ni+j\}}x_{2i-1}x_j + \alpha_{\{2n^2+2ni+j\}}x_{2i}x_j \\
&+ \alpha_{\{4n^2+2ni+j\}}x_{2i-1}x_{2i}x_j\Big\} \\
&+ \sum_{i=1}^{n}\{c_{2i}x_{2i-1} + c_{2i-1}x_{2i}\}.
\end{aligned}
\tag{4.3}
$$

Therefore, with the equations from (4.1) to (4.3), we are able to consider the conserved nonlinear dynamical system with external perturbations by employing piecewise continuous constant terms, c_{2k-1}, c_{2k}.

The physical meaning of conserved quantities in a biological system is difficult to define contrary to classical mechanics in physics, and so we would like to explain differences between Ψ-function and

Hamiltonian. The Ψ-function in this study is derived from Noether's theorem with Euler-Lagrange equations of motion applied to the $2n$-ND system. We discussed the binary-coupled form to generalize Lotka-Volterra type competitive system in the previous work.

The binary-coupled system has the conserved quantity (Ψ-function) and the Ψ-function may have similar physical meanings as the Hamiltonian of a system. However, the Hamiltonian is defined as the total energy of a system, and the energy has the dimension of the work, which is defined as force $\times$ displacement [31, 73]. The conserved quantity Ψ is constant along with time, but it is constructed from interactions of $2n$-ND system, not from the force, kinetic energy and potentials which are, in principle, converted to the work produced by the system. Hence, the Ψ-function may well be called as the 'conserved quantity', but not as the Hamiltonian of the system. The Ψ-function may correspond to (generalized) kinetic and potential energies of a system, but it is not possible to prove that the Ψ-function is equivalent to the Hamiltonian in terms of physics. In the $2n$-ND model, variables denote population densities of a system of extended Lotka-Volterra type differential equations, and it is inappropriate to directly interpret the Ψ-function as the total energy or biomass of the system. However, it is important to comprehend that the conserved Ψ-function controls behaviors and properties of the system.

We showed that the conserved quantity, Ψ-function, can reproduce the Lyapunov function of classical Lotka-Volterra equations in the previous work [130]. It is essential to understand that Lyapunov functions for certain systems of differential equations can be derived from Noether's theorem when a system has conserved quantities. Hence, in conserved systems such as $2n$-ND systems, the conservation law and Noether's theorem are fundamental to study properties of the system. The system with Lyapunov function has limit cycles and attractors, which designate energy dissipations of the system. The systems with Ψ-functions are strictly conserved systems, which should correspond to limit cycles at a given time. The dynamics of the system of Ψ-function evolves according to the conservation law Ψ, which is equivalent to Lagrangian dynamics in physical systems.

4.2.2 Properties of 2-variable ND model

The equations of 2-variable ND model are produced by setting $n = 1$ ($k = 1$) in equations (4.1) to (4.3), resulting in

$$\dot{x}_1 = \frac{1}{d_{21}}\{(\alpha_4 + \alpha_5)x_1 + 2\alpha_6 x_2 + 2\alpha_8 x_1 x_2 + \alpha_7 x_1^2\} + \frac{c_1}{d_{21}}, \tag{4.4}$$

$$\dot{x}_2 = \frac{1}{d_{12}}\{2\alpha_3 x_1 + (\alpha_4 + \alpha_5)x_2 + 2\alpha_7 x_1 x_2 + \alpha_8 x_2^2\} + \frac{c_2}{d_{12}}, \tag{4.5}$$

and the 2-variable ND model has the following conservation law,

$$\begin{aligned}\Psi \equiv &\alpha_3 x_1^2 + (\alpha_4 + \alpha_5)x_1 x_2 + \alpha_6 x_2^2 + \alpha_7 x_1^2 x_2 + \alpha_8 x_1 x_2^2 \\ &+ c_2 x_1 + c_1 x_2.\end{aligned} \tag{4.6}$$

The nonlinear interactions can generally represent, for example, Lotka-Volterra type prey-predator, competitive interactions, food-chain relations by adjusting nonlinear parameters $\alpha_1, \ldots, \alpha_8$. The piecewise continuous constants, c_1 and c_2 are used as external perturbations in computer simulations, such as environmental conditions which increase or decrease interacting species in questions. The equations (4.4) $\sim$ (4.6) form 2-variable BCF nonlinear differential equations with a conservation law.

By employing eqs. (4.4) ~ (4.6), we will show:
(1) solutions to the binary-coupled nonlinear equations maintain a characteristic (x_1, x_2) phase-space of solutions and recovery from external perturbations. The external perturbations can numerically reproduce environmental conditions such as temperature, climate and chemical substances which affect interacting species. The nonlinear binary-coupled model can be applied to examine responses of a system whether they are induced from internal interactions or external perturbations.
(2) The binary-coupled nonlinear equations with conservation law exhibit stable phase-space solutions, which are interpreted as stability and recovery of population-change in a biological system. The properties of the binary-coupled nonlinear interactions will be shown explicitly in numerical simulations.
(3) By employing the 2-variable binary-coupled model, it is possible to simulate cycles of maxima and minima in population-change, delays of periodic times of population cycles for competitive species. Hence, cycles of population-change will be discussed in terms of the conservation law and nonlinear interactions.

Figure 4.1(a) shows the nonlinear interactions between species without external perturbations ($c_1 = 0$ and $c_2 = 0$), whose coefficients of nonlinear equations are set as in Table 1 (Condition 1). In a view of the classical Lotka-Volterra competitive system, it can be interpreted as that x_1 and x_2 represent prey and predator, respectively. Figure 4.1(b) is the phase-space given by solutions (x_1, x_2). The solutions (x_1, x_2) are periodic with respect to time, the maximum and minimum of (x_1, x_2) appear with a time-delay. Figure 4.1(c) shows the numerical value of the conserved function Ψ defined by (4.6), which is constant with respect to time.

The solutions (x_1, x_2) in Figure 4.1(a) show explicitly a time-delay of the peak for interacting species. The timings of peak and delayed peak are determined by nonlinear interactions and strength of coupling constant. The solutions (x_1, x_2) in Figure 4.1(b) show phase-space solutions, which are stable in the meaning that the conserved quantity Ψ is maintained constant and phase-space solutions are in the same trajectory for all time. The unit of time should be considered to adjust to the time scale of a system in consideration, because biological unit times are generally different from microbes to mammals.

The phase-space diagram 4.1(b) and the straight line of Figure 4.1(c) show that the solution is exact and stable [130]. The three figures exhibit important properties of solutions to the system of prey-predator type of competitive nonlinear interactions.

One of the important properties shown by the stable, conserved nonlinear system is that the interacting species repeat the rhythm of maxima and minima of the population. The periods of the rhythm are the result of complicated nonlinear interactions, but the system keeps the constant quantity Ψ with respect to time. The interesting applications of the BCF model are shown by employing in the reference '*Mysis* in the Okanagan Lake food web' [111], Canadian Lynx and snowshoe hare [21], which will be explained in Section 4.3.

Table 1: The list of nonlinear coefficients.

	α_1	α_2	α_3	α_4	α_5	α_6	α_7	α_8
Condition 1	1.0	401.0	-0.35	1.5	10.5	-0.01	-0.006	-0.011
Condition 2	1.0	401.0	-0.35	1.5	10.5	-0.51	-0.006	-0.011

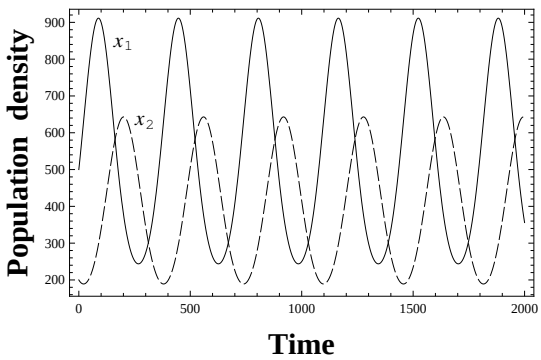

(a) 2-variable ND solutions. Solid and dashed lines represent x_1 (prey) and x_2 (predator), respectively. One should note that the unit of time should be defined with respect to a system in consideration.

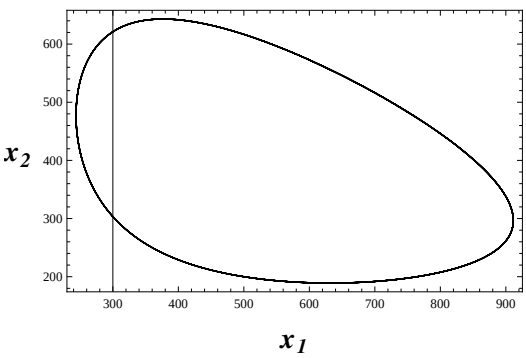

(b) Phase-space of 2-variable ND solutions.

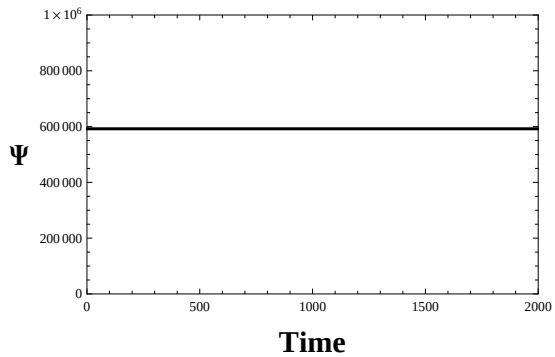

(c) Conservation law Ψ of 2-variable ND. It is constant with respect to time.

Figure 4.1: A 2-variable ND solution and Conservation law Ψ.

4.2.3 Recovering and restoration from perturbations

In order to investigate responses of a system to external perturbations, we introduce piecewise continuous constants, c_1 and c_2, by using θ-functions such that

$$c_i = f_i\{\theta(t - t_{start}) - \theta(t - t_{end})\}, \quad (i = 1, 2), \tag{4.7}$$

where $\theta(t - t')$ represents a step function:

$$\theta(t - t') = \begin{cases} 1, & (t \geq t'), \\ 0, & (t < t'), \end{cases} \tag{4.8}$$

and coefficients f_i $(i = 1, 2)$ are positive or negative constants to express strength of external perturbations. The constants are adjusted to produce reasonable maxima and minima in numerical simulations.

Figures 4.2(a), 4.2(b) and 4.2(c) show the reaction and recovery of the nonlinear interacting system from an external perturbation. One of the typical recovery of a system from a perturbed state is shown. In

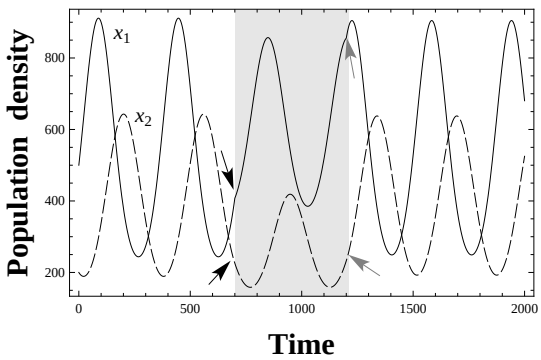

(a) 2-variable ND solutions with a negative perturbation on prey x_1. The perturbation is introduced from $t = 700$ to $t = 1200$ which is represented as gray background.

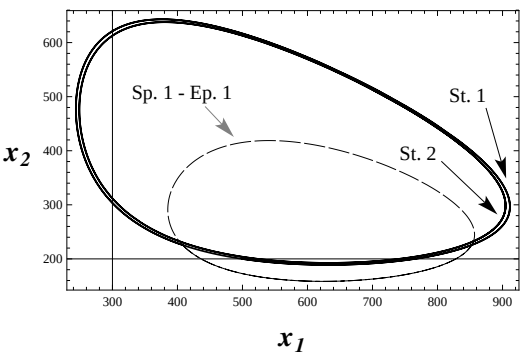

(b) The (x_1,x_2) phase-space transition with the negative perturbation as in (a). Solid line (St. 1) is initial state, and St. 2 is the recovered state after the end of perturbation. Dashed line is phase-space during Sp. 1 - Ep. 1.

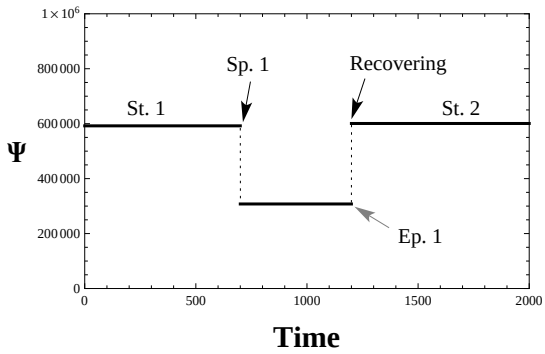

(c) Conservation law Ψ of 2-variable ND with one perturbation. Ψ changed Ψ ≃ 60000 to Ψ ≃ 30000 by introducing perturbation. It recovers after Ep. 1.

Figure 4.2: An external perturbation and a recovery.

Figure 4.2(a), an external perturbation starts at $t = 700$ (Sp. 1), and the coefficient f_1 equals to -1260.0 and f_2 equals to zero in this example. The black arrow is the starting point of perturbation, and the gray arrow is the end of perturbation in Figures 4.2(a) and 4.2(c). The nonlinear coefficients are listed in Table 1 (Condition 1). The solutions (x_1, x_2) are deformed by the perturbation (Figure 4.2(a) and 4.2(b)). However, the system does not disintegrate but finds a new stable phase-space close to the original phase-space and maintains a new conserved relation. The perturbation ends at $t = 1200$ (Ep. 1), and the system recovers the original state (x_1, x_2).

The timing of negative perturbation which reduces the population number x_1 or x_2 produces different results. When a negative perturbation is exerted in the increasing phase of x_1 or x_2, the system will find a new conserved stable solution near the original solution, but when a negative strong perturbation is exerted before x_1 or x_2 gets to its minimum, the system may collapse: the system exhibits no solutions (x_1, x_2), which would be interpreted as disintegration or extinction in biological systems.

The conserved nonlinear system naturally exhibits maxima and minima without external perturbations, and so we call these maxima and minima as endogenous maximum and minimum. It is needed to

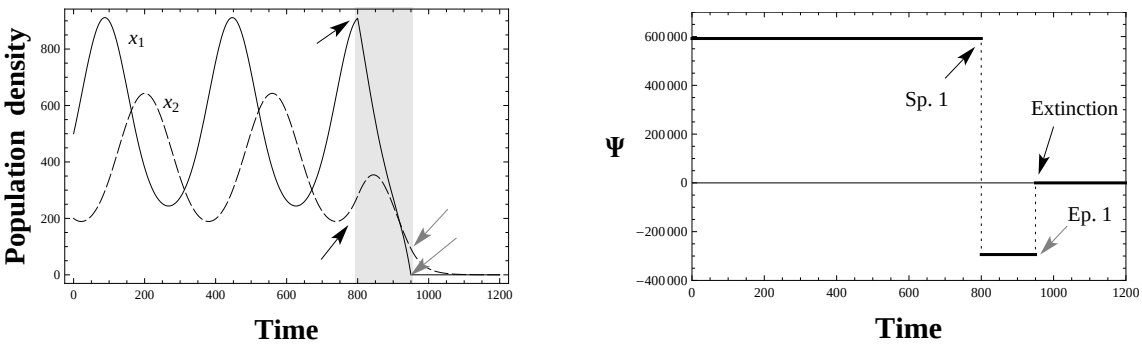

(a) 2-variable ND solutions with a critical negative perturbation on prey, x_1. Solutions converge to zero after the perturbation.

(b) Conservation law Ψ with a critical negative perturbation. Ψ converges to zero after the critical perturbation.

Figure 4.3: Critical negative perturbation and extinction.

distinguish them from enhanced maxima and minima by external perturbations.

In Figure 4.3, the response of a strong negative perturbation to prey after the peak of endogenous maximum is shown. The values of coefficients are listed in Table 1 (Condition 1). The starting point of this perturbation is at $t = 800$ and the end point of the perturbation is at $t = 950$. The negative constant of perturbation is $f_1 = -3175.3879$. The prey, x_1, rapidly declines with negative perturbation, and (x_1, x_2) converges to zero for $t \gtrsim 1000$. These computer simulations may be compatible with known empirical results, for example, in pest control. A pest control is not so effective if it is performed in the season when harmful insects are in peak and active, because species are energetic enough to find a new stable life to live. It is effective when a pest control is performed in the season when harmful insects are not so active or in a declining state after endogenous maximum.

In the nonlinear interacting system, positive perturbations which will increase x_1 or x_2 do not always mean a positive effect on stability of the system. There is a limit to the value of a positive perturbation, because an increase of x_1 leads to a decrease of x_2 in a stable system (x_1, x_2), which indicates that a system has internally allowed maximum and minimum populations.

Figures 4.4 shows the behaviors of (x_1, x_2) at normal and critical values of positive perturbations, c_1, for x_1. The values of coefficients are listed in Table 1 (Condition 2). Figures 4.4(a) and 4.4(b) show that the normal positive perturbation which increases interacting species will increase the peak of (x_1, x_2) populations. However, at certain critical values of coupling constants, the prey-predator interaction cannot keep and support the rhythm of maxima and minima, and the system diverges. Figures 4.4(c) and 4.4(d) show that the system cannot maintain a stable, interacting system when the positive perturbation surpasses the critical value ($c_1 = 1599.924999$ in the current simulation). The unstable solutions branch out at $t \simeq 1100$ when the value of perturbation changes from $f_1 = 1160.0$ to $f_1 = 1599.924999$.

Hence, in a conserved stable system, species seem to strictly control each other by seeking a new stable solution so that they can survive together. The competitive interacting system such as the conserved prey-predator relations may be considered to be a cooperative system for species to survive. It should be noted that if a dynamical prey-predator system is active, the rhythms of maxima and minima are clearly repeated, which is known in real prey-predator systems. However, if an external perturbation (exogenous interaction) exceeds a certain critical value of the competitive system, the rhythms of maxima and

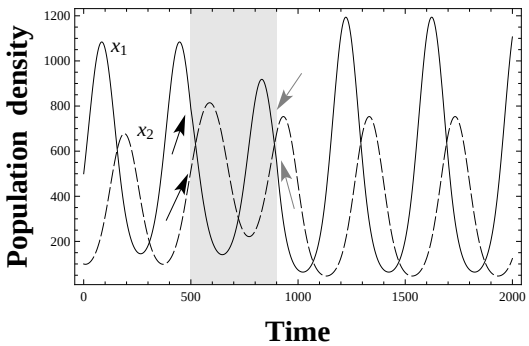

(a) 2-variable ND solutions with a positive perturbation. The perturbation starts at $t = 500$ and ends at $t = 900$ represented as gray background. The amplitudes of x_1 and x_2 become larger than before.

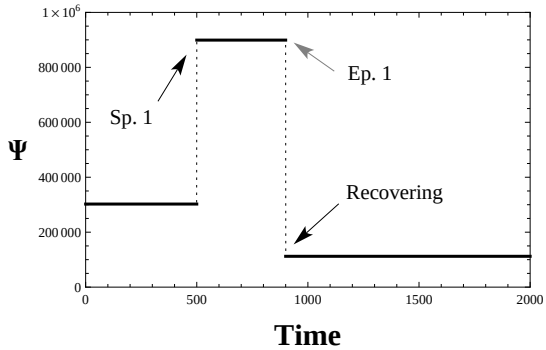

(b) The Conserved quantity Ψ with a positive perturbation. It recovers after perturbation but finds another equilibrium state.

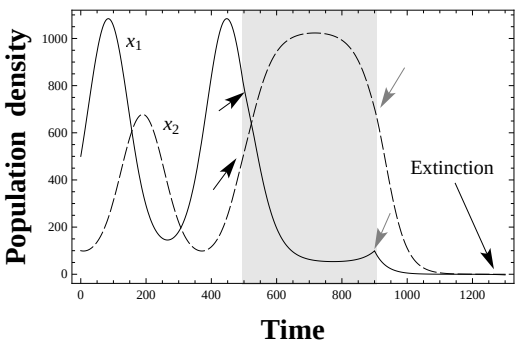

(c) 2-variable ND solutions with a critical perturbation. x_1 and x_2 converge to zero after a critical perturbation.

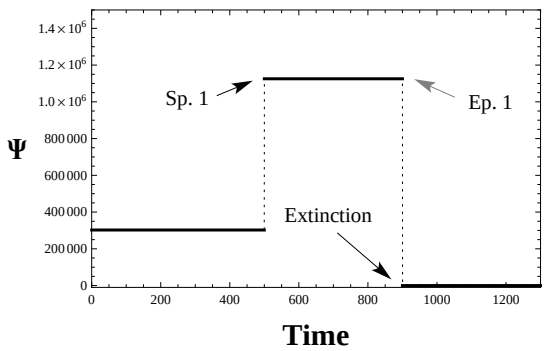

(d) Conservation law of 2-variable ND with a critical perturbation. The Ψ converges to zero after a critical perturbation.

Figure 4.4: Critical perturbations and divergence of solutions.

minima will disappear first and then after a time, the system will diverge (disintegrate). Therefore, the rhythm of wild-life indicates that the dynamical interactions between species are active and stable. When the rhythm of change disappear or does not come back, it may indicate that related species are in danger of extinction. The rhythm is important to examine if the wild life is normal and active, or harmed by human activities and external perturbations.

On the other hand, by adding another perturbation, we can show that it is possible to save species from extinction. Figure 4.5(a) is a result of a positive perturbation to save species (x_1, x_2) in a danger of extinction in Figure 4.3(a). We exerted a positive perturbation after Sp. 1 - Ep. 1 in Figure 4.5. The positive perturbations start at $t = 1000$ (Sp. 2) and end at $t = 1300$ (Ep. 2), the strengths of c_1 and c_2 are $f_1 = 200$, $f_2 = -1000$. Figure 4.5(a) shows that species are in danger of extinction, however, if positive external perturbations are properly inserted, the system will come back to life again.

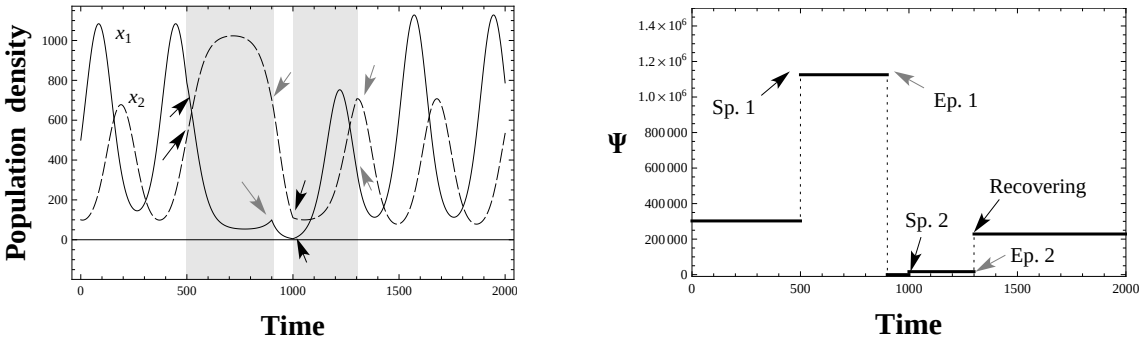

(a) 2-variable ND solutions with perturbations to avoid converging to zero after a critical perturbation. x_1 and x_2 come back to life after the second perturbations.

(b) Conservation law Ψ with two perturbations in (a). Ψ recovers from the perturbation after Sp. 2 - Ep. 2.

Figure 4.5: The critical behavior and restoration.

4.2.4 Comments on "atto-fox problem"

It should be noticed that a problem known as "atto-fox problem" [61, 89] in a system of differential equations will not occur in a conserved system of differential equations, because the problem is related to properties of the conserved or non-conserved system of differential equations. The $2n$-ND system has the conservation law and the Ψ-function characterizes behaviors of solutions and systems. If Ψ-function is conserved and not equal to zero, the solution will converge and the system will be stable. The nonlinear ordinary differential equations with a conservation law can have a stable solution controlled by the Ψ-function, and solutions consist of a closed hyper-surface of $(x_1, x_2, \ldots, x_{2n})$ for $2n$-dimensional case. It should be noted that the admissible coefficients of nonlinear interactions are strictly confined by Ψ-function of the system.

The Ψ-function will not be constant when there are no solutions or unphysical solutions, and the property to maintain Ψ-function as constant will confine admissible solutions [130]. For example, if the 2-variable nonlinear interacting system has solutions which are extremely different as 10^{-18} orders like "atto-fox problem", it is not possible that the system can maintain Ψ-function as constant in time. The phenomenon like "atto-fox problem" would appear in dissipative or non-conserved systems, because non-conserved and dissipative systems do not have the conservation law to control admissible solutions, and a large class of (unphysical) solutions can be allowed compared to the system of Ψ-function, which is the reason why the "atto-fox problem" could happen in non-conserved and dissipative systems. Therefore, the conserved system with Ψ-function will produce physical solutions controlled by the conservation law, and the phenomenon like the "atto-fox problem" will not be allowed in a conserved system with Ψ-function.

4.3 Conservation law and population cycles

4.3.1 The food-web of Microbes in Okanagan Lake

One of interesting data of the ecological interactions is the interaction described in '*Mysis* in the Okanagan Lake food web: a time-series analysis of interaction strengths in an invaded plankton commu-

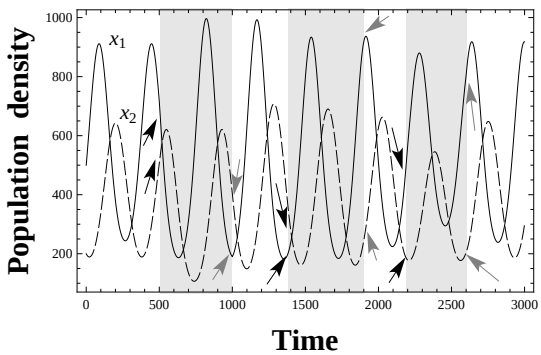

(a) 2-variable ND solutions with three external perturbations. The rhythm of x_1 and x_2 recovers from several perturbations. Gray backgrounds represent periods of perturbations.

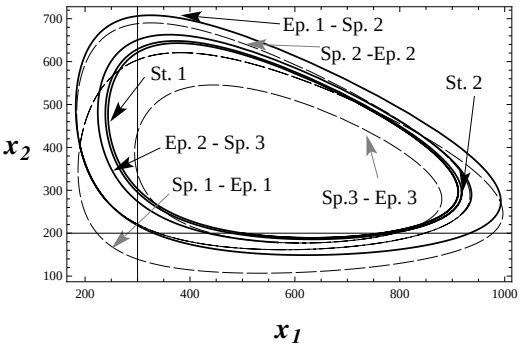

(b) Phase-space transitions of x_1 and x_2. Dashed lines represent solutions, x_1 and x_2, during perturbations. Solid line represent solutions without perturbations.

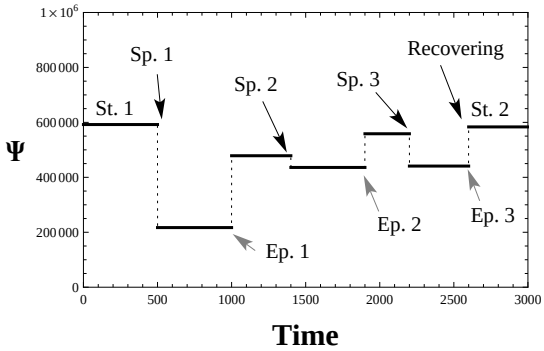

(c) Conservation law Ψ with three perturbations. It recovers from three perturbations. $\Psi \simeq 60000$ in the St. 1 and St. 2.

Figure 4.6: Several external perturbations and recoveries.

nity' [111]. Although the food-web in Okanagan Lake is not clarified definitely, mysis introduction to lakes is known as an effective method to enhance ecological interactions and its strengths among microbes and other creatures so as to increase fisheries productions.

The time-series of dominant crustacean zooplankton densities in Okanagan lake has been measured monthly and suggested that mysis and zooplankton populations are synchronous and characterized by the cycle of the peak and bottom population densities. The cycles of population densities are primarily due to cycles of season and climate and then to mutual interaction of microbes. The analysis of microbes suggests that the density-dependent and delayed population regulation of microbes is evident. In addition to the seasonal factors, the regular cycles and the delayed peak and bottom populations densities of microbes are the results of strong nonlinear interactions of species. We numerically examined changes of population densities of microbes by employing the 2-variable conserved ND model.

The current conserved nonlinear model shows that the interacting species designate a *standard rhythm* of the peak and bottom population densities. There are some fluctuations at the peak and bottom densities, but they show the stable dynamic life as demonstrated in Figure 4.6 (a) ~ (c). Although, normal

peak and bottom densities can be readily explained by adjusting coupling strength of model's internal interactions, a sudden change of maxima which is often encountered in a biological data cannot be easily simulated by only adjusting internal coupling constants in the 2-variable nonlinear interacting model.

In Figure 4.6, several perturbations are exerted on the interacting 2-variable system. The first external perturbation starts at $t = 500$ (Sp. 1) and ends at $t = 1000$ (Ep. 1). The strength of perturbations in Sp. 1-Ep. 1 are $f_1 = -800$, $f_2 = -100$. The second external perturbation starts at $t = 1400$ (Sp. 2) and ends at $t = 1900$ (Ep. 2). The strengths of perturbations in Sp. 2-Ep. 2 are $f_1 = -50$, $f_2 = -120$. The third external perturbation starts at $t = 2200$ (Sp. 3) and ends at $t = 2600$ (Ep. 3). The strength of perturbations in Sp. 3-Ep. 3 is set as $f_1 = -500$, $f_2 = -50$. The lines (x_1, x_2) may represent for instance, the prey-predator interactions, species of food-chain, and species interacting with its environmental factors (temperature or some environmental effects). Black arrows are starting point of perturbations, and gray arrows are the end of perturbations; parameters are listed in Table 1 (Condition 1). The time period is within $t = 4000$, initial values are $x_1 = 500$, $x_2 = 300$.

The significant properties of the stable nonlinear conserved system are that if external perturbations are not large enough to disintegrate the system, the system will find a stable conserved solution near the original system and continue a stable cycle (maxima and minima). It is clearly seen from (x_1, x_2)-phase space solutions in Figure 4.6(b). The system recovers from several external perturbations.

The numerical analysis can be applied to examine the change of population densities of microbes. For example, the time-series data of dominant crustacean zooplankton densities in the Figure 2 of the refernece '*Mysis* in the Okanagan Lake food-web ', show that the sudden maxima of dominant zooplankton densities are seen in the period '99 ∼ '02. The sudden increase of the peak is readily adjusted when an external perturbation is assumed in the simulation, however, it is not reproduced by adjusting internal coupling constants in the 2-variable nonlinear model. Hence, it is concluded in the 2-variable model that there would have been certain positive external perturbation to the system of microbes in Okangan Lake during '98 ∼ '01 considering a time-delay of external perturbations.

It is interesting to check what kind of external or internal perturbations is affecting the peak of population density during the period '98 ∼ '01. If there are no explicit changes in external or internal factors during the period, a sudden increase of the peak could be a result of more complex internal interactions. For example, the rhythm of the peak and bottom population densities should be explained by 4-variable or 6-variable nonlinear interactions of microbes. The unusual rhythm indicates how exogenous (environmental) and endogenous (internal interactions) variables are affecting the dynamics of each component and environmental nature related to the species. The analysis of nonlinear model suggests that the sudden peak and bottom densities have important information on the dynamics of the system of species and environment. Hence, it is important to understand the *standard rhythm* of the peak and bottom population densities in order to distinguish them from unusual maxima and minima.

One should be careful that a positive perturbation on one of interacting species not only enhances the peak of maxima but also decreases minima in the rhythm of species. It is often true that the effect of enhancement is usually emphasized without taking care after negative effects. Hence, the enhancement of the number of population of a specific species may be harmful to other species in the food-web and consequently it endangers itself. Our analyses in Figure 4.4 and 4.5 show that if we carefully control the increase or decrease of the population of certain species after introduction of a positive effect, we can keep normal and stable dynamics of species suitable for the environment. For this purpose, it is essential to explicitly understand the *standard rhythm* from real observed data.

4.3.2 Population regulation in Canadian lynx and snowshoe hare

It is difficult to identify population regulation mechanisms about prey-predator patterns of large mammals because the large mammal's life span is relatively long compared with microbes. The prey-predator cycle such as wolves and caribous takes some decades of years to observe, their interacting relation and behaviors have been recently revealed with modern technology (GPS-colored animals) [122]. However, the food-web configuration between snowshoe hare and Canadian lynx is well-known prey-predator type phenomena, and a ten-year cycle of Canadian lynx was examined from the data of Canada lynx fur-trades return of the Northern Department of the Hudson's Bay Company (the data are from C. Elton and M. Nicholson [21]).

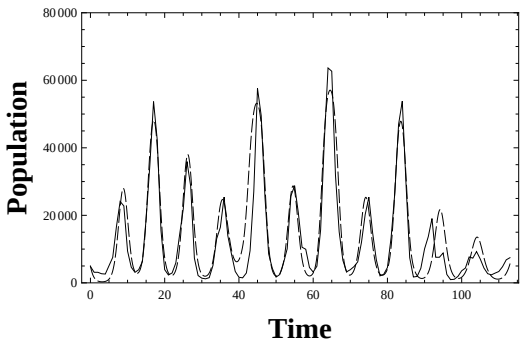

(a) The 2-variable ND simulation of Canadian lynx population. The solid line represents Canadian lynx population [21], and the dashed line represents a theoretical solution of 2-variable ND with several perturbations.

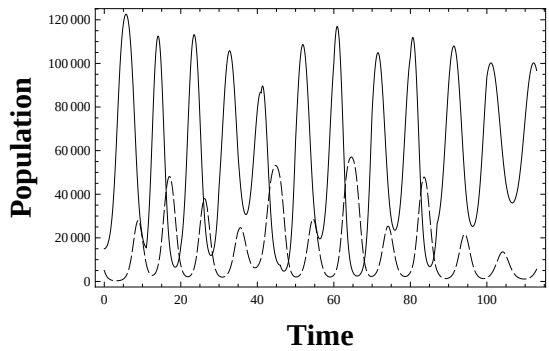

(b) The estimated population of Canadian lynx and snowshoe hare. The dashed line represents Canadian lynx population simulated by 2-variable ND model with perturbations, and the solid line represents approximate population of snowshoe hare.

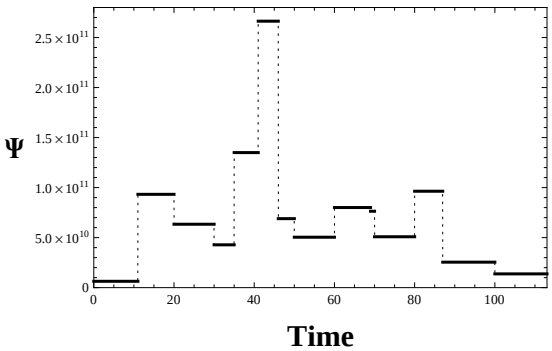

(c) Transition of conservation law Ψ with respect to time. Several perturbations are introduced.

Figure 4.7: Simulation of Canadian lynx and snowshoe hare.

The Canadian lynx and snowshoe hare have a synchronous ten-year cycle in population numbers [121,122]. The fundamental mechanisms for these cycles are maintained by the important factors such as nutrient, predation and social interactions [63]. In addition to the important factors, the nonlinear model with conservation law suggests that species of a system consequently find a strategy or a mechanism to

survive for long-time periods. In other words, the cycle of population density is a manifestation of the strategy or mechanism to survive, which is suggested by stability of phase-space solutions determined by conservation law of a system.

The nonlinear interactions with conservation law show a *standard rhythm* and stability from external perturbations as shown in Figure 4.6. The feeding and nutrient experiments in [63] are considered as external perturbations to the system. As shown in Figure 4.6, the perturbations cause certain effects on the system, but the system will find a rhythm to maintain the dynamics of species, which is not so different from the original *standard rhythm*. Our numerical results agree with conclusions derived from feeding experiments and nutrient-addition experiments. Therefore, we propose that the properties of the system which has a conservation law should be a key to understand the unanswered question: why do these cycles exist?

The results of computer simulations show that the timing of perturbation leads to different results. This is also confirmed by the feeding experiment of snowshoe hare: " ... during the peak of the cycle in 1989 and 1990 had no impact on reproductive output ... however, during the decline phase in 1991 and 1992, the predator exposure plus food treatment caused a dramatic increase in reproductive output ..." [63]. This fact can be examined in our model calculations. The perturbation in the peak phase does not cause large effects on *standard rhythm*, but negative and positive perturbations during a decreasing or increasing phase induce dramatic effects.

The cycle of *standard rhythm* for Canadian lynx and snowshoe hare indicates that the stable dynamical system of lynx and hare functions normally and environmental nature is conserved in reasonable conditions. However, as we have shown in Figure 4.4(c) and 4.4(d), if a strong negative perturbation is applied persistently for a long period, the system would fall into a danger of extinction. The important results of our simulation tell that before a system gets in danger of extinction, the *standard rhythm* of the system will tend to become ambiguous or disappear. Hence, if we carefully observe the *standard rhythm* of a specific system of species, we could help the dynamical system save and preserve related natural environment.

In Figure 4.7, we simulated the Canadian lynx data of the Hudson's Bay Company from 1821 to 1910, which is approximately thought as the lynx-population density. The interpolated Elton's data was downloaded from `http://www.atomosyd.net/spip.php?action=dw2_out&id=42`. The solid-line in Figure 4.7(a), is lynx-population data and the dashed-line is the results of our numerical simulation using 2-variable nonlinear interactions between lynx and snowshoe hare (Figure 4.7(b)). Based on parameters of the classical Lotka-Volterra equation, we introduced external perturbation f_1 to fit 2-ND model to the Canadian lynx data (see, Table 2 and Table 3). The nonlinear coefficients α_1-α_8 are fixed for all time. The conserved binary-coupled model tells that there should have been some external perturbations, although we cannot make sure at the present what kinds of external perturbations were exerted. The actual population density of snowshoe hare is not known, and so we assumed a reasonable population density and several external perturbations for numerical simulations in order to fit the lynx population data.

Table 2: The list of nonlinear coefficients of simulation in Figure 4.7.

α_1	α_2	α_3	α_4	α_5	α_6	α_7	α_8
1.0	635.0	-0.35	700.5	300.5	-0.35	-0.0068	-0.016

Table 3: The list of external perturbations in Figure 4.7. The periods of positive and negative perturbations to numerically simulate Canadian lynx population. Note that the values of f_1 have the meaning of velocity (number/time).

Perturbation	Time	Strength of f_1
Sp. 1 - Ep. 1	$0 \leq t \leq 11$	-11000000
Sp. 2 - Ep. 2	$20 \leq t \leq 30$	-4000000
Sp. 3 - Ep. 3	$30 \leq t \leq 35$	-12000000
Sp. 4 - Ep. 4	$35 \leq t \leq 41$	-8000000
Sp. 5 - Ep. 5	$41 \leq t \leq 46$	4200000
Sp. 6 - Ep. 6	$50 \leq t \leq 60$	-9000000
Sp. 7 - Ep. 7	$60 \leq t \leq 69$	1140000
Sp. 8 - Ep. 8	$70 \leq t \leq 80$	-11000000
Sp. 9 - Ep. 9	$87 \leq t \leq 100$	-14500000
Sp. 10 - Ep. 10	$100 \leq t \leq 113$	21500000

The snowshoe hare gets several positive and negative perturbations, but the overall rhythms of lynx and hare are not altered. As suggested by in Figure 4.6(b), the phase-space of lynx and snowshoe hare is stable against several external perturbations. This is also compatible with the empirical fact that the ten-year cycle in snowshoe hare is resilient to a variety of natural disturbances from forest fires to short-term climatic fluctuations. However, as shown in our model calculation in Figure 4.4(c), a long-term (more than ten years) negative perturbations and a vast environmental change that humans could cause would definitely endanger the *standard rhythm* of snowshoe hare, lynx and related species.

4.4 Conservation law for Turing pattern

In this section, we refer to the application of our methods in this thesis for Reaction-Diffussion systems and Turing model. The emergence of spatio-temporal patterns in biological systems such as the skin of the marine angelfish, zebras and butterflies are observed in nature, and studying these patterns are considered to be a primary subject not only in physics but also in other fields, such as chemistry, ecology and economy. One of the remarkable models to express spatiotemporal patterns is Turing model defined as a reaction-diffusion system by using partial differential equations. Moreover, Turing patterns have stability and characteristic phenomena to maintain these patterns from external perturbations or damages. It is shown that the skin of the marine angelfish Pomacanthus could recover stripe patterns from external damages and the corresponding Turing model could correctly predict future patterns. In our previous research, we showed that there exists a conservation law in nonlinear interacting systems such as competitive systems, and the competitive systems with a conservation law have stability and restoration phenomena from external effects. In this section, we try to construct a conservation law from Turing model directly, since we hypothesize that stable spatio-temporal patterns in biological systems are relevant to a conservation law. We apply Lagrangian approach and Noether's theorem for reaction-diffusion types of partial differential equation systems and examine the condition for emergent patterns in terms of conservation law. The emergences of patterns are also explained from the perspective of a conservation

law and deterministic approaches. In addition, we try to show the condition of parameters to produce Tuirng patterns explicitly. It is known that spontaneous emergence of patterns in animals and morphogenesis are relevant to Reaction-Diffusion systems proposed by A. M. Turing [129]. Reaction-Diffusion system can predict pattern in *Pomacanthus* and restoration phenomena. However, reaction-Diffusion system has sometimes unrealistic solutions and sensitive to changing parameters. In our research, we try to apply Lagrangian approach for Turing models to fit realistic phenomena.

4.4.1 Noether's theorem for the system of partial differential equations

Lagrangian and Noether's theorem for the system of partial differential equations are defined as follows

$$-E_k(\xi_s^k - \dot{x}_\alpha^k \tau_s^\alpha) = \frac{\partial}{\partial t^\alpha}\left[\left(\mathcal{L}\delta_\beta^\alpha - \dot{x}_\beta^k \frac{\partial \mathcal{L}}{\partial \dot{x}_\alpha^k}\right)\tau_s^\beta + \frac{\partial \mathcal{L}}{\partial \dot{x}_\alpha^k}\xi_s^k\right] \quad (s = 1, \ldots, r). \tag{4.9}$$

where E_k is the Euler-Lagrange equation for the system of partial differential equations. In the current analysis, we consider $\alpha = 1$ (for time transformation).

4.4.2 Conservation law for Reaction-Diffusion system

In this study, we tried to construct conservation law for linear type of Reaction-Diffusion system as follows

$$\begin{aligned} \frac{\partial u}{\partial t} &= a_5 u + a_3 u + a_8 - a_6 \Delta u, \\ \frac{\partial v}{\partial t} &= -a_3 v - a_4 u - a_7 + a_6 \Delta v, \end{aligned} \tag{4.10}$$

and its respecitive conservation law is given as follows

$$\Psi_1 \equiv a_3 uv + a_4/2u^2 + a_5/2v^2 + a_6 \frac{\partial u}{\partial x} \cdot \frac{\partial v}{\partial x} + a_7 u + a_8 v.$$

Using explicit method, we tried to simulate u, v and Ψ_1 In the one dimentional case, we could get the soulutions of u, v and Ψ_1, and Ψ_1 became constant with respect to time and space. It is observed that $u(t, x)$ and $v(t, x)$ oscillate with respect to time, and Ψ_1 is constant with respect time and space. As well as the case of one dimensional case, we tried to calculate in the case of two dimensional case as follows. Based on the parameters on the model which we derived, we could obtain spatial-strip pattern. In this analysis, We could derive conservation law for Turing models using Noether's theorem and found that the parameters in Reaction-Diffusion system have restricted conditions when the system has conservation law. Although the condition for parameters are not consistent to Turing models, spatial-temporal pattern are observed. We also observed oscillation phenomena like the system of ordinary differential equations in one-dimensional case. In two-dimensional case, the Ψ_1 are constant with respect to time when initial conditions for $u(t, x, y)$ and $v(t, x, y)$ are uniform and constant. However, if we choose random values for initial conditions for $u(t, x, y)$ and $v(t, x, y)$, Ψ_1 are not constant with respect to time.

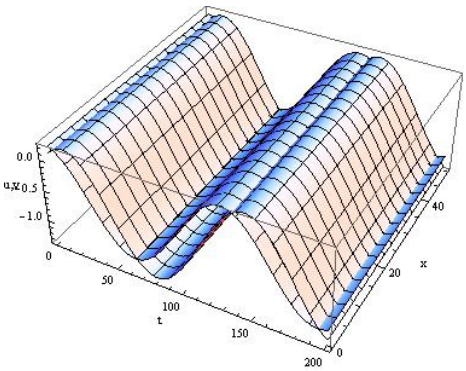

(a) Solution of $u(t,x)$, $v(t,x)$.

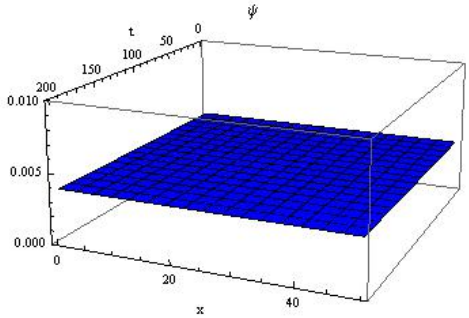

(b) Solution of Ψ_1.

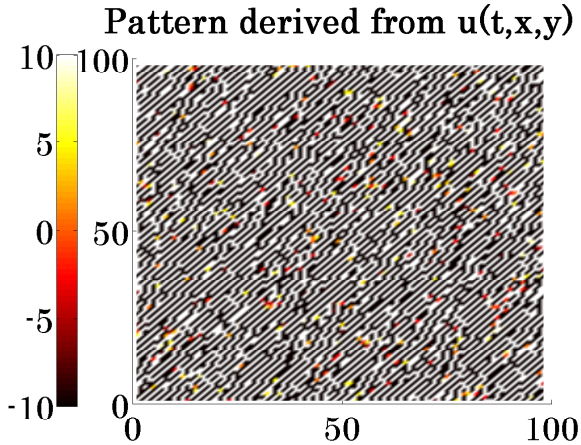

(c) Spatial pattern by $u(t,x,y)$

4.5 Concluding remarks

In this chapter, we examined characteristic properties of several ecological systems based on conserved nonlinear interactions which include generalized Lotka-Volterra type prey-predator, competitive interactions. In Section 4.2.1, we extended our $2n$-variable ND model by including external perturbations in order to apply the model to more realistic biological phenomena and to study responses of a biological system to external perturbations.

We simulated external positive and negative perturbations by employing piecewise constant terms in our nonlinear equations. As it is discussed in the analysis, the results of simplified perturbations agreed with the experiments and empirical data reasonably well. The numerical simulations showed the existence of the *standard rhythm* which is characteristic to a nonlinear conserved system. It is essential to understand *standard rhythm* by observing and taking data of a system so that we can distinguish unusual maxima and minima from *standard rhythm*. This gives a possibility to examine signatures that distinguish internal effects from external ones.

The ten-year cycle of lynx and hare is a very interesting biological phenomenon. Though a cycle of a biological system should be a phenomenon composed of complex and multi-biological interactions, the 2-variable BCF analysis has revealed the interesting results on properties of the biological phenomena. The ten-year cycle of lynx and hare is stable and resilient to external perturbations, which is reproduced in our model calculations. The system with conservation law shows stable cycles and recovering phenomena, which are displayed numerically in phase-space solutions. The stability and conservation law are constructed at least by binary-coupled species in biological and ecological systems, and they are maintained in a more complicated multi-coupled system, as we proved in a general form [130].

The coupling constants of interacting species expressed in nonlinear differential equations are considered to have been determined in a long time by complicated environmental and internal factors of a specific system, such as the landforms, seasons, climate and temperature. Once members and structures of dynamical systems were constructed, appropriate dynamical systems would be maintained for long-time periods with internal factors such as nutrient, predation and social interactions. The predation and social interactions are expressed as complicated nonlinear relations in mathematical terms. This may be explained by the fact that members of a system have a well-conserved rhythm respectively and these rhythms also have a well-determined slight delay to each other, which indicates that certain nonlinear interactions among members exist.

The important factors (nutrient, predation and social interactions) are needed for all species to survive in nature, but they easily change by natural conditions. In addition, an unusual increase of population numbers of a species would endanger the survival of a species itself as well as other species (see the numerical simulations in Figure 4.4). The important property of the nonlinear model with conservation law is that the binary-coupled system can have the persistent stability and recovering strength to external perturbations. As a predator needs a prey for its food, a prey needs a predator for the conservation of their own species. The conservation law and rhythm of species are considered to be constructed by species and natural conditions in a system for a long time, and hence, the cycle (rhythm) of species would be interpreted as a manifestation of the survival of the fittest to the balance of a biological system.

Chapter 5

Model of expected impact degree for multiple knockouts

5.1 Background

The features of stability, robustness and symmetry are essential to understand and control natural systems. It is well known that complex network systems in nature have several properties such as stability, robustness, scalability and adaptability to external effects and robustness is a key feature in the analysis of complex systems, especially for complex biological systems. Many organisms have strong adaptability to external environmental effects or changes, and they can survive if some of their genes are mutated. Understanding the origin of stability and robustness of cells has become an important topic.

The system of metabolic network has robust structure and the robustness is measured by impact degree [93, 123]. Impact degree is defined as the number of reaction inactivated by artificial knockouts of specific reactions in metabolic networks. The efficient method to calculate impact degree that of large scale metabolic network is recently proposed and investigated [124]. However, it takes much computational times and costs to find precise impact degree with multiple knockouts more than 3 because of computational complexity.

In this study, we develop a model of expected impact degree using recurrence and difference equation to estimate the impact degree with multiple knockouts and evaluate which model is suitable for simulating the expected impact degree for multiple knockouts. There are several methods to handle discrete network system such as boolean dynamics [45]. We propose a model of discrete recurrence equations inspired by branching process and percolation.

5.2 Defenition of Impact degree

Impact degree is one of the measurements to evaluate the importance of a reaction in a certain metabolic network quantifying damage spreads by artificial knockouts of reaction nodes. It was proposed by Jiang *et al.* as a measure of the importance of each reaction in a metabolic network and defined as the number of inactivated reactions caused by the knockout of a single reaction. Recently, the definition of impact degree is extended for including cycles using maximal valid assignment since it is found that the effects of cycles in metabolic networks play important roles.

Let consider a network system with sets of vertex $V_c = \{C_1, \ldots, C_m\}$ and $V_r = \{R_1, \ldots, R_n\}$, where $V_c \cap V_r = \{\}$, which express sets of compound nodes and reaction nodes respectively. A metabolic network is defined as a bipartite directed graph $G(V_c \cup V_r, E)$ in which each edge is directed either from a node in V_c to a node in V_r, or from a node in V_r to a node in V_c. Each reaction and compound take one of the two states as 0 or 1, where 0 and 1 correspond to inactive and active state of reactions or compounds. The calculation of impact degree is defined as following rules.
(i) A reaction is inactivated if any of its consumed or produced compound is inactivated.
(ii) A compound is inactivated if all of its consuming reactions or all of its producing reactions are inactivated. That is to say, the state of reaction and compound nodes at time t are determined as following equations,

$$\begin{cases} R_i(t+1) = C_1(t) \wedge C_2(t) \wedge \cdots \wedge C_m(t), \quad (i = 1, \ldots, n), \\ C_j(t+1) = (R_1^p(t) \vee R_2^p(t) \vee \cdots \vee R_n^p(t)) \wedge (R_1^c(t) \vee R_2^c(t) \vee \cdots \vee R_n^c(t)), \quad (j = 1, \ldots, m), \end{cases} \tag{5.1}$$

where $R_1^p, \ldots$ and $R_1^c, \ldots$ are producing reactions and consuming reactions of compound C_j, respectively.

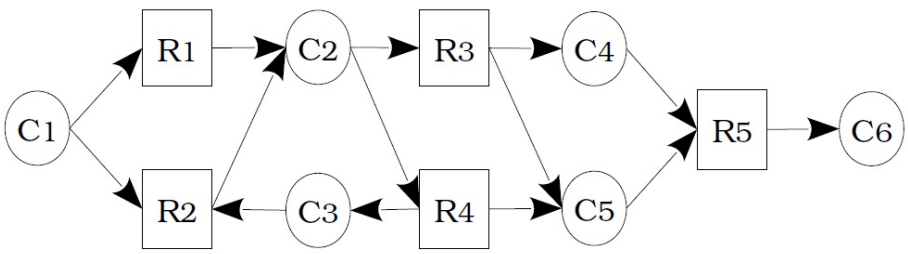

Figure 5.1: The model of metabolic network.

$$\begin{aligned} R_1(t+1) &= (C_1(t) \wedge C_2(t)), & C_1(t+1) &= R_1(t) \vee R_2(t), \\ R_2(t+1) &= (C_1(t) \wedge C_3(t)) \wedge (C_2(t)), & C_2(t+1) &= (R_1(t) \vee R_2(t)) \wedge (R_3(t) \vee R_4(t)), \\ R_3(t+1) &= C_2(t) \wedge (C_4(t) \wedge C_5(t)), & C_3(t+1) &= R_4(t) \wedge R_2(t), \\ R_4(t+1) &= C_2(t) \wedge (C_3(t) \wedge C_5(t)), & C_4(t+1) &= R_3(t) \vee R_5(t), \\ R_5(t+1) &= (C_4(t) \wedge C_5(t)) \wedge C_6(t), & C_5(t+1) &= (R_3(t) \vee R_4(t)) \wedge R_5(t), \\ & & C_6(t+1) &= R_5(t), \end{aligned} \tag{5.2}$$

Table 5.1: The transition of impact in a metabolic network for R_5 knockout.

	R_1	R_2	R_3	R_4	R_5	C_1	C_2	C_3	C_4	C_5	C_6
$t = 0$	1	1	1	1	1	1	1	1	1	1	1
$t = 1$	1	1	1	1	0	1	1	1	1	1	1
$t = 2$	1	1	1	1	0	1	1	1	0	0	0
$t = 3$	1	1	0	0	0	1	1	1	0	0	0
$t = 4$	1	1	0	0	0	1	0	0	0	0	0
$t = 5$	0	0	0	0	0	1	0	0	0	0	0
$t = 6$	0	0	0	0	0	0	0	0	0	0	0

Table 5.2: The transition of impact in a metabolic network for R_4 knockout.

	R_1	R_2	R_3	R_4	R_5	C_1	C_2	C_3	C_4	C_5	C_6
$t = 0$	1	1	1	1	1	1	1	1	1	1	1
$t = 1$	1	1	1	0	1	1	1	1	1	1	1
$t = 2$	1	1	1	0	1	1	1	0	1	1	1
$t = 3$	1	0	1	0	1	1	1	0	1	1	1

5.3 Model of expected impact degree

5.3.1 Expect impact degree with fixed coefficients for infinite network systems

Let I_n be the expected impact degree under n knockouts of reaction nodes, then we have the following recurrence equation,

$$I_n = \begin{cases} 0 & (n = 0), \\ \alpha + \beta \sum_{i=0}^{n'} p_n^i I_i & (n \geq 1), \end{cases} \tag{5.3}$$

where α and β expresses constant or arbitrary function and p_n^i express a coefficient or probability that I_n have I_i trees under the number of n knockouts. The n' denotes maximum infected trees caused by n knockouts.

If β and p_n^i take constant value as $\beta = 1$ and $p_n^i = \mu$, it is possible to solve the (5.3) in any value of n' using generating functions approach. The approach using generating function is well known and used in the complex networks theory [95, 135]. We define generating function $f(x)$ for the expected impact degree I_k which means expected impact degree under k-th knockout nodes. The generating function of expected impact degree is given as follows,

$$f(x) = \sum_{k=0}^{\infty} I_k x^k. \tag{5.4}$$

We can derive analytical solutions under the condition of $n' = n$ of (5.3) as follows using Taylor expansion. Therefore, we get the analytical solution of expected impact degree (5.3) I_n as

$$I_n = \frac{1}{\mu}\{\frac{1}{(1-\mu)^n} - 1\}, \ (\mu \neq 1). \tag{5.5}$$

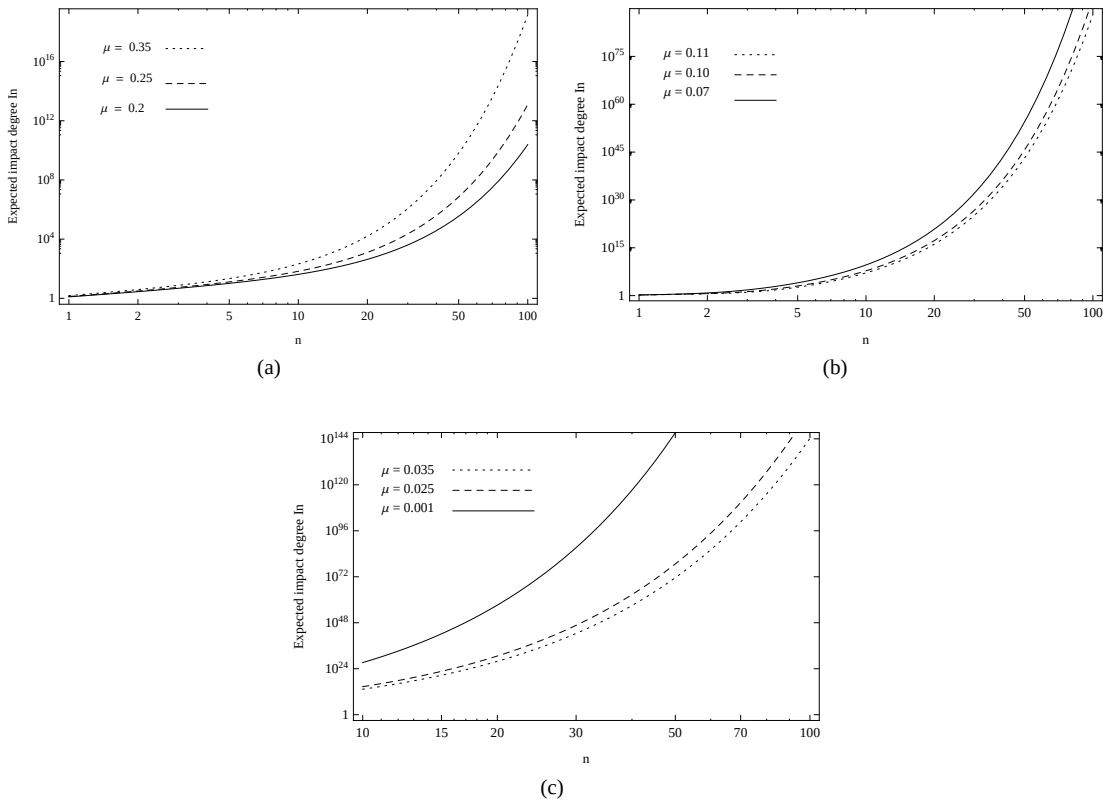

Figure 5.2: The solutions of expected impact degree I_n.

The solution increase exponentially with respect to n and μ. As the same approach, if $n' = n + 1$ the solution of expect impact degree with n-th knockout is obtained as follows,

$$\begin{aligned} I_n = & \frac{\mu c_1}{r_+ - r_-}\Big\{\Big(\frac{1}{r_-^n} - \frac{1}{r_+^n}\Big) - \Big(\frac{1}{r_-^{n-1}} - \frac{1}{r_+^{n-1}}\Big)\Big\} \\ & - \frac{1}{r_+ - r_-}\Big\{\frac{1}{r_- - 1}\Big(1 - \frac{1}{r_-^{n-1}}\Big) + \frac{1}{r_+ - 1}\Big(1 - \frac{1}{r_+^{n-1}}\Big)\Big\}, \end{aligned} \tag{5.6}$$

where $r_+ = (1 + \sqrt{1 - 4\mu})/2$, $r_- = (1 - \sqrt{1 - 4\mu})/2$, $I_0 = 0$, $I_1 = c_1$. Note that expected impact degree

with n-th knockout is $I_n > 0$ and real value. If $n' = n + 2$,

$$\begin{aligned}
I_n =& \frac{1}{(1-\alpha_3)(\alpha_1-\alpha_2)}\Big\{\frac{1}{\alpha_1-1}\Big(1-\frac{1}{\alpha_1^{n-2}}\Big)-\frac{1}{\alpha_2-1}\Big(1-\frac{1}{\alpha_2^{n-2}}\Big)\Big\} \\
&-\frac{1}{1-\alpha_3}\Big\{\frac{1}{\alpha_1-\alpha_2}\Big(\frac{1}{\alpha_2^{n-2}}-\frac{1}{\alpha_1^{n-2}}\Big)-\frac{1}{\alpha_2-\alpha_3}\Big(\frac{1}{\alpha_3^{n-2}}-\frac{1}{\alpha_2^{n-2}}\Big)\Big\} \\
&+\frac{\mu c_1}{\alpha_1-\alpha_3}\Big\{\frac{1}{\alpha_1-\alpha_2}\Big(\frac{1}{\alpha_2^{n}}-\frac{1}{\alpha_1^{n}}\Big)-\frac{1}{\alpha_2-\alpha_3}\Big(\frac{1}{\alpha_3^{n}}-\frac{1}{\alpha_2^{n}}\Big)\Big\} \\
&-\frac{\mu c_1}{\alpha_1-\alpha_3}\Big\{\frac{1}{\alpha_1-\alpha_2}\Big(\frac{1}{\alpha_2^{n-2}}-\frac{1}{\alpha_1^{n-2}}\Big)-\frac{1}{\alpha_2-\alpha_3}\Big(\frac{1}{\alpha_3^{n-2}}-\frac{1}{\alpha_2^{n-2}}\Big)\Big\} \\
&+\frac{\mu c_2}{\alpha_1-\alpha_3}\Big\{\frac{1}{\alpha_1-\alpha_2}\Big(\frac{1}{\alpha_2^{n-1}}-\frac{1}{\alpha_1^{n-1}}\Big)-\frac{1}{\alpha_2-\alpha_3}\Big(\frac{1}{\alpha_3^{n-1}}-\frac{1}{\alpha_2^{n-1}}\Big)\Big\} \\
&+\frac{\mu c_2}{\alpha_1-\alpha_3}\Big\{\frac{1}{\alpha_1-\alpha_2}\Big(\frac{1}{\alpha_2^{n-2}}-\frac{1}{\alpha_1^{n-2}}\Big)-\frac{1}{\alpha_2-\alpha_3}\Big(\frac{1}{\alpha_3^{n-2}}-\frac{1}{\alpha_2^{n-2}}\Big)\Big\},
\end{aligned} \tag{5.7}$$

where $I_1 = c_1$, $I_2 = c_2$. The coefficients α_1, α_2 and α_3 are solutions of a cubic equation defined as $x^3 - x + \mu = 0$, which is derived from generating function.

5.3.2 Model of expected impact degree for multiple knockouts with effects of finite size

We consider the model of expected impact degree with effects of size of network. The solution of I_m increases exponentially with m. In this case, the expected impact degree of multiple impacted degree are larger than sum of the expected impact degree with single impacted degree. Therefore, we include the nonlinear effects of size of network system and consider the model described as follows.

$$I_n = \begin{cases} 0 & (n = 0), \\ n + \kappa n(N-n)/N \displaystyle\sum_{i=0}^{N} p_n^i I_i & (n \geq 1), \end{cases} \tag{5.8}$$

where N is the size of considering network and κ is constant of proportionality. The maximum infected node n' is fixed as N for all number of knockouts n.

5.4 Evaluation of model of expected impact degree

We evaluate the model of expected impact degree using metabolic networks data sets. We can compute the impact degree with multiple knockouts by comprehensive method using SIMPLE ALGORITHM [124]. Since it is impossible to evaluate experiment with a Large-Scale network because of the computational complexity, we use the subnetwork *E. coli*, *B. subtilis*, *S. cerebisiae* and *H. sapiens* from KEGG database. We experienced the eco00010.xml, eco00020.xml and eco00030.xml, bsu00010.xml, bsu00020.xml and bsu00030.xml, sce00010.xml, sce00020.xml and sce00030.xml, hsa00010.xml, hsa00020.xml and hsa00030.xml respectively. Using SIMPLE ALGORITHM, it is able to derive the expected impact degree of multiple knockouts $n \simeq 30$.

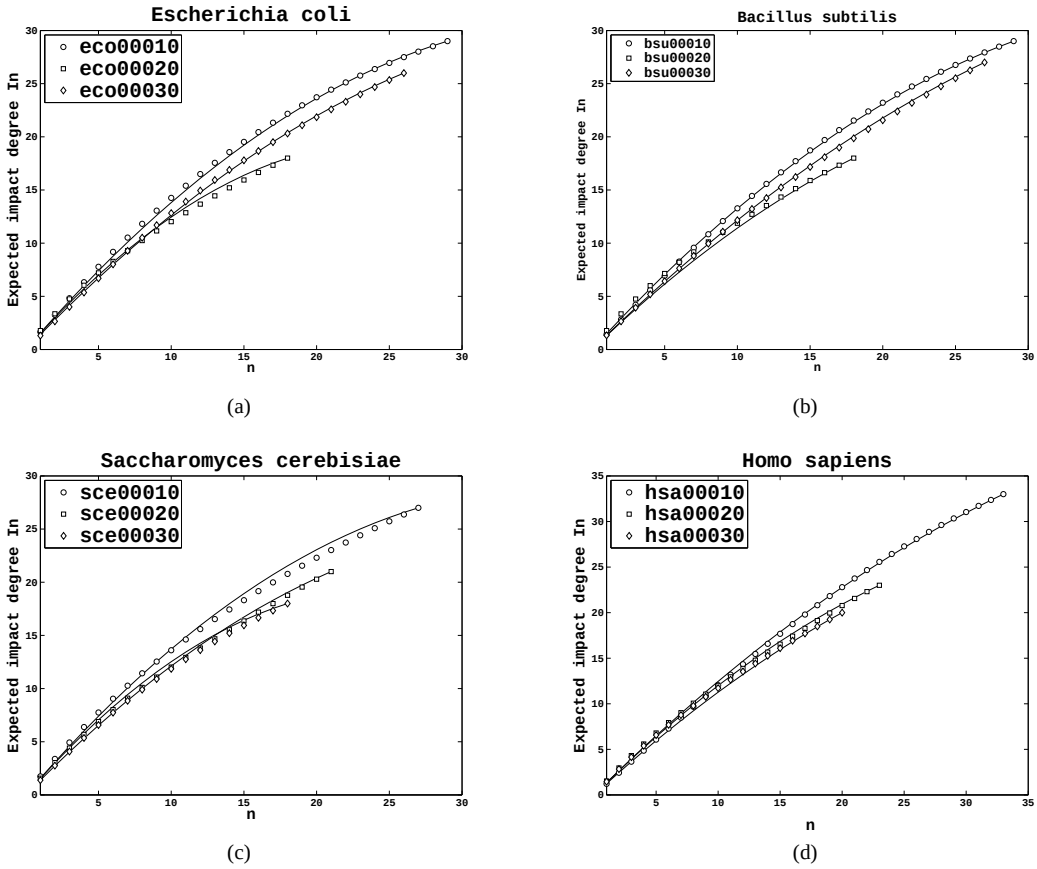

Figure 5.3: The solutions of expected impact degree I_n for subnetworks.

5.5 Concluding remark

In this chapter, we proposed the model of expect impact degree using simple recurrence equations inspired by branching process and compared to data of metabolic network from KEGG database. We compare the model of expected impact degree with finite size effects of network system and the model with infinite size of network. Through computational experiments, it is observed that the model of expected impact degree with finite size effects well fits to the changing of impact degree of metabolic network from KEGG database. We can predict the expected impact degree for full metabolic networks for arbitrary n using the model of expected impact degree and reaction network extracted from KEGG database.

It is found that the solutions of expected impact degree increases linearly until knockouts of half size of whole metabolic network. However, the solutions of expected impact degree reach the limit with convex curve when we give knockouts more than half size of whole metabolic network. These phenomena are observed in both partial metabolic network and complete metabolic network. The damage expansion rates take highest value when we give knockouts half size of considering metabolic network.

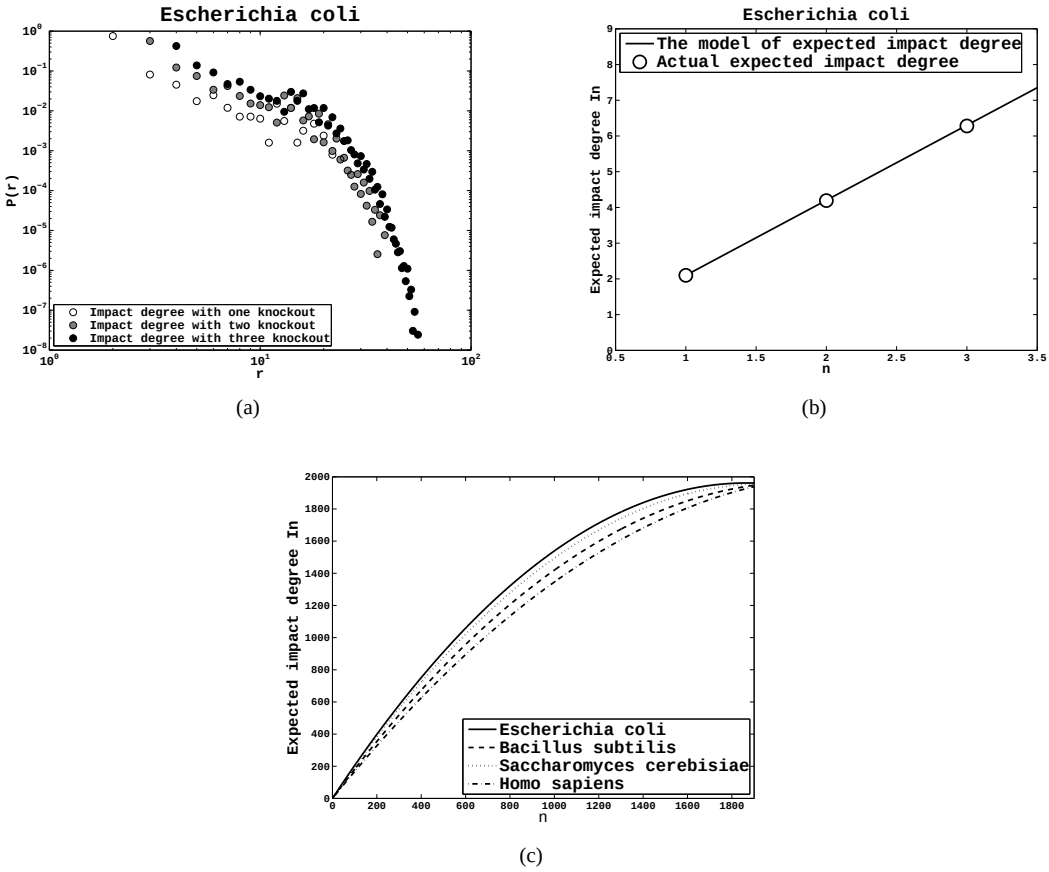

Figure 5.4: The solutions of expected impact degree I_n for metabolic networks for all data set.

The solution of expected impact degree with finite network size and KEGG database show convex curve with respect knockouts.

It tells us data of metabolic networks obtained from KEGG database have properties of scalability and symmetric structure. Although we need to evaluate importance of each reaction for metabolic network, the numerical experiments of expected impact degree and KEGG database showed scalability of metabolic network for both eucaryote and prokaryote from perspective of network systems. It indicates that we can obtain valuable results of experiments concerning partial metabolic network without examining whole metabolic network data. Moreover, it supports the property that addition law of metabolic network in both theoretical and experimental case. In addition to the scalability of metabolic network from KEGG database, symmetric structures in metabolic network are also observed through the model of expected impact degree and KEGG database.

The numerical simulations of the model of expected impact degree for full metabolic networks of E. coli, B. subtilis, S. cerebisiae and H. sapiens are obtained using reaction network for arbitrary size of knockouts. In the case of whole metabolic network for each species from KEGG database, it is impossible to obtain impact degree more than 3 knockouts because of computational complexity. It is

found that the solution of the model of expected impact degree show lowest values in the case of H. sapiens. It would be related to the stability or robustness of network structure which are characteristic to each species, however, the difference between eucaryote and prokaryote are not observed.

We have investigated and discussed the model of expected impact degree with nonlinear finite size effects. The model of expected impact degree well fits to observed data from KEGG database and show qualitative behavior of metabolic network from artificial or external impact. It would be useful to evaluate the stability of considering metabolic network with arbitrary knockouts, and there would be possibility that the stability of metabolic network is related to properties of scalability and symmetric structure of metabolic network.

Chapter 6

Sector dominance ratio analysis of financial markets

6.1 Background

Economical and Financial markets are highly complex adaptive systems, resulting from multi-scale interactions amongst individuals, institutions, companies and countries [82]. To better understand the dynamics and structure of financial markets, one can draw on the tools developed in the discipline of complexity science, which has focused on the extraction of useful information for understanding and controlling dynamic interacting systems such as economic, biological, and other complex systems [10, 34, 91, 101, 117, 127, 133]. Physics-based approaches also have been proposed for avoiding and controlling systemic risks and crises in financial markets [9, 75]. While complex phenomena such as chaos generally lead to unpredictability [110], classical dynamics and quantum statistical mechanics in physics have been applied to many fields of science [112]. Such methods have been successful in analyzing information and conservation laws, and have contributed to the understanding of nonlinear and complex dynamical interacting systems that are not in a state of equilibrium [78, 130, 131].

The network approach also has been used to analyze connections between world financial markets, especially since the coupling between markets has strengthened in recent years [52]. The evolution of dependencies in the global market can be quantified by constructing the dependency network for each market [53]. At a smaller scale, the network structure of markets and the interactions and dependencies among economic sectors within national markets also can be modeled using such a structure [18]. The structure of economic sectors within each market is relevant not only to intramarket properties, but also affects the relation across markets. In addition, each market has a unique structure of economic sectors; for example, the energy and financial sectors are of relatively high importance in the U.S. stock market. Uncovering which economic sectors play a dominant role in each market is fundamental to understanding their structure.

Many methods have been applied to studying information embedded in the interactions in stock markets. One key statistically based approach is the use of empirical correlation analysis, and the analysis of empirical correlations between different financial assets [27, 51, 67]. A major contribution of statistical physics to these efforts has been the use of Random Matrix Theory (RMT) to uncover latent information embedded in the observed empirical correlations [11, 22, 48, 54, 68, 94, 99, 103, 108]. RMT is a method-

ology to evaluate the eigenvalues of empirical correlation matrices, originally developed in the field of nuclear physics by Wigner and Dirac to explain energy levels of complex quantum systems.

In their seminal work, Plerou *et al.* [99] tested the eigenvalue statistics of the empirically measured correlation matrix C, of historical returns from the U.S. stock market against the null hypothesis of a random correlation matrix. This allowed them to distinguish genuine correlations from spurious correlations that are present even in random matrices. They found that the bulk of the eigenvalue spectrum of C shares universal properties with the Gaussian orthogonal ensemble of random matrices. Further, by analyzing deviations from RMT, they showed that the largest eigenvalue and its corresponding eigenvector represent the influence of the entire market on all stocks; using the remaining deviating eigenvectors, they were able to partition stocks into distinct subsets whose identity corresponds to conventionally identified economic sectors. Finally, they introduced an approach which utilizes these results for the construction of portfolios that have a stable ratio of risk to return.

Recently, Kinlaw *et al.* [60] introduced a method to measure systemic importance using the absorption ratio and variance of eigenvectors introduced by [64], which is equal to the fraction of a market's total variance explained by a subset of important factors. This method provides the possibility to assess whether a market is fragile or resilient to shocks or external effects by examining the value of the absorption ratio. Furthermore, this tool was extended to measure the centrality of an economic sector in a given market, by the use of a centrality score.

In this chapter, we propose to extend previous work by introducing a new approach to uncover the functional dominance of economic sectors, using RMT. We propose a new indicator, the Sector Dominance Ratio (SDR), to examine economic sectoral makeup at a certain reference time interval using both raw correlation and partial correlation matrices. Here we term standard Pearson correlation coefficients [98] as raw correlations. Partial correlations are the correlation between two variables after removing the mediating effect of a third variable (see Methods section), and provides the means to uncover the nature of the hidden embedded relationships between different sectors of the market. We will introduce the SDR methodology and study the dynamic changes of SDR employing eigenvectors obtained from both raw and partial correlation matrices. The SDR uses RMT to identify the informative components of the empirical correlation matrices, and thus, unlike other factor models or principal components-based indicators, does not require making assumptions on where the meaningful system information is embedded. As such, the SDR can shed additional light into the functional structure of financial markets.

We examine the SDR for both yearly and monthly bases for raw correlation and partial correlation matrices. We apply the SDR methodology to study the structure of four different stock markets, those of the U.S., U.K., Germany, and Japan, and investigate whether the economic sectoral makeup is indeed apparent in the observed prices and their evolution over time. The information obtained from the model of SDR provides important insights into the underlying driving forces in the dynamics of real stock markets: not only the importance of each sector, but also the state of the sector and whether its activity or growth rate is increasing or decreasing. Finally, we show the SDR is useful for predicting the behavior of VIX indexes using a Granger causality and cross correlation tests for both raw and partial correlation.

The chapter is organized as follows. Section 6.2 refers to methods for the analysis of stock market data, correlation coefficients and the introduction of the RMT approach as well as the relation between RMT and the factor model. In section 6.3, we present the formal model of the SDR using components of eigenvectors for raw and partial correlations. In section 6.4, we examine the distribution of eigenvalues and the components of the largest and second largest eigenvector. We present the results obtained from

the SDR analysis in section 6.5 focusing on the sectoral content of the different markets in different time periods. We show that the method of raw and partial correlations and the model of SDR provide important information on the underlying structure of financial markets and their dynamics. Finally, we discuss the main results and conclusions in section 6.7.

6.2 Materials and methods

6.2.1 Data

We employ the daily adjusted closing price from four major stock markets (see [52]) downloaded from Thomson Reuters Datastream. For the U.S., the U.K. and Japan, we include stocks belonging to each country's most important stock indices, the S&P 500, FTSE 350, and Nikkei 500. For Germany, we start with the entire set of DAX composite shares since the DAX index has only 30 members. After filtering out stocks that did not actively trade over the entire period, we are left with 89 stocks, mainly DAX members and some stocks from the MDAX and SDAX. The number of stocks finally used for the analysis shrinks significantly when we select only stocks that trade actively from January 2000 to December 2010. We also use volume data to filter for very illiquid stocks.

Economic sectors and their market share in each country are shown in Table 6.1. Each market has unique makeup of economic sectors; for example, the energy sector is substantial in the U.S. and Japan, but not in the U.K. and Germany. The services and health care sectors have a large share in the U.K. and German markets, but not in the U.S. and Japan. The communications sector does not appear in the German stock market. We consider the percentage of representative economic sectors in Table 6.1 as benchmark values to compare with random data, and employ the data of Table 6.1 for the analysis of SDR for normalization.

Table 6.1: The table presents the number and percentage (in parentheses) of representative economic sectors in the U.S., U.K., German and Japanese stock markets. Each sector is indexed by s. The total number of stocks is 403 for U.S. stock market, 116 for the U.K., 89 for Germany and 315 for Japan.

s	Sector	U.S.	U.K.	Germany	Japan
1	Basic materials	21 (5.21%)	9 (7.76%)	4 (4.49%)	36 (11.4%)
2	Communications	29 (7.2%)	1 (0.86%)	0 (0%)	12 (3.81%)
3	Consumer goods	136 (33.8%)	12 (10.34%)	24 (27.0%)	113 (35.9%)
4	Energy	32 (7.94%)	0 (0%)	0 (0%)	2 (0.63%)
5	Financial	62 (15.4%)	33 (28.5%)	10 (11.2%)	39 (12.4%)
6	Health care	0 (0%)	4 (3.45%)	9 (10.1%)	0 (0%)
7	Industrial goods	52 (12.9%)	12 (10.3%)	11 (12.4%)	89 (28.3%)
8	Services	0 (0%)	32 (27.6%)	14 (15.7%)	0 (0%)
9	Technology	45 (11.2%)	6 (5.17%)	13 (14.6%)	19 (6.03%)
10	Utilities	26 (6.45%)	7 (6.03%)	4 (4.49%)	5 (1.59%)

6.2.2 Stock correlation metrics

The stock return $r_i(t)$ is defined as

$$r_i(t) = \log[p_i(t + \Delta t)] - \log[p_i(t)], \tag{6.1}$$

where $p_i(t)$ is the daily adjusted closing price of stock i at time t, and Δt is the time interval which is taken as $\Delta t = 1$ (1 trading day) for this analysis. The raw correlation (Pearson's correlation, [98]) coefficient between two stocks i and j is defined as

$$C(i, j) = \frac{\langle (r_i - \mu_i) \cdot (r_j - \mu_j) \rangle}{\sigma_i \sigma_j}, \tag{6.2}$$

where r_i and r_j are returns of stocks i and j, μ_i and μ_j are respective means, σ_i and σ_j are standard deviations of corresponding stocks, and the bracket $\langle\rangle$ denotes the average over time. Note that $C(i, j)$ is a symmetric square matrix and $C(i, i) = 1$ for all i.

Recently, a new method to study relationships of influence, or dependency, by using partial correlations to construct a new type of network was introduced in [49, 55]. In their study, they applied this approach to the analysis of stock relationships, and were able to uncover important information regarding the underlying dependency relationships between stocks traded on the New York Stock Exchange (NYSE). This methodology is also capable of providing important information on the evolution of the network [50] and recently, on the investigation of the immune system [77] and semantic networks [56], validating the applicability of the methodology to different types of complex systems.

Partial correlation is another useful tool to investigate correlations between two stocks. The partial correlation measures correlation between two variables after accounting for any common dependence on a third mediating variable. For stocks, we wish to measure correlation after removing the mutual dependence on a systematic economy-wide factor such as the market index. The residual, or partial, correlation between stocks i and j, after accounting for the mediating effect of the market index, m, is defined by [3, 54, 106] as:

$$\rho(i, j|m) = \frac{C(i, j) - C(i, m)C(j, m)}{\sqrt{(1 - C^2(i, m))(1 - C^2(j, m))}}, \tag{6.3}$$

where $C(i, j)$ is the raw correlation between stock i and j, $C(i, m)$ is the pairwise correlation between stock i and the mediating variable m, and $C(j, m)$ is the pairwise correlation between stock j and the mediating variable m.

While much work has made use of RMT to study empirical correlation matrices, there is very little work using RMT to investigate partial correlation matrices [54]. An important question is how similar the leading eigenvectors of the correlation matrix and the partial correlation matrix are, and what additional information is provided by the eigenvectors of the partial correlation matrix.

6.2.3 Application of Random Matrix Theory (RMT)

One important application of RMT in Finance is its use in determining the number of factors to use in a factor model. In order to assess stock returns, the factor model developed by Fama *et al.* [24] is widely

used for a multivariate system [87, 109]. The general multifactor model for $x_i(t)$ is defined as

$$x_i(t) = \left\{ \sum_{j=1}^{K} \gamma_i^{(j)} f_j(t) \right\} + \gamma_i^{(0)} \varepsilon_i(t), \tag{6.4}$$

where $x_i(t)$ is the return from stock i and $\gamma_i^{(j)}$ is a constant describing the weight of factor j in the dynamics of the variable $x_i(t)$. The maximum number of factors, which are described by the time series $f_j(t)$ is K, and the last term $\varepsilon_i(t)$ is a zero mean noise with unit variance.

The factors can be selected on theoretical ground such as interest rates for bonds, industrial production for stocks, or alternately on empirical grounds. In our approach, a factor can be also associated with each relevant eigenvalue and eigenvector; the multifactor model with eigenvalue and eigenvector is given as follows

$$x_i(t) = \sum_{h=1}^{K} \gamma_i^{(h)} \sqrt{\lambda_h}\ f^{(h)}(t) + \sqrt{1 - \sum_{h=1}^{K} \gamma_i^{(h)^2} \lambda_h}\ \ \varepsilon_i(t). \tag{6.5}$$

In this multifactor model, K is the maximum number of relevant eigenvalues and $\gamma_i^{(h)}$ is the i-th component of the h-th eigenvector of correlation matrix C. The λ_h is h-th eigenvalue and $f^{(h)}$ is defined as h-th factor. The term $\varepsilon_i(t)$ is idiosyncratic firm-specific component of returnterm. In this multifactor model, the eigenvalues which have "meaningful" information on factor $f^{(h)}$ should be included. Using RMT, we can select meaningful eigenvalues for the multifactor model by examining the number of eigenvalues deviating from λ_{max} given by Equation (2.40).

6.3 Sector dominance ratio (SDR)

We propose the following Sector Dominance Ratio (SDR) to study evolution of sectoral makeup using eigenvectors derived from empirical correlation matrices and benchmark values in Table 6.1. After ordering the eigenvalues obtained from an empirical correlation matrix as $\lambda_1 > \lambda_2 \cdots > \lambda_k > \lambda_{k+1} \cdots > \lambda_{max}$, we assess the components of the k-th eigenvector $\boldsymbol{v}_k = (v_{1k}, v_{2k}, \ldots, v_{Nk})$ corresponding to k-th largest eigenvalue deviating from λ_{max}, using SDR. The SDR, Φ_s, is given as follows

$$\Phi_s = N_\theta \sum_{i=1}^{N} \delta_{si} \theta(v_{ik} - \tau) - \varepsilon_s, \tag{6.6}$$

where s is the sector number in Table 6.1 and N is the number of stocks for each market. The N_θ is a normalization term defined as $N_\theta = 1/\sum_{i=1}^{N} \theta(v_{ik} - \tau)$. Note that threshold τ is fixed under the maximum value of component of $\boldsymbol{v}_k$, therefore, N_θ always takes finite and positive values. The second term ε_s is a normalization term defined as $\varepsilon_s = n_s/N$ where n_s is the number of stocks belonging to sector s, and values listed in Table 6.1 are applied to ε_s. The function δ_{si} is Kronecker delta function; if stock i belongs to sector s, it returns $\delta_{si} = 1$ and $\delta_{si} = 0$ otherwise. Each stock i is classified into 10 economic sector (basic materials (s=1), communications (s=2), consumer goods (s=3), energy (s=4), financial (s=5), health care (s=6), industrial goods (s=7), services (s=8), technology (s=9) and utilities (s=10)) as listed in Table 6.1.

The function $\theta(v_{ik} - \tau)$ represents a step function defined as

$$\theta(v_{ik} - \tau) = \begin{cases} 1, & (v_{ik} \geq \tau), \\ 0, & (v_{ik} < \tau), \end{cases} \tag{6.7}$$

where τ is a threshold. The function $\theta(v_{ik} - \tau)$ determines whether or not stock i has an active role in its stock market during a certain reference time. The threshold τ can be interpreted as an average value of activity of a financial market obtained from an empirical correlation matrix. If $\theta(v_{ik} - \tau)$ returns 1, the stock i is considered to play an active role at the given reference time, reflecting that the weight of the given stock in the corresponding eigenvector is larger than the activity threshold, τ. The range of SDR is $-1 \leq \Phi_s \leq 1$, and if a certain sector s plays a dominant role at a given reference time, Φ_s takes a positive value close to $\Phi_s \simeq 1$. If SDR takes a negative value close to $\Phi_s \simeq -1$, it indicates that the activity of sector s is low or declining during the given time interval. For the case of random data, it can be shown that $\Phi_s \simeq 0$ (see B.1). Here we define the threshold to be $\tau = 1/\sqrt{N}$ (for additional information, see B.2).

Defined this way, the proposed SDR measure provides new information, which is not present in either standard factor models, or RMT, or both. The SDR does not require any assumptions regarding the number of factors, rather only the num- ber of stocks in each sector. The SDR provides a quantitative, empirically based approach to study how different sectors dominate the behavior of other sectors, as reflected by their relative size in the empirical eigenvectors. The larger their size, the larger is their effect on the empirical correlations, which reflects how they in- fluence changes in the price changes of other sectors in the market. Thus, for a given sector classification system, this measure provides the means to quantita- tively monitor the difference in the contributions of the individual sectors in the real behavior of the market. This information can be used to monitor changes in individual sectors, shifts in market structure, and if needed, reconsideration of the classification scheme.

6.4 Spectral properties of similarity metrics

For each market (U.S., U.K., Germany and Japan), we calculate the empirical correlation matrix from the stock time series, and derive the eigenvalue distribution of each correlation matrix, for both raw and partial correlation. We study the numbers and values of eigenvalues deviating from λ_{max} compared to the distributions obtained from random matrices. The values of the parameters, Q, λ_{max} and λ_{min} for all markets are listed in Table 6.2.

The distributions of eigenvalues of the similarity measures from the U.S., U.K., German and Japanese stock markets are presented using raw and partial correlations in Figure 6.1. The number and percentage of empirical eigenvalues that exceed the theoretical maximal eigenvalue, λ_{max}, for the raw and partial correlations and value of parameters for distributions of a random matrix are listed in Table 6.2. Eigenvalues for the case of partial correlations for each market are more prone to exceed λ_{max}, which implies that there is more information present in these matrices, after removing the mediating effect of the market index. In the case of raw correlation, the U.K. stock market has the largest percentage of deviating eigenvalues and the Japanese stock market has the lowest percentage of deviating eigenvalues.

In factor models and financial RMT analysis, the largest eigenvalue is considered the principal eigenvalue, and its corresponding eigenvector is associated with the market mode, specifically, the general movement of the market. As such, an important question is the extent of additional information provided

Table 6.2: Value of Q, λ_{min} and λ_{max} for distribution of random matrices (2.39) derived from data for each stock market, and the number and percentage (value in parenthesis) of empirical eigenvalues which deviate from λ_{max} for raw and partial correlation matrices.

	Value of parameters			Eigenvalues deviating from λ_{max}	
Market	Q	λ_{min}	λ_{max}	Raw correlation	Partial correlation
U.S.	6.86	0.38	1.91	17 (4.22%)	26 (6.45%)
U.K.	24.0	0.63	1.45	8 (6.90%)	13 (11.2%)
Germany	31.4	0.68	1.39	6 (6.74%)	10 (11.2%)
Japan	8.57	0.43	1.80	11 (3.49%)	23 (7.30%)

by the partial correlations, after removing the mediating effect of the market index. For example, one can ask whether the largest eigenvalue of the partial correlation matrix is similar to the second largest eigenvalue of the raw correlation matrix. We observe that the largest eigenvalue of raw correlation is generally speaking $3 \sim 5$ times larger than that of the partial correlation matrix, testifying to the importance of the common market factor in driving raw correlations among stocks. The value of the principal eigenvalue is 116.0 for the U.S. stock market, 36.4 for the U.K. stock market, 23.9 for the German stock market and 105.6 for the Japanese stock market. By contrast, the value of the largest eigenvalue for partial correlation is only 35.5 for the U.S., 8.2 for the U.K., 8.9 for Germany, and 20.2 for Japan.

To further understand the additional embedded information present in the partial correlations, we examine the values of the components of the largest eigenvector for both raw correlation and partial correlation for each market. The scatter plots of weights (magnitudes) of components of eigenvectors $\boldsymbol{v}_1$ from raw and partial correlations are given in Figure 6.2. We plot each component of eigenvector $\boldsymbol{v}_1$ for both raw and partial correlations (gray circles in Figure 6.2) and compare to comparable values obtained from random data (white circles in Figure 6.2, see B.1 for more information). Using raw correlations, all components of eigenvector $\boldsymbol{v}_1$ have positive values; however, the components of the largest eigenvector derived from partial correlations contain negative values in all stock markets. Moreover, in the case of partial correlation for the U.S. and Japanese markets, there are several negative values in the components of eigenvector $\boldsymbol{v}_1$. For Germany negative value in the partial correlation principal eigenvector are also observed; however, Germany has the smallest number of such negative values. Compared to the U.S., U.K. and Japanese stock markets, Germany's stock market is not significantly influenced by its index. All components of $\boldsymbol{v}_1$ derived from the random matrix have positive values for all stocks for both raw and partial correlation.

6.5 Uncovering the sectoral makeup of financial markets

To investigate and monitor the dynamical evolution of the structure of financial markets, we apply the SDR methodology. First, we study the SDR for the entire time period. The values of the SDR, Φ_s ($s = 1, \ldots, 10$), using $\boldsymbol{v}_1$ from raw and partial correlations during the period from January 2000 to December 2010 are presented in Table 6.3. The threshold τ is given as $\tau = 1/\sqrt{N}$ where N is the number of stocks for each stock market (see also B.2 and B.3).

Table 6.3 demonstrates that implied sectoral importance can be meaningfully inferred from raw ver-

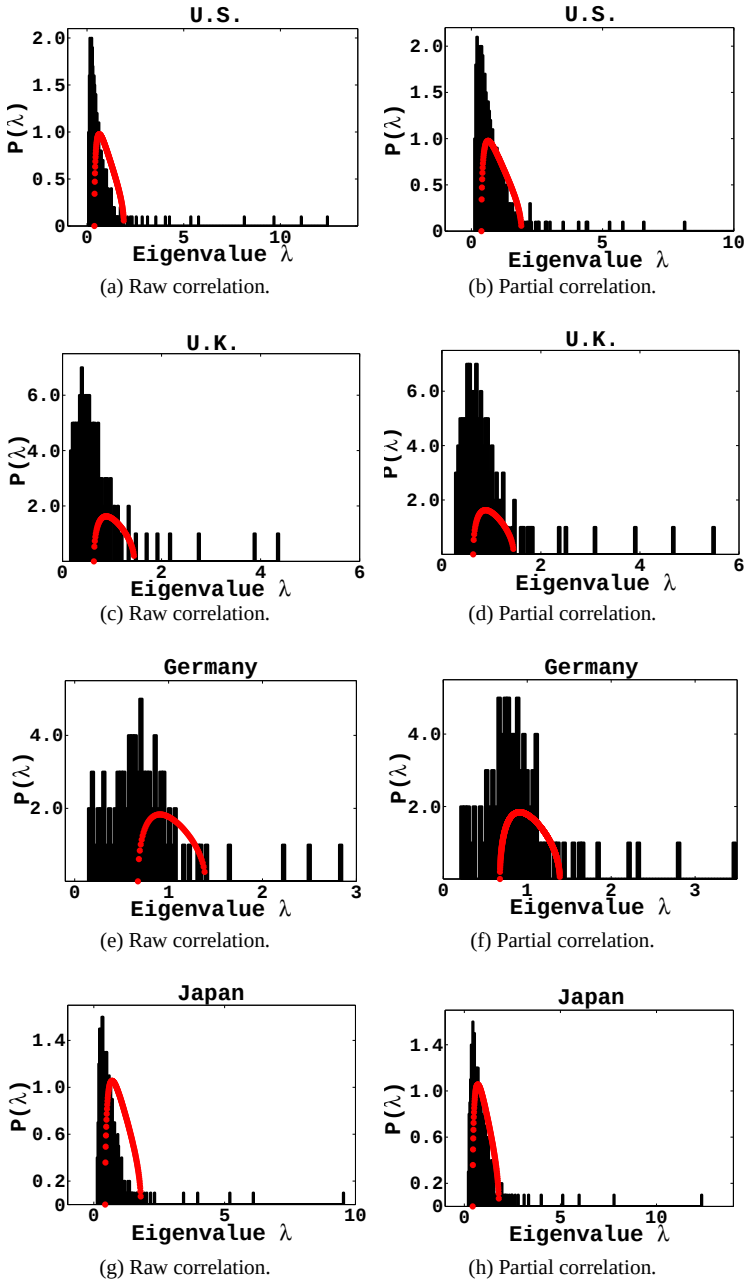

(a) Raw correlation. (b) Partial correlation.

(c) Raw correlation. (d) Partial correlation.

(e) Raw correlation. (f) Partial correlation.

(g) Raw correlation. (h) Partial correlation.

Figure 6.1: Probability distribution of the eigenvalues of the raw and partial correlation matrices of U.S. (a,b), U.K. (c,d), Germany (e,f), and Japanese (g,h) stock markets. The distributions are presented using black straight lines and the distributions of random matrices are presented using red circles.

sus partial correlation. This emphasizes the influence of the different sectors with and without the mediating effect of the market index. For example, the SDR using $\boldsymbol{v}_1$ for the U.S. stock market exhibits a

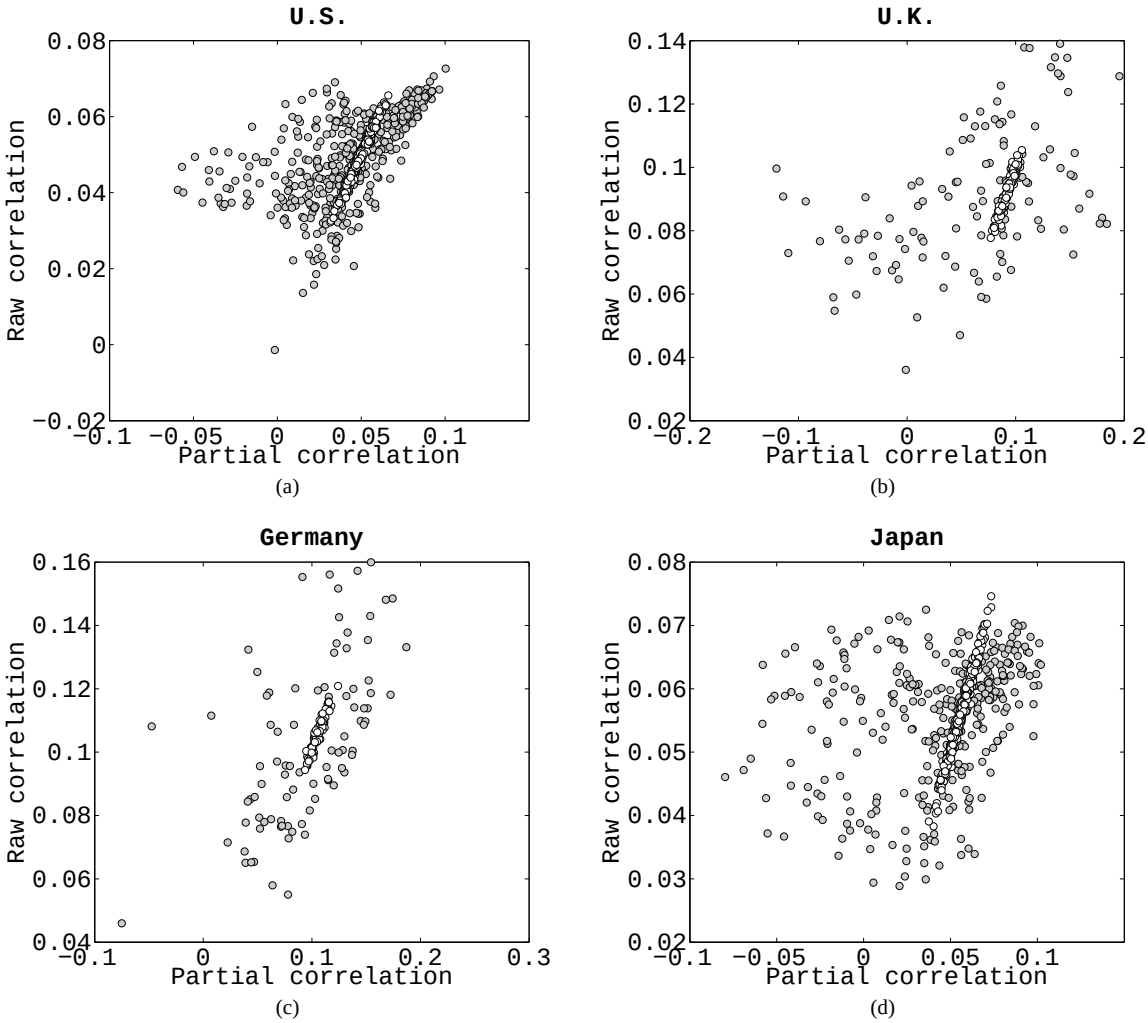

Figure 6.2: The weight of components of eigenvector $\boldsymbol{v}_1$ from the U.S. (a), U.K. (b), Germany (c) and Japanese (d) stock markets. The x-axis indicates the value of components of $\boldsymbol{v}_1$ derived from partial correlation and y-axis indicates the value of components for raw correlation for corresponding stocks. Gray circles indicate components of $\boldsymbol{v}_1$ from each stock, and white circles are components of $\boldsymbol{v}_1$ from random data.

large value in the financial sector using both raw and partial correlations, while the basic materials sector is lower in the case of $\boldsymbol{v}_1$ using partial rather than raw correlation. This shows that the influence of the basic materials sectors to a large extent results from the market index. In the case of the SDR for the U.K. stock market, the basic material sector and financial sector is lower in the case of $\boldsymbol{v}_1$ for partial correlation. This again shows that the influence of both these sectors, which is large when studying the raw correlations, is significantly decreased once the effect of the index is removed and the underlying structure of the market is uncovered. The financial sector dominates in both the U.S. and U.K. stock

Table 6.3: The SDR from the largest eigenvector $\boldsymbol{v}_1$ using raw correlation (R.C.) and partial correlation (P.C.) from January 2000 to December 2010. The threshold is $\tau = 1/\sqrt{N}$, where N is the number of stocks for each market.

	U.S.		U.K.		Germany		Japan	
Sector	R.C.	P.C.	R.C.	P.C.	R.C.	P.C.	R.C.	P.C.
Basic materials	4.84%	3.55%	2.44%	-7.76%	5.51%	5.51%	4.61%	9.62%
Communications	-2.96%	-0.86%	-0.86%	-0.86%	0%	0%	-2.74%	-3.81%
Consumer goods	-11.5%	-7.47%	-4.22%	-5.08%	-1.97%	5.53%	-8.6%	-2.04%
Energy	2.64%	0.09%	0%	0%	0%	0%	-0.63%	0.87 %
Financial	11.6%	18.9%	26.7%	16.3%	3.76%	3.76%	2.59%	4.16%
Health care	0%	0%	-3.45%	-3.45%	-7.61%	-7.61%	0%	0%
Industrial goods	6.14%	5.34%	-2.18%	10.7%	7.64%	7.64%	6.51%	-3.44%
Services	0%	0%	-7.18%	1.36%	-5.73%	1.77%	0%	0%
Technology	-8.52%	-10.4%	-5.17%	-5.17%	-4.61%	-14.6%	-0.15%	-6.03%
Utilities	-2.22%	-5.72%	-6.03%	-6.03%	3.01%	-1.99%	-1.59%	0.67%

markets, but has very little influence in the case of Germany and Japan, which emphasizes the difference in the structure and makeup of these four markets. Another esample is the Energy sector, which is found to be influential only for the U.S. and Japanese stock markets, emphasizing their strong dependence on energy resources.

Next, we examine dynamical changes and the evolution of SDR on both a yearly and monthly basis by using $\boldsymbol{v}_1$ for both raw correlation and partial correlation. We divide the stock return data for each stock market into yearly and monthly periods, and calculate raw and partial correlation matrices. The SDR was calculated for both raw and correlation matrices.

The transitions of SDR on a yearly basis for the U.S., U.K., German, and Japanese stock markets using $\boldsymbol{v}_1$ for raw correlation and partial correlation with threshold $\tau = 1/\sqrt{N}$ are presented in Figure 6.3. We observe that the financial sector exhibited negative values in 2008, which correspond to the shocks in this sector resulting from the 2008 financial crisis in U.S. stock market. The footprints of the financial crisis can also be found when observing the negative or low values of SDR in the U.K. stock market, which are not observed in the case of Germany and Japan. In contrast, it can be observed, especially after removing the mediating effect of the index, that both Germany and Japan exhibit strong variations in the dominance of the different sectors.

Next, we study the SDR on a monthly basis (Figure 6.4). For the U.S. stock market, the monthly based SDR analysis provides important information on the change in the structure of the market. First, we observe that the raw correlations do not provide sufficient information. However, when removing the effect of the index, the changes in the underlying structure of the market become apparent. For example, the growing influence of the Financial sector is clearly visible, together with the weakening influence of the technology and industrial sectors. This provides new information into the evolution of this market leading up to the 2008 financial crisis. For the other three markets, similar results are observed to those found for the yearly based SDR analysis, emphasizing the dominance of the Financial sector in the U.K. stock market, and the changes in market structure observed for Germany and Japan.

6.6 SDR Investigation of the dominance of the financial sector

As an example of the application of the introduced methodology, we compare the SDR indicator to the index of implied volatility (VIX) for all stock markets on both a yearly and monthly basis (see Figure 6.5), for the period of January 2006 to December 2010. High values for the VIX are interpreted as a forecast of high volatility of returns in the near future. In this example, we focus on the SDR values calculated for the Financial sector, for both yearly and monthly time horizons. The SDR derived for this sector is denoted as Φ_5.

We compare the CBOE VIX index for the period January 2006 until December 2010 to $-\Phi_5$, for the U.S. and U.K. stock markets, the VDAX index to $-\Phi_5$ for the German stock market and compare the Nikkei Stock Average Volatility Index for $-\Phi_5$ for the Japanese stock market. Since we define the SDR with a positive value as an expression of the dominance of a sector in a given time period, the negative of the value of SDR for financial sector, $-\Phi_5$, corresponds to the VIX for each market. When we compared $-\Phi_5$ to VIX on a yearly basis, the peak of VIX and $-\Phi_5$ are consistent in the case of the U.S. (Figure 6.5(a)) and U.K. (Figure 6.5(b)) stock markets for both raw and partial correlation cases. However, in the case of Germany and Japan, the peaks of $-\Phi_5$ with partial correlation do not agree with those of VIX. This indicates that the financial sector plays a more dominant role in the U.S. and U.K. stock markets, and we find that $-\Phi_5$ is consistent with the VIX index.

To quantitatively compare the SDR to the VIX, we make use of Granger Causality Analysis (GCA) to analyze the extent to which the SDR predicts changes in the VIX indexes, or vice versa. Granger causality uses temporal precedence to identify the direction of causality from information in the data [6,35,36,51]. Thus, given the two time series $-\Phi_5$ and $I_{vix,k}$ (VIX index for country k), we can independently identify both the influence from $-\Phi_5$ to $I_{vix,k}$, and influence in the reverse direction with suitable models.

Let "y" and "x" be stationary time series. To test the null hypothesis that "x" does not Granger-cause "y", one first finds the proper lagged values of "y" to include in a univariate autoregression of "y":

$$y_t = a_0 + a_1 y_{t-1} + a_2 y_{t-2} + \cdots + a_m y_{t-m} + \text{residual}. \tag{6.8}$$

Next, the autoregression is augmented by including lagged values of "x":

$$y_t = a_0 + a_1 y_{t-1} + a_2 y_{t-2} + \cdots + a_m y_{t-m} + b_p x_{t-p} + \cdots + b_q x_{t-q} + \text{residual} \tag{6.9}$$

One retains in this regression all lagged values of "x" that are individually significant according to their t-statistics, provided that collectively they add explanatory power to the regression according to a standard F-test (whose null hypothesis is no explanatory power jointly added by the "x"'s). In the notation of the above augmented regression, "p" is the shortest, and "q" is the longest, lag length for which the lagged value of "x" is significant. The null hypothesis that "x" does not Granger-cause "y" is not rejected if and only if no lagged values of "x" are retained in the regression. A measure of linear dependence $F_{-\Phi_5,I_{VIX,k}}$, between $-\Phi_5$ and $I_{VIX,k}$, which implements Granger causality in terms of vector autoregressive models, has been proposed by Geweke [29]. $F_{-\Phi_5,I_{VIX,k}}$ is the sum of three components

$$F_{-\Phi_5,I_{VIX,k}} = F_{-\Phi_5 \to I_{VIX,k}} + F_{I_{VIX,k} \to -\Phi_5} + F_{-\Phi_5 \cdot I_{VIX,k}}. \tag{6.10}$$

$F_{-\Phi_5 \cdot I_{VIX,k}}$ is a measure of the total linear dependence between the series $-\Phi_5$ and $I_{VIX,k}$. If nothing of the value at a given instant of one can be explained by a linear combination of all the values (past, present, and future) of the other, $F_{-\Phi_5 \cdot I_{VIX,k}}$ will evaluate to zero. This term will then contain no directional

information, and implies residual correlations in the data that cannot be assigned to causally directed influence. $F_{-\Phi_5 \to I_{VIX,k}}$ is a measure of linear directed influence from $-\Phi_5$ to $I_{VIX,k}$. If past values of $-\Phi_5$ improve the prediction of the current value of $I_{VIX,k}$, then $F_{-\Phi_5 \to I_{VIX,k}} > 0$. The results of the GCA are presented in Table 6.4. We find that the SDR $-\Phi_5$ Granger causes the VIX index for both the U.S. and U.K., when calculated from raw correlations.

Table 6.4: The table represents the results of Granger causality tests between $-\Phi_5$ and VIX for raw correlation and partial correlation for all stock markets. If the value of F-statistic is larger than the value of critical value, $-\Phi_5$ Granger cause VIX. The significance level is 0.05 for all Granger causality tests.

Market	Granger causality test	F-statistic	Critical value
U.S. (R.C.)	$-\Phi_5$ Granger VIX	7.48	3.85
U.S. (P.C.)	$-\Phi_5$ does not Granger VIX	3.32	3.85
U.K. (R.C.)	$-\Phi_5$ Granger VIX	12.5	3.85
U.K. (P.C.)	$-\Phi_5$ does not Granger VIX	0.56	3.85
Germany (R.C.)	$-\Phi_5$ does not Granger VIX	0.71	3.85
Germany (P.C.)	$-\Phi_5$ does not Granger VIX	1.27	3.85
Japan (R.C.)	$-\Phi_5$ does not Granger VIX	0.21	3.85
Japan (P.C.)	$-\Phi_5$ does not Granger VIX	2.78	3.85

Furthermore, to study the similarity between $-\Phi_5$ and the VIX indexes, we perform a cross-correlation analysis between the two. Cross correlation is a standard method in signal processing for estimating the degree to which two series are correlated at different time lags. The discrete cross-correlation function between two time series X and Y is given by [14]

$$XCF(d) = \frac{\sum_{i=1}^{N-d} [(X(i) - \langle X \rangle) \cdot (Y(i-d) - \langle Y \rangle)]}{\sqrt{\sum_{i=1}^{N-d} (X(i) - \langle X \rangle)^2} \cdot \sqrt{\sum_{i=1}^{N-d} (Y(i-d) - \langle Y \rangle)^2}} \tag{6.11}$$

$$d = \pm 1, \pm 2, ..., \pm N - 1 \tag{6.12}$$

where d is the lag. We consider values of $d = \pm 1, \pm 2, \pm 3, \pm 4, \pm 5, \pm 6$. We investigate the monthly values of $-\Phi_5$ and $I_{VIX,k}$ for each year separately, for both raw correlations and partial correlation cases (Figure 6.6). In this analysis, the large value of $d = +1$ means that the VIX would have similarity to previous month's value of $-\Phi_5$, and a large value of $d = -1$ means $-\Phi_5$ would have similarity to previous month's value of VIX.

6.7 Concluding remarks

In this chapter we present a new measure to investigate the functional micro structure of financial markets, the Sector Dominance Ratio (SDR). To demonstrate the capabilities of this measure, we analyze data from the U.S., U.K., German, and Japanese stock markets from January 2000 to December 2010, a period in which these markets went through different structural changes. Using this data, our aim is

threefold: 1) introduce the SDR measure to study the micro structure of financial markets; 2) use the SDR to emphasize the structural differences between the investigated markets; and 3) to present and emphasize the additional information embedded in the stock partial correlations, after removing the mediating effect of the market index.

Significant patterns for the financial sector are evident from the SDR calculated for the raw and partial correlations, especially in the case of the U.S. and U.K. stock markets. Compared to Germany and Japan, these two markets exhibit a strong dominance of the financial sector, as is captured by the SDR analysis. This is further emphasized when we observe that for the U.S. market, the largest eigenvector from partial correlations and the second largest eigenvector from raw correlations are similar and exhibit similar values as the SDR of the financial sector. This finding emphasizes and highlights the extent of the dominance of the financial sector in this market. With regard to the time period surrounding the 2008 financial crisis, the SDR in the financial sectors in the U.S. and U.K. showed negative values in 2008; this tendency was also seen in Germany, but the Japanese stock market did not show such large negative values. This demon- strates the differences between the structural makeup of these four markets, and the extent of the damage of the 2008 financial crisis.

To further study the impact of the financial sector in these four markets, and as an example of the application of the SDR methodology, we compare the SDR measure to the VIX in all stock markets using both yearly and monthly averages. We compare the VIX index with the SDR for the financial sector, $-\Phi_5$, on a yearly basis and find that it is consistent with VIX in the U.S. and U.K. stock markets, especially in the partial correlation case. However, peaks of $-\Phi_5$ do not coincide with those of VIX for the German or Japanese stock markets. This is consistent with the fact that the financial sector plays a more dominant role in U.S. and U.K. stock market; in those markets, therefore, $-\Phi_5$ would be relevant to VIX. The Granger causality tests indicates that $-\Phi_5$ using raw correlations Granger-causes VIX in the U.S. and U.K. stock markets. We further examined the cross correlations between $-\Phi_5$ with the largest eigenvector from raw correlation and partial correlation matrices; therefore, the $-\Phi_5$ would be an indicator for VIX indexes for both U.S. and U.K. stock markets. We conclude that $-\Phi_5$ does not Granger cause VIX for the German and Japanese stock markets, because while the financial sector plays a dominant role in U.S. and U.K. stock markets, it does not do so in the German and Japanese stock markets. For the cross correlation analysis, we examine the cross correlation between $-\Phi_5$ and VIX for each year for all stock markets. The similarities between $-\Phi_5$ and VIX at $d = -1, \ldots, -6$ are observed especially for partial correlations case for all stocks and in the raw correlation case for the German stock market. This indicates that the $-\Phi_5$ using partial correlation can be useful for predicting the behavior of VIX indexes.

In summary, we present a new measure to quantify the evolution of activity of economic sectors reflected in financial markets. The SDR provides a quantitative measure to study structural versus functional activity in financial markets. As such, it provides a means to identify economic sectors with increasing dominance, which could indicate an increase in systemic risk. Further, the SDR also provides a means to identify markets in which the functional makeup is extremely different from the structural makeup, which could indicate structural reforms. As such, the SDR parameter provides both practitioners and policy makers an important tool useful for understanding the functional structure of financial markets, and its dynamics, and provides valuable information for monitoring and managing systemic risk.

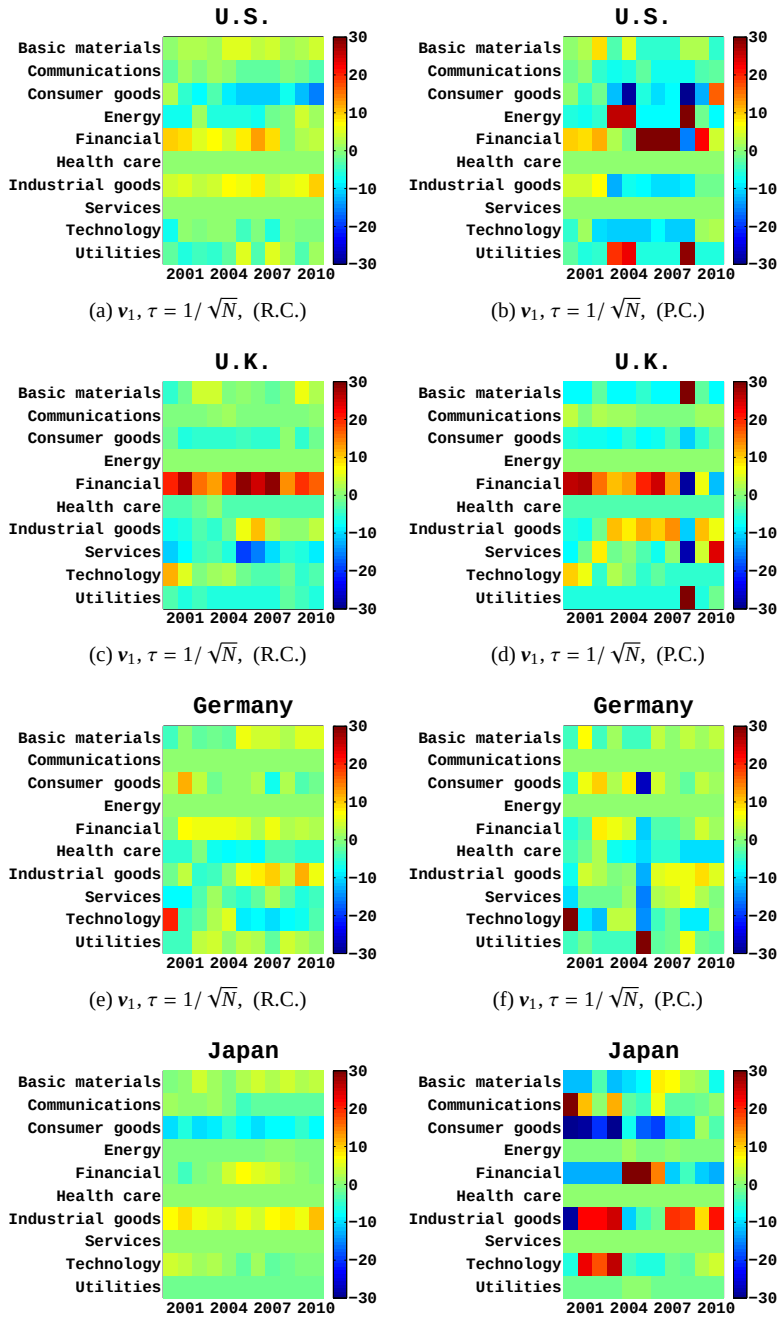

(a) $\boldsymbol{v}_1$, $\tau = 1/\sqrt{N}$, (R.C.)

(b) $\boldsymbol{v}_1$, $\tau = 1/\sqrt{N}$, (P.C.)

(c) $\boldsymbol{v}_1$, $\tau = 1/\sqrt{N}$, (R.C.)

(d) $\boldsymbol{v}_1$, $\tau = 1/\sqrt{N}$, (P.C.)

(e) $\boldsymbol{v}_1$, $\tau = 1/\sqrt{N}$, (R.C.)

(f) $\boldsymbol{v}_1$, $\tau = 1/\sqrt{N}$, (P.C.)

(g) $\boldsymbol{v}_1$, $\tau = 1/\sqrt{N}$, (R.C.)

(h) $\boldsymbol{v}_1$, $\tau = 1/\sqrt{N}$, (P.C.)

Figure 6.3: Yearly based SDR analysis obtained from the largest eigenvector $\boldsymbol{v}_1$ for the raws and partial correlations of U.S. (a,b), U.K. (c,d), Germany (e,f), and Japanese (g,h) stock markets. The threshold is given as $\tau = 1/\sqrt{N}$.

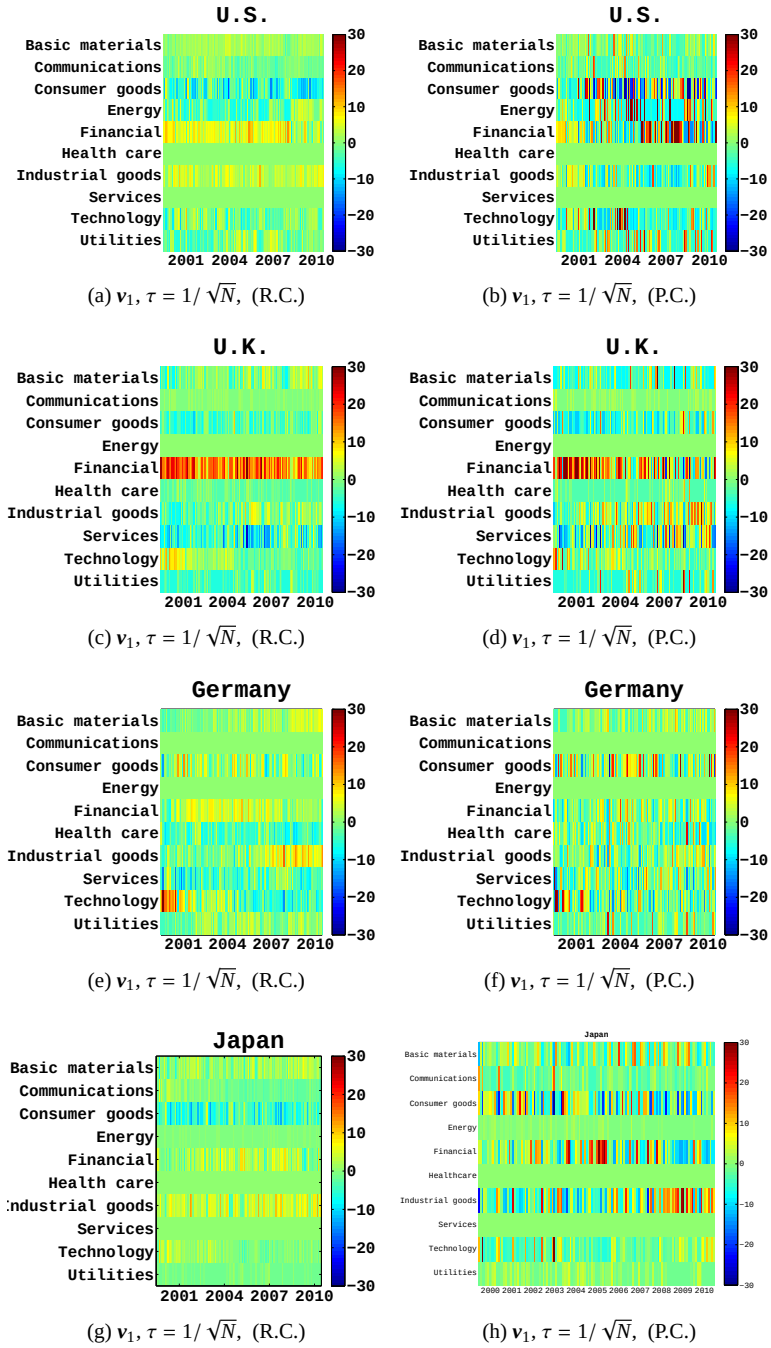

(a) $\boldsymbol{v}_1$, $\tau = 1/\sqrt{N}$, (R.C.)

(b) $\boldsymbol{v}_1$, $\tau = 1/\sqrt{N}$, (P.C.)

(c) $\boldsymbol{v}_1$, $\tau = 1/\sqrt{N}$, (R.C.)

(d) $\boldsymbol{v}_1$, $\tau = 1/\sqrt{N}$, (P.C.)

(e) $\boldsymbol{v}_1$, $\tau = 1/\sqrt{N}$, (R.C.)

(f) $\boldsymbol{v}_1$, $\tau = 1/\sqrt{N}$, (P.C.)

(g) $\boldsymbol{v}_1$, $\tau = 1/\sqrt{N}$, (R.C.)

(h) $\boldsymbol{v}_1$, $\tau = 1/\sqrt{N}$, (P.C.)

Figure 6.4: Monthly based SDR analysis for the raw and partial correlations of the U.S. (a,b), U.K. (c,d), Germany (e,f), and Japanese (g,h) stock markets. The dominance of the Financial sector is observed in both U.S. and U.K. stock market, but not in the German and Japanese stock markets. Furthermore, the monthly based SDR analysis highlights changes in market structure, emphasizing changes that led up to the 2008 financial crisis.

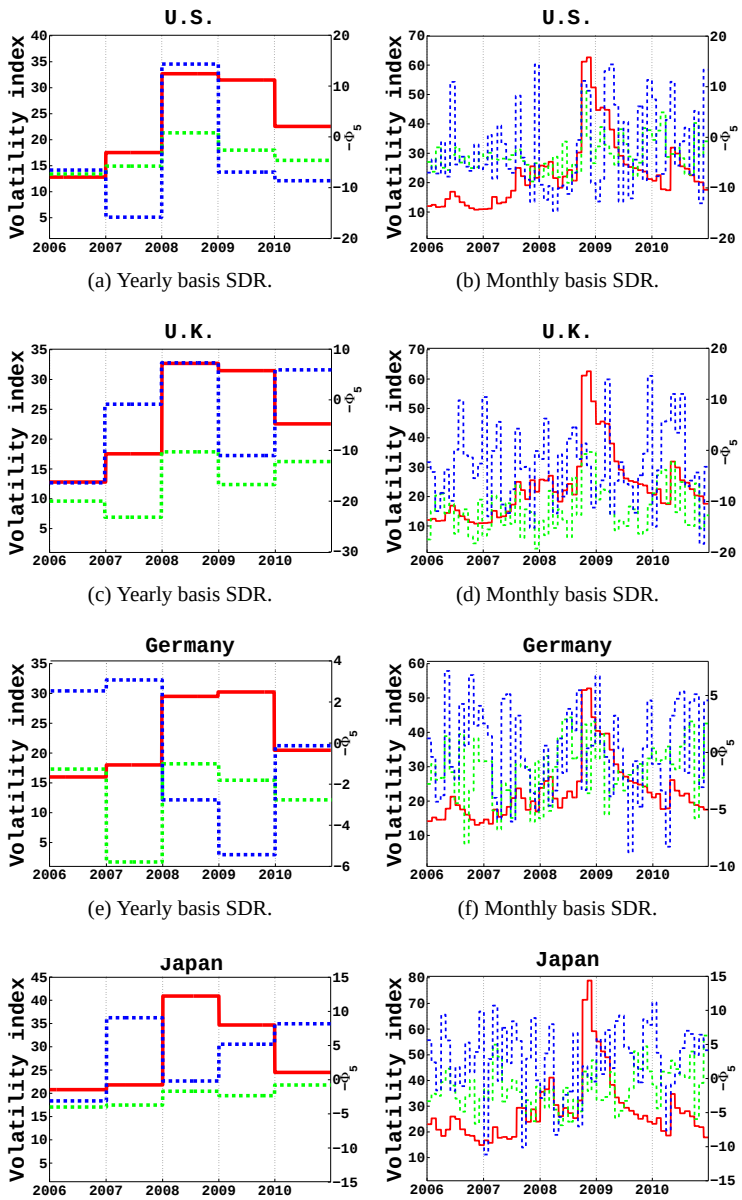

(a) Yearly basis SDR. (b) Monthly basis SDR.

(c) Yearly basis SDR. (d) Monthly basis SDR.

(e) Yearly basis SDR. (f) Monthly basis SDR.

(g) Yearly basis SDR. (h) Monthly basis SDR.

Figure 6.5: The comparison of Financial sector based SDR and VIX for the period of 2006-2010, on a yearly and monthly based time horizon for the U.S. (a,b), U.K. (c,d), Germany (e,f), and Japanese (g,h) stock markets. The red line corresponds to the VIX index on either yearly or monthly time horizon, and green and blue dashed lines correspond to dynamical change of $-\Phi_5$, which expresses deactivation of SDR for financial sector using $\boldsymbol{v}_1$ for raw and partial correlation, respectively. The left y-axis displays the value of volatility index and the right y-axis displays the value of $-\Phi_5$.

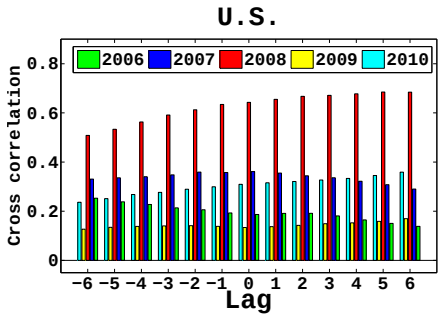

(a) R.C.

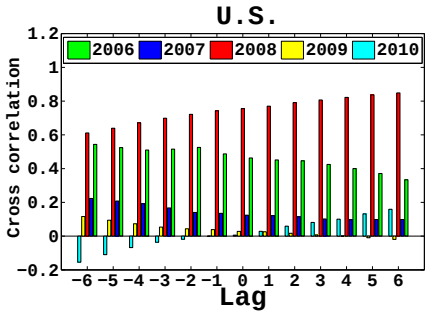

(b) P.C.

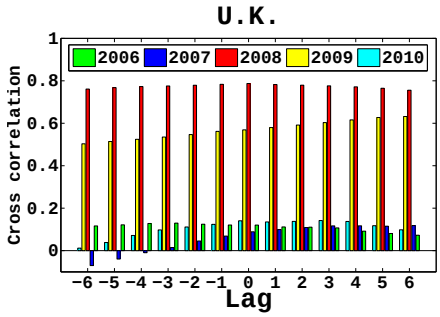

(c) R.C.

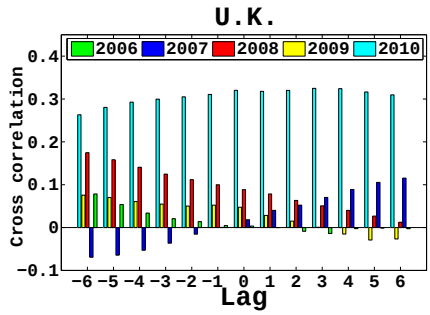

(d) P.C.

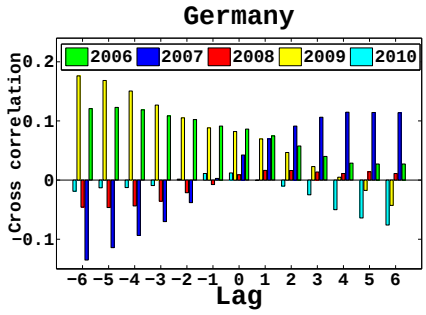

(e) R.C.

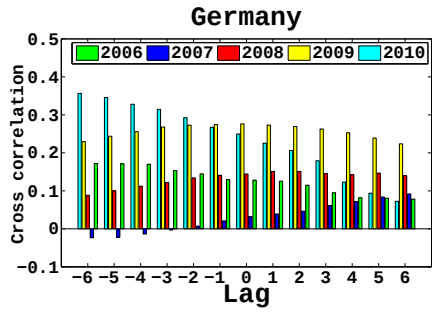

(f) P.C.

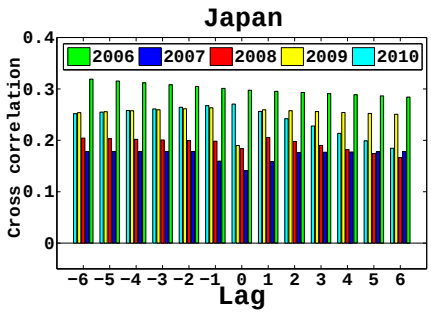

(g) R.C.

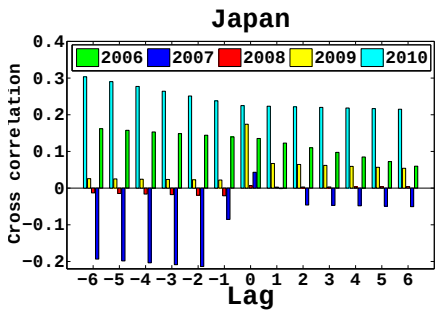

(h) P.C.

Figure 6.6: Cross correlation function (XCF) between the SDR calculated for the financial sector, $-\Phi_5$, and VIX by monthly basis for each year using raw and partial correlation, for the U.S. (a,b), U.K. (c,d), Germany (e,f), and Japanese (g,h) stock market.

Chapter 7

Conclusion and future work

7.1 Summary and Discussion

In this thesis, we have investigated several formation mechanisms of complex system such as ecology, molecular biology and economical system.

In Chapter 3, we have investigated a system of $2n$-dimensional, coupled first-order differential equations which contains self-interactions, and mixing interactions by using Noether's theorem. We discussed that the nonlinear differential equations with a conserved quantity, Ψ, calculated by Noether's theorem have converged stable solutions, and the coefficients of nonlinear interactions are strictly confined by the conservation law of the system. The conserving converged solutions have been shown by a closed curve in (x_1, x_2)-coordinates for 2-dimensional case, and in general, it should be discussed by a closed hypersurface in $(x_1, x_2, \ldots, x_{2n})$-coordinates for $2n$-dimensional case. We investigated a system of symmetric nonlinear coupled first order differential equations has a conservation law and exists in the form of the $2n$-independent variables $(x_1, x_2, \ldots, x_{2n})$. We have named the system of symmetric first-order differential equations composed of the $2n$-dimensional nonlinear interactions as the binary-coupled form. We have found that if a coupled nonlinear system exists in a form of symmetric first-order differential equations, which has a velocity-independent conserved quantity as discussed in this thesis, the system tends to be composed of the binary-coupled form. The predator-prey type system, food-web system, and gene regulation network system may be typical examples, and the computer network seems to be expressed by $2n$-coupled form. However, if a competitive system is the odd-variable type, the system of the first-order differential equations becomes little different. The conservation law we derived in Chapter 3 also used to check the accuracy of numerical solutions of nonlinear differential equations. The binary-coupled differential equations have several interesting properties, and the system of binary-coupled form seems to be found in social, natural and biological sciences. If a system of binary-coupled form is naturally discovered in nature, the consequences discussed in binary-coupled form system would help understand structures, interactions, evolution mechanism of biological systems as well as social, economic and environmental systems. We have investigated and discussed the property of $2n$-dimensional ND system in general, such as addition law and exchangeability. Although $2n$-dimensional ND system is discussed as a continuous system by employing differential equations, it is useful to examine their qualitative character of the classical Lotka Volterra system.

In Chapter 4, we have examined characteristic properties of several ecological systems based on con-

served nonlinear interactions which include generalized Lotka-Volterra type prey-predator, competitive interactions. We have extended our $2n$-variable ND model by including external perturbations in order to apply the model to more realistic biological phenomena and to study responses of a biological system to external perturbations. We have also simulated external positive and negative perturbations by employing piecewise constant terms in our nonlinear equations. The results of simplified perturbations agreed with the experiments and empirical data reasonably obtained. It is shown that the numerical simulations have showed the existence of the *standard rhythm* which is characteristic to a nonlinear conserved system. We have found that it is essential to understand *standard rhythm* by observing and taking data of a system so that we can distinguish unusual maxima and minima from *standard rhythm*. Based on the concept of *standard rhythm*, the ten-year cycle of lynx and hare is examined. Though a cycle of a biological system should be a phenomenon composed of complex and multi-biological interactions, the 2-variable ND analysis has revealed the interesting results on properties of the biological phenomena. The ten-year cycle of lynx and hare is stable and resilient to external perturbations, which is reproduced in numerical calculations of our model. The stable cycles and recovering phenomena are shown with the system with conservation law, which are displayed numerically in phase-space solutions. We assume that the stability and conservation law are constructed at least by binary-coupled species in biological and ecological systems, and they are maintained in a more complicated multi-coupled system. The important factors are needed for all species to survive in nature, but they easily change by natural conditions. In addition, an unusual increase of population numbers of a species would endanger the survival of a species itself as well as other species. The important property of the nonlinear model with conservation law is that the binary-coupled system can have the persistent stability and recovering strength to external perturbations.

In Chapter 5, we have develop a model of expected impact degree using recurrence and difference equation to estimate the impact degree with multiple knockout and evaluate which model is suitable for simulating the impact degree with multiple knockout. The model of expected impact degree with effects of network size has well fitted to the observed data from Kyoto Encyclopedia of Genes and Genomes database. It is found that the solutions of the model of expected impact degree increases linearly until knockouts of half size of whole metabolic network. However, the solutions of expected impact degree reach the limit with convex curve when we give knockouts more than half size of whole metabolic network. These phenomena are observed in both partial metabolic network and complete metabolic network. The damage expansion rates take highest value when we give knockouts half size of considering metabolic network. The solution of expected impact degree with finite network size and Kyoto Encyclopedia of Genes and Genomes database show convex curve with respect knockouts. We assume that structure of metabolic networks obtained from Kyoto Encyclopedia of Genes and Genomes database have properties of scalability and symmetric structure. Although we need to evaluate importance of each reaction for metabolic network, the numerical experiments of expected impact degree and database showed scalability of metabolic network for both eucaryote and prokaryote from perspective of network systems. It indicates that we can obtain valuable results of experiments concerning partial metabolic network without examining whole metabolic network data. Moreover, it supports the property that addition law of metabolic network in both theoretical and experimental case. In addition to the scalability of metabolic network from database, symmetric structures in metabolic network are also observed through the model of expected impact degree. It would be useful to evaluate the stability of considering metabolic network with arbitrary knockouts, and there would be possibility that the stability of metabolic network is related to properties of scalability and symmetric structure of metabolic network.

In Chapter 6, we have presented a new measure to investigate the functional micro structure of

financial markets, the Sector Dominance Ratio (SDR). To demonstrate the capabilities of this measure, we have analyzed data from the U.S., U.K., German, and Japanese stock markets from January 2000 to December 2010, a period in which these markets went through different structural changes. We have compared the SDR measure to the VIX in all stock markets using both yearly and monthly averages. We compare the VIX index with the negative value of SDR for the financial sector on a yearly basis and find that it is consistent with VIX in the U.S. and U.K. stock markets, especially in the partial correlation case. However, peaks of negative value of SDR do not coincide with those of VIX for the German or Japanese stock markets. This is consistent with the fact that the financial sector plays a more dominant role in U.S. and U.K. stock market; in those markets, therefore, negative value of SDR would be relevant to VIX. The SDR provides a quantitative measure to study structural versus functional activity in financial markets. As such, it has been provided a means to identify economic sectors with increasing dominance, which could indicate an increase in systemic risk. Further, the SDR has also provided a means to identify markets in which the functional makeup is extremely different from the structural makeup, which could indicate structural reforms.

7.2 Future direction

In this thesis, we have investigated structural properties in complex phenomena such as ecology, biology and economy using analytical and statistical mechanics. We found several hypotheses for complex phenomena related by dissipative structure, nonlinear competitive systems and conservation law. We understand that the conservation law Ψ depends sensitively on the values of nonlinear coefficients, and we also hope to investigate the relations between coefficients and stability of solutions of $2n$-ND systems. In this thesis, it was difficult to find the conservation law Ψ for odd variables systems. However, special cases such as one variable would be possible to be expressed as constraint condition would have conservation law Ψ since we it would be same problem as even variable systems. Besides odd variable systems, various type of Lagrangian and Ψ would be investigated using binary-coupled form and exponential function. The conservation law Ψ shows several interesting behaviors. For example, if nonlinear coefficients are not appropriate value, Ψ oscillate while solutions have finite values. We need further examination for numerical simulation of Ψ In Chapter 4, we assume that stability and conservation law are constructed by species in mutual dependency or cooperation to survive for long-time periods in severe nature, and the *standard rhythm* should be regarded as the result of strategy for species to live in nature. Whatever roles they have to play, the species that can fit and balance with other creatures can survive in nature. A strong predator cannot even survive if it ignores the law of the *standard rhythm* and conservation law of a system constructed by other members and the environment. We will have to consider quantitative algorithm for numerical simulation to fit realistic data. Moreover, considering population not only Canadian lynx but also snowshoe hare will be important future work. We hope that this study will help understand both activities of animals and humans in natural life.

In Chapter 5, we need to more computational experiments for several species and consider the differences of robustness among species. Moreover, the reason why considering nonlinear effects of size of network is useful for calculating expected impact degree from perspective of mathematical model. In addition, the model of expected impact degree would be useful for applying other fields such as economy since there are many phenomena described by network systems. As future work, we need to focus on properties of scalability and symmetry of these network systems. It is because the methods of conserva-

tion law might be able to apply and it would be useful for controlling network structure.

In Chapter 6, the SDR parameter has provided both practitioners and policy makers an important tool useful for understanding the functional structure of financial markets, and its dynamics, and has provided valuable information for monitoring and managing systemic risk. In this thesis, we took the largest eigenvalue from raw correlation as an indicator of SDR for convenient. However, it will be needed to investigate the reason why the largest eigenvalue is successful for monitoring financial market. As future work, we would like to reveal the structural correlation among SDR, random matrix theory and financial market.

Appendix A

Invariance of Single Integrals

A.1 r-parameter transformations

Under the hypothesis that the fundamental integrals is invariant under the r-parameter family transformations, we derive a set of basic invariant identities which considering Lagrangian and infinitesimal generators of the transformation. Let us consider the transformation of $(t, x', \ldots, x^n)$-space with parameter $(\varepsilon^1, \ldots, \varepsilon^r)$ depending on real value r. We denote the general transformation considering time transformation $\bar{t}$ and space transformation $\bar{x}^k$. Using arbitrary function ϕ and ψ^k, we express these transformations as follows.

$$\begin{aligned} \bar{t} &= \phi(t, x, \varepsilon), \\ \bar{x}^k &= \psi^k(t, x, \varepsilon) \quad (k = 1, ..., n). \end{aligned} \tag{A.1}$$

Applying Taylor expansion around $\varepsilon = 0$, the properties are given from continuity as

$$\begin{aligned} \phi(t, x, 0) &= t, \\ \psi^k(t, x, 0) &= x^k \quad (k = 1, \ldots, n). \end{aligned} \tag{A.2}$$

The time transformation $\bar{t}$ and space transformation $\bar{x}^k$ are expressed as follows

$$\begin{aligned} \bar{t} &= t + \tau_s(t, x)\varepsilon^s + o(\varepsilon), \\ \bar{x}^k &= x^k + \xi^k_s(t, x)\varepsilon^s + o(\varepsilon). \end{aligned} \tag{A.3}$$

Moreover, there are relations among the transformation function ψ^k, ϕ, τ_s and ξ^k_s as

$$\tau_s(t, x) = \frac{\partial \phi}{\partial \varepsilon^s}(t, x, 0), \quad \xi^k_s(t, x) = \frac{\partial \psi^k}{\partial \varepsilon^s}(t, x, 0). \tag{A.4}$$

It is called as infinitesimal transformation.

A.2 Invariant Definitions

Suppose that the difference of functional is infinitesimal under the time transformation $t \to \bar{t}$ and space transformation $x(t) \to \bar{x}(\bar{t})$. That is

$$J(x) = \int_a^b \mathcal{L}(t, x(t), \dot{x}(t))dt \tag{A.5}$$

and $J(\bar{x})$ which is after transformation

$$J(\bar{x}) = \int_{\bar{a}}^{\bar{b}} \mathcal{L}(\bar{t}, \bar{x}(\bar{t})), \frac{d\bar{x}}{d\bar{t}}(\bar{t}))d\bar{t} \tag{A.6}$$

have invariant property in the perspective of Lagrangian. We hypothesize that Lagrangian is invariant under the transformation as follows.

$$\mathcal{L}(\bar{t}, \bar{x}(\bar{t})), \frac{d\bar{x}}{d\bar{t}}(\bar{t}))\frac{d\bar{t}}{dt} - \mathcal{L}(t, x(t), \dot{x}(t)) = O(\varepsilon). \tag{A.7}$$

Note that $O(\varepsilon)$ is also infinitesimal, if $\varepsilon \to 0$, $O(\varepsilon)/\varepsilon \to 0$. Based on these hypothesis and integral equations, we calculate following equations using Jacobian.

$$\begin{aligned} J(\bar{x}) - J(x) &= \int_{\bar{t_1}}^{\bar{t_2}} \mathcal{L}(\bar{t}, \bar{x}(\bar{t})), \frac{d\bar{x}}{d\bar{t}}(\bar{t}))d\bar{t} - \int_{t_1}^{t_2} \mathcal{L}(t, x(t), \dot{x}(t))dt \\ &= \int_{\bar{t_1}}^{\bar{t_2}} \mathcal{L}(\bar{t}, \bar{x}(\bar{t})), \frac{d\bar{x}}{d\bar{t}}(\bar{t}))\frac{d\bar{t}}{dt}dt - \int_{t_1}^{t_2} \mathcal{L}(t, x(t), \dot{x}(t))dt \\ &= \int_{t_1}^{t_2} \Big\{\mathcal{L}(\bar{t}, \bar{x}(\bar{t})), \frac{d\bar{x}}{d\bar{t}}(\bar{t}))\frac{d\bar{t}}{dt} - \mathcal{L}(t, x(t), \dot{x}(t))\Big\}dt \\ &= O(\varepsilon). \end{aligned} \tag{A.8}$$

Note that $O(\varepsilon)$ is the function which has an order over the ε^2. There is a relation between Lagrangian before transformation and Lagrangian after transformation as follows

$$\mathcal{L}(\bar{t}, \bar{x}(\bar{t}), \frac{d\bar{x}}{d\bar{t}}(\bar{t}))\frac{d\bar{t}}{dt} - \mathcal{L}(t, x(t), \dot{x}(t)) = \varepsilon^s \frac{d\Phi_s}{dt}(t, x(t)) + O(\varepsilon). \tag{A.9}$$

The function Φ_s is an arbitrary function. Invariant properties are derived from the differentiation of Lagrangian before transformation and after transformation, and if $\varepsilon \to 0$ it is found that $O(\varepsilon)$ is 0. Therefore, there is an invariant property of Φ_s which is proportional to ε. In term of physics, Φ_s is often called as gauge function and it is also considered the symmetric property of Lagrangian.

A.3 The Fundamental Invariance Identities

Theorem A.3.1. *The Lagrangian $\mathcal{L}(t, x, \dot{x})$ and its derivative satisfy following r-identities under the r-parameter transformation*

$$\frac{\partial \mathcal{L}}{\partial t}\tau_s + \frac{\partial \mathcal{L}}{\partial x^k}\xi_s^k + \frac{\partial \mathcal{L}}{\partial x^k}\Big(\frac{d\xi_s^k}{dt} - \dot{x}^k\frac{d\tau_s}{dt}\Big) + \mathcal{L}\frac{d\tau_s}{dt} = \frac{d\Phi_s}{dt}. \tag{A.10}$$

$(s = 1, \ldots, r)$, *where the τ_s and ξ_s^k are defined by the transformations.*

Proof. In the proof, we will need following expressions which are derived from transformations.

$$\bar{t} = t + \tau_s(t,x)\varepsilon^s + o(\varepsilon). \tag{A.11}$$

$$\bar{x}^k = x^k + \xi^k_s(t,x)\varepsilon^s + o(\varepsilon). \tag{A.12}$$

We also use the definition of partial and basic differentiation $\varepsilon \to 0$.

$$\Big(\frac{\partial \bar{t}}{\partial t}\Big)_0 = 1, \Big(\frac{\partial \bar{x}^k}{\partial t}\Big)_0 = \Big(\frac{\partial \bar{t}}{\partial x^k}\Big)_0 = 0, \Big(\frac{\partial \bar{x}^k}{\partial x^h}\Big)_0 = \delta^k_h, \tag{A.13}$$

$$\Big(\frac{\partial^2 \bar{x}^k}{\partial \varepsilon^s \partial t}\Big)_0 = \frac{\partial}{\partial t}\xi^k_s(t,x) = \frac{\partial \xi^k_s}{\partial t}, \tag{A.14}$$

$$\Big(\frac{\partial \bar{x}^k}{\partial \varepsilon^s \partial x^h}\Big)_0 = \frac{\partial \xi^k_s}{\partial x^h}, \tag{A.15}$$

$$\Big(\frac{\partial^2 \bar{t}}{\partial \varepsilon^s \partial t}\Big)_0 = \frac{\partial}{\partial t}\tau_s(t,x) = \frac{\partial \tau_s}{\partial t}, \tag{A.16}$$

$$\Big(\frac{\partial^2 \bar{t}}{\partial \varepsilon^s \partial x^h}\Big) = \frac{\partial \tau_s}{\partial x^h}. \tag{A.17}$$

Note that $(\cdot)_{\varepsilon=0}$ is expressed as $(\cdot)_0$. Applying derivation of (A.10) by ε^s, we get following

$$\begin{aligned}
&\frac{\partial \mathcal{L}}{\partial t}\tau_s + \frac{\partial \mathcal{L}}{\partial x^k}\xi^k_s + \frac{\partial \mathcal{L}}{\partial x^k}\Big(\frac{d\xi^k_s}{dt} - \dot{x}^k\frac{d\tau_s}{dt}\Big) + \mathcal{L}\frac{d\tau_s}{dt} = \varepsilon^s\frac{d\Phi_s}{dt} + O(\varepsilon)\\
&\frac{d}{d\varepsilon^s}\Big\{\frac{\partial \mathcal{L}}{\partial t}\tau_s + \frac{\partial \mathcal{L}}{\partial x^k}\xi^k_s + \frac{\partial \mathcal{L}}{\partial x^k}\Big(\frac{d\xi^k_s}{dt} - \dot{x}^k\frac{d\tau_s}{dt}\Big) + \mathcal{L}\frac{d\tau_s}{dt}\Big\} = \frac{d}{d\varepsilon^s}\Big\{\varepsilon^s\frac{d\Phi_s}{dt} + O(\varepsilon)\Big\}\\
&\Big\{\frac{\partial \bar{\mathcal{L}}}{\partial \bar{t}}\frac{d\bar{t}}{d\varepsilon^s} + \frac{\partial \bar{\mathcal{L}}}{\partial \bar{x}}\frac{d\bar{x}}{d\varepsilon^s} + \frac{\partial \bar{\mathcal{L}}}{\partial \dot{\bar{x}}}\frac{d\dot{\bar{x}}}{d\varepsilon^s}\Big\}\Big(\frac{d\bar{t}}{dt}\Big) + \mathcal{L}\Big(\frac{\partial}{\partial \varepsilon^s}\Big)\Big(\frac{d\bar{t}}{dt}\Big) = \frac{d\Phi_s}{dt}\\
&\Big(\frac{d\bar{t}}{dt}\Big)\Big(\frac{\partial \bar{\mathcal{L}}}{\partial \bar{t}}\tau_s + \frac{\partial \bar{\mathcal{L}}}{\partial \bar{x}}\xi^k_s + \frac{\partial \bar{\mathcal{L}}}{\partial \dot{\bar{x}}}\Big(\frac{\partial}{\partial \varepsilon^s}\cdot\frac{d\bar{x}}{dt}\Big)\Big) + \mathcal{L}\Big(\frac{\partial}{\partial \varepsilon^s}\Big)\Big(\frac{d\bar{t}}{dt}\Big) = \frac{d\Phi_s}{dt}
\end{aligned} \tag{A.18}$$

By the definition of basic derivation, it is clear that we can obtain as following formulations,

$$\frac{d\bar{t}}{dt} = \frac{\partial \bar{t}}{\partial t} + \frac{\partial \bar{t}}{\partial x}\dot{x}, \tag{A.19}$$

$$\frac{d\bar{x}}{dt} = \frac{\partial \bar{x}}{\partial t} + \frac{\partial \psi}{\partial x}\dot{x}. \tag{A.20}$$

$$\Big(\frac{\partial}{\partial \varepsilon^s}\Big)\Big(\frac{d\bar{t}}{dt}\Big) = \frac{\partial \tau_s}{\partial t} + \frac{\partial \tau_s}{\partial x}\dot{x} = \frac{d\tau_s}{dt}. \tag{A.21}$$

$$\frac{\partial \bar{x}}{\partial t} + \frac{\partial \bar{x}}{\partial x}\dot{x} = \frac{d\bar{x}}{d\bar{t}}\Big(\frac{\partial \bar{t}}{\partial t} + \frac{\partial \bar{x}}{\partial x}\dot{x}\Big) \tag{A.22}$$

If we apply derivation by ε,

$$\frac{\partial}{\partial\varepsilon}\frac{\partial\bar{x}^k}{\partial t}+\frac{\partial}{\partial\varepsilon}\frac{\partial\bar{x}^k}{\partial x^h}\dot{x}^k=\frac{d\bar{x}}{d\bar{t}}\Big(\frac{\partial^2\bar{t}}{\partial\varepsilon^s\partial t}+\frac{\partial^2 t}{\partial\varepsilon^s\partial x^h}\dot{x}^h\Big)+\frac{\partial}{\partial\varepsilon}\frac{d\bar{x}}{d\bar{t}}\Big(\frac{\partial\bar{t}}{\partial t}+\frac{\partial\bar{t}}{\partial x^h}\dot{x}^h\Big) \tag{A.23}$$

Setting $\varepsilon\to 0$ in this expression,

$$\frac{\partial\xi^k_s}{\partial t}+\frac{\partial\xi^k_s}{\partial x^h}=\dot{x}\Big(\frac{\partial\tau_s}{\partial t}+\frac{\partial\tau_s}{\partial x^h}x^h\Big)+\Big(\frac{\partial}{\partial\varepsilon^s}\frac{d\bar{x}}{dt}\Big)_0 \tag{A.24}$$

$$\frac{d\xi^k_s}{dt}-\dot{x}\frac{d\tau_s}{dt}=\Big(\frac{\partial}{\partial\varepsilon^s}\frac{d\bar{x}}{dt}\Big) \tag{A.25}$$

Now, we obtain

$$\frac{\partial\mathcal{L}}{\partial t}\tau_s+\frac{\partial\mathcal{L}}{\partial x}\xi^k_s+\frac{\partial\mathcal{L}}{\partial\dot{x}}\Big(\frac{d\xi^k_s}{dt}-\dot{x}\frac{d\tau_s}{dt}\Big)+\mathcal{L}\frac{d\tau_s}{dt}=\frac{d\Phi_s}{dt}. \tag{A.26}$$

□

Appendix B

Supplementary data

B.1 Results for shuffled data

To validate the empirical values observed for the SDR, we make use of a shuffling analysis procedure. For each stock, we first shuffle its price time series in time, thus breaking the temporal order. We then recalculate the returns, the stock correlation matrices, and from them the shuffled based SDR values. For example, in Figure B.1 we compare the raw correlations calculated for the U.S. market empirical data versus those calculated from the randomly shuffled data. Using the same color code to represent the correlation value, it is clear that the correlations for the random case are significantly different, and are very close to zero.

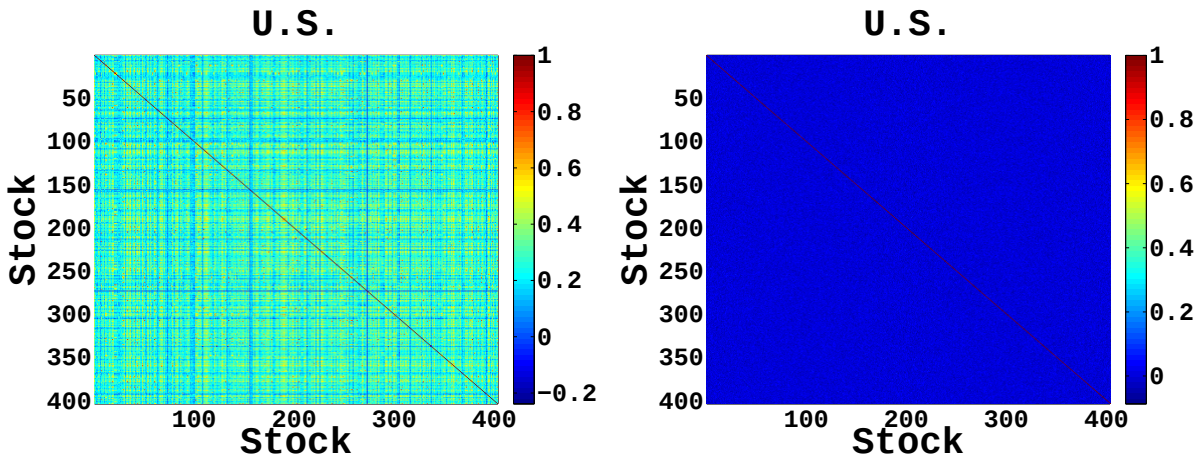

(a) R.C. matrix

(b) R.C. matrix for Shuffled data.

Figure B.1: Stock raw correlation matrix for the U.S. market, calculated from empirical data (a) and from the random ally shuffled time series (b), using the same color code.

B.2 Comparing the effect of the different thresholds

We compare the results of the SDR calculated using the $\tau = 1/\sqrt{n}$ threshold with other threshold values. The SDR, Φ_s ($s = 1, \ldots, 10$), using $\boldsymbol{v}_1$ from raw and partial correlations during the period from January 2000 to December 2010 are presented in Table B.1. The threshold τ is $\tau = \mu$ for $\boldsymbol{v}_1$, where μ is the mean of components of eigenvectors $\boldsymbol{v}_1$ for each market. The components of the eigenvectors $\boldsymbol{v}_1$ for raw correlation are always positive; on the other hand, the components of the eigenvectors $\boldsymbol{v}_2$ for raw correlation and partial correlation take both positive and negative values; therefore, we use the value of τ for $\boldsymbol{v}_1$ and $\boldsymbol{v}_2$.

Table B.1 shows the SDR for basic materials sector decreased in the German, U.K. and U.S. stock markets in the case of partial correlation. The SDR for the communications sector showed larger percentage in the U.K. stock market and the SDR for consumer goods showed a larger percentage in the German, U.S., and Japanese stock markets in the case of partial correlation. The SDR for energy sector increased in the U.S. and Japanese stock markets and the SDR for the financial sector decreased for all stock markets in the case of partial correlation.

Table B.1: The SDR obtained from the largest eigenvector $\boldsymbol{v}_1$ for raw correlation (R.C.) and partial correlation (P.C.). The threshold is $\tau = \mu$, where μ is the mean of components of eigenvector $\boldsymbol{v}_1$ for each market from January 2000 to December 2010.

	U.S.		U.K.		Germany		Japan	
Sector	R.C.	P.C.	R.C.	P.C.	R.C.	P.C.	R.C.	P.C.
Basic materials	4.06%	1.62%	5.20%	-3.41%	5.26%	4.39%	4.27%	5.06%
Communications	-2.81%	-2.80%	-0.86%	0.59%	0%	0%	-2.76%	-3.28%
Consumer goods	-9.85%	-4.96%	-4.78%	-5.99%	-0.14%	6.36%	-8.12%	1.89%
Energy	2.79%	3.77%	0%	0%	0%	0%	-0.63%	0.43 %
Financial	3.39%	2.09%	25.3%	15.0%	10.47%	9.98%	2.80%	1.98%
Health care	0%	0%	-3.45%	-3.45%	-7.67%	-5.66%	0%	0%
Industrial goods	4.66%	1.73%	-2.94%	4.15%	7.15%	7.64%	6.30%	-1.13%
Services	0%	0%	-7.22%	4.30%	-5.97%	2.04%	0%	0%
Technology	-7.76%	-5.80%	-5.17%	-5.17%	-4.85%	-14.6%	-0.27%	-6.03%
Utilities	-1.57%	-3.52%	-6.03%	-6.03%	2.82%	-2.26%	-1.59%	1.07%

The yearly based SDR derived from $\boldsymbol{v}_1$ and $\boldsymbol{v}_2$ using raw and partial correlations for the U.S. stock market are presented in Figure B.2. We calculate the yearly based SDR for the U.S. stock market using $\boldsymbol{v}_1$ and $\boldsymbol{v}_2$, and study the effect of different threshold values. In the case of the SDR using $\boldsymbol{v}_1$ for raw correlation and partial correlation with the threshold $\tau = \mu$, the consumer goods, energy and utilities sector show a larger SDR value using partial correlation. The changes in SDR of the financial sector are also greater using partial correlation. Low SDR values for the financial sector are observed for both raw correlation and partial correlation in 2008. In the case of the SDR for $\boldsymbol{v}_2$ for raw and partial correlations with threshold $\tau = 0$, the technology sector shows a higher value of SDR in raw correlation and partial correlation, compared to that of the SDR obtained from $\boldsymbol{v}_1$ with threshold $\tau = \mu$. Low values of the SDR for the financial sector were also observed during 2008.

The yearly based and monthly based SDR calculated from $\boldsymbol{v}_1$ with threshold $\tau = \mu$ for the U.S., U.K., German, and Japanese stock markets are presented in Figure B.3 and Figure B.4, respectively, for both

raw correlation and partial correlation.

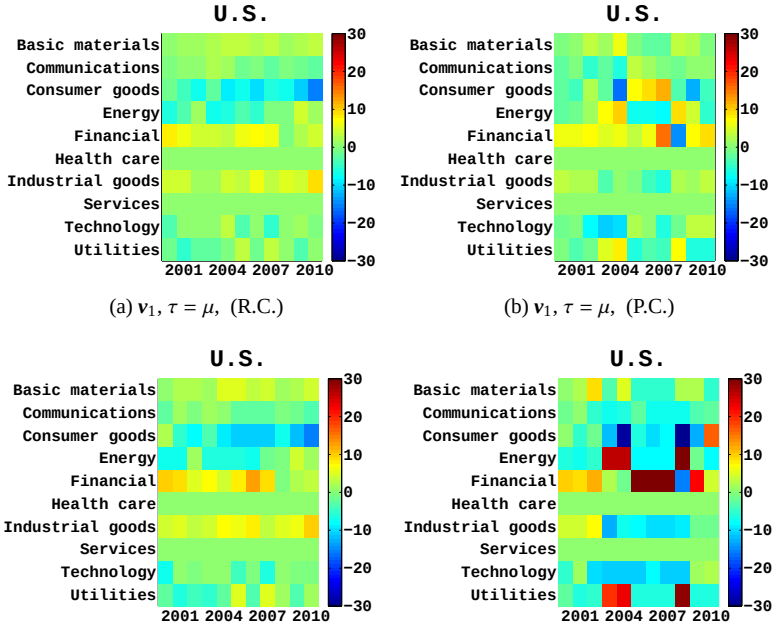

(a) $\boldsymbol{v}_1$, $\tau = \mu$, (R.C.) (b) $\boldsymbol{v}_1$, $\tau = \mu$, (P.C.)

(c) $\boldsymbol{v}_1$, $\tau = 1/\sqrt{N}$, (R.C.) (d) $\boldsymbol{v}_1$, $\tau = 1/\sqrt{N}$, (P.C.)

Figure B.2: The yearly based SDR calculated from $\boldsymbol{v}_1$ for the U.S. stock market for different thresholds and for the first and second largest eigenvectors: (a) SDR calculated from $\boldsymbol{v}_1$ and $\tau = \mu$ for raw correlations; (b) SDR calculated from $\boldsymbol{v}_1$ and $\tau = \mu$ for partial correlations; (c) SDR calculated from $\boldsymbol{v}_1$ and $\tau = 1/\sqrt{N}$ for raw correlations; and (d) SDR calculated from $\boldsymbol{v}_1$ and $\tau = 1/\sqrt{N}$ for partial correlations.

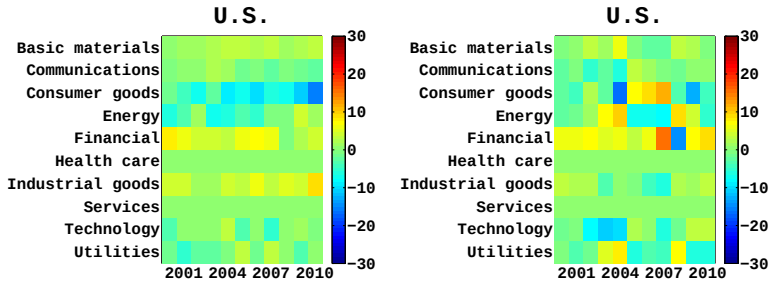

(a) $\boldsymbol{v}_1$, $\tau = \mu$, (R.C.)

(b) $\boldsymbol{v}_1$, $\tau = \mu$, (P.C.)

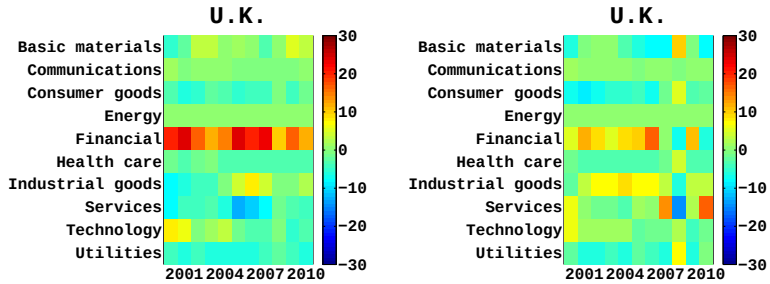

(c) $\boldsymbol{v}_1$, $\tau = \mu$, (R.C.)

(d) $\boldsymbol{v}_1$, $\tau = \mu$, (P.C.)

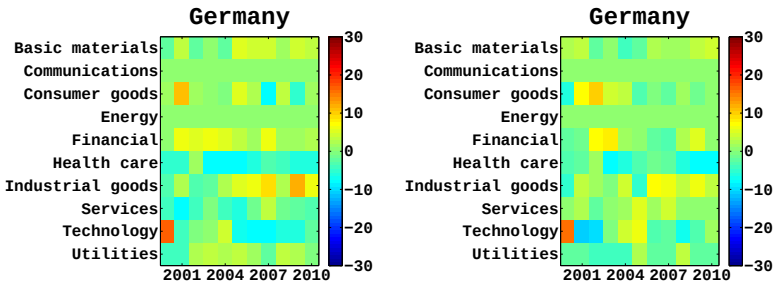

(e) $\boldsymbol{v}_1$, $\tau = \mu$, (R.C.)

(f) $\boldsymbol{v}_1$, $\tau = \mu$, (P.C.)

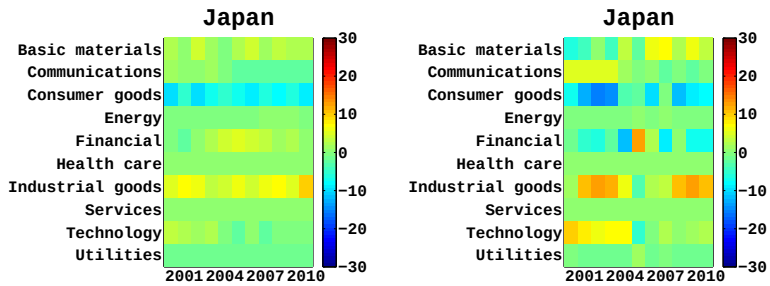

(g) $\boldsymbol{v}_1$, $\tau = \mu$, (R.C.)

(h) $\boldsymbol{v}_1$, $\tau = \mu$, (P.C.)

Figure B.3: The yearly based SDR calculated from $\boldsymbol{v}_1$ with $\tau = \mu$ for raw and partial correlations, for the U.S. (a,b), U.K. (c,d), Germany (e,f), and Japanese (g,h) stock markets.

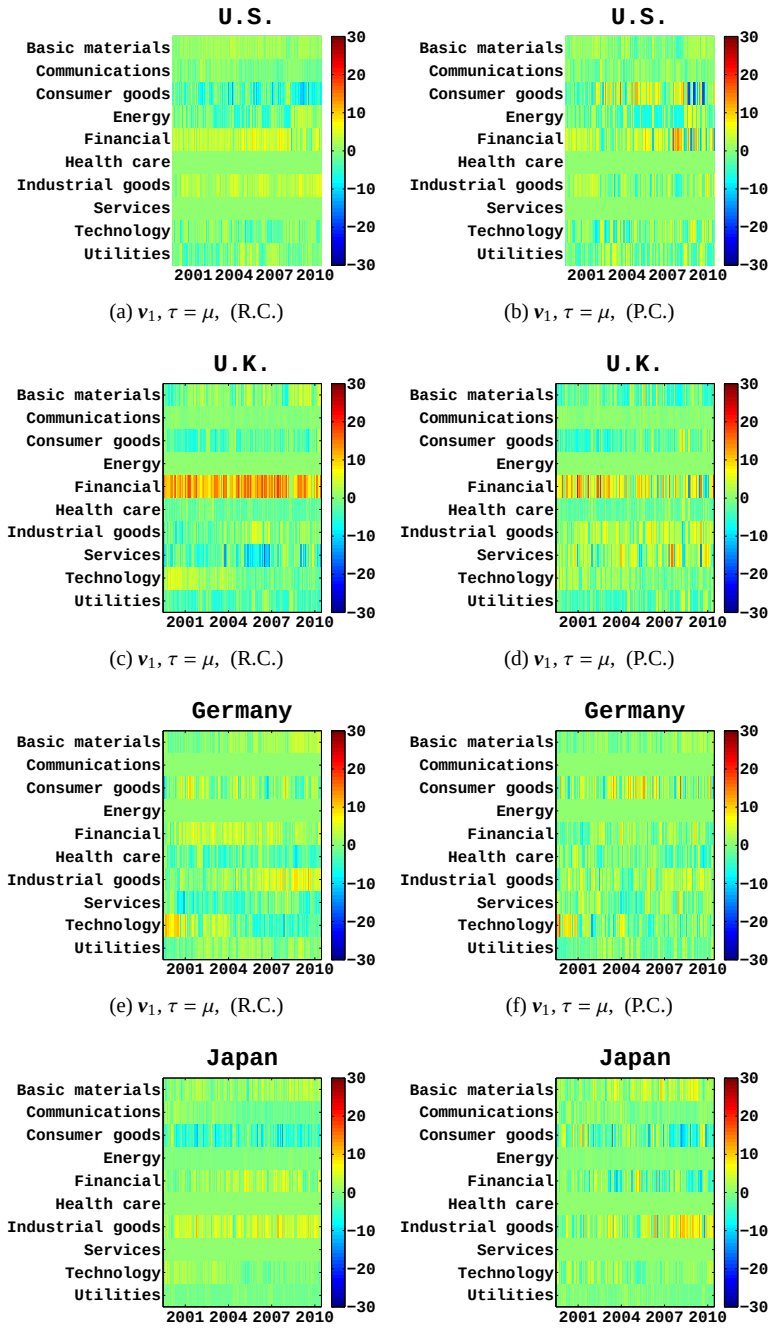

(a) $\boldsymbol{v}_1$, $\tau = \mu$, (R.C.) (b) $\boldsymbol{v}_1$, $\tau = \mu$, (P.C.)

(c) $\boldsymbol{v}_1$, $\tau = \mu$, (R.C.) (d) $\boldsymbol{v}_1$, $\tau = \mu$, (P.C.)

(e) $\boldsymbol{v}_1$, $\tau = \mu$, (R.C.) (f) $\boldsymbol{v}_1$, $\tau = \mu$, (P.C.)

(g) $\boldsymbol{v}_1$, $\tau = \mu$, (R.C.) (h) $\boldsymbol{v}_1$, $\tau = \mu$, (P.C.)

Figure B.4: The monthly based SDR calculated from $\boldsymbol{v}_1$ with $\tau = \mu$ for raw and partial correlations, for the U.S. (a,b), U.K. (c,d), Germany (e,f), and Japanese (g,h) stock markets.

B.3 Results for the second-largest eigenvector

Table B.2 and Table B.3 present the values of the SDR, Φ_s ($s = 1, \ldots, 10$), using $\boldsymbol{v}_2$ from raw and partial correlations during the period January 2000 to December 2010. The threshold used for the calculation is $\tau = 0$ for $\boldsymbol{v}_2$ in Table B.2 and $\tau = 1/\sqrt{N}$ for $\boldsymbol{v}_2$ in Table B.3. While the components of eigenvectors $\boldsymbol{v}_1$ for raw correlation are always positive, the components of eigenvectors $\boldsymbol{v}_2$ for raw correlation and partial correlation take both positive and negative values; therefore, we changed the value of τ for $\boldsymbol{v}_1$ and $\boldsymbol{v}_2$.

Table B.2 implies that the SDR for basic materials sector decreased in all stock markets; however, the SDR for the financial sector increased in all markets. The similarities are not observed among SDR for $\boldsymbol{v}_1$ and $\boldsymbol{v}_2$ for both raw and partial correlations.

The SDR obtained for a different threshold τ using $\boldsymbol{v}_2$ for raw and partial correlations during the period January 2000 to December 2010 are presented in Table B.3; the threshold τ is given as $\tau = 1/\sqrt{N}$ where N is the number of stocks for each stock market. The SDR listed in Table B.3 shows larger values, especially in the finance, industrial goods and technology sectors compared to the results using thresholds $\tau = \mu$ or $\tau = 0$ which are listed in Table B.1 and Table B.2.

Table B.2: The SDR obtained from the second largest eigenvector $\boldsymbol{v}_2$ for raw correlation (R.C.) and partial correlation (P.C.) from January 2000 to December 2010. The threshold is $\tau = 0$.

	U.S.		U.K.		Germany		Japan	
Sector	R.C.	P.C.	R.C.	P.C.	R.C.	P.C.	R.C.	P.C.
Basic materials	-2.07%	-2.78%	-4.86%	-7.76%	3.51%	2.82%	-1.62%	-7.26%
Communications	2.66%	2.51%	0.59%	1.70%	0%	0%	3.38%	1.75%
Consumer goods	-2.81%	-0.74%	-6.00%	-7.78%	5.03%	4.73%	-10.4%	9.27%
Energy	-7.49%	-7.45%	0%	0%	0%	0%	-0.63%	0.75%
Financial	12.0%	13.7%	7.78%	12.6%	-3.24%	-1.48%	-5.19%	9.15%
Health care	-6.11%	-2.79%	-3.45%	-0.88%	0%	0%	0%	0%
Industrial goods	-1.69%	-5.13%	2.70%	-7.78%	5.64%	7.15%	10.3%	-13.7%
Services	0%	0%	7.20%	5.74%	6.27%	1.34%	0%	0%
Technology	5.87%	6.31%	2.07%	10.2%	-14.6%	-14.6%	5.73%	-1.17%
Utilities	-6.45%	-6.45%	-6.03%	-6.03%	3.51%	2.82%	-1.59%	1.19%

Table B.3 shows that the SDR using $\boldsymbol{v}_2$ for the U.S. stock market has a large value for the financial sector for both raw and partial correlations. The value of SDR using $\boldsymbol{v}_2$ and partial correlation is more than 50% in the case of the financial sector. The basic materials sector is not detected in the case of $\boldsymbol{v}_2$ using raw correlation. The basic material and financial sector SDRs in the U.K. fall in the case of $\boldsymbol{v}_2$ for both raw and partial correlations. In contrast, the SDR for the communications sector increased in the case of $\boldsymbol{v}_2$ for both raw and partial correlations. The technology sector also exhibits larger values in the case of SDR using $\boldsymbol{v}_2$ for both raw and partial correlations. The SDR of the industrial goods sector using $\boldsymbol{v}_2$ for raw correlation also shows a large value. The SDR for the German stock market shows a large value in the basic materials and industrial goods sectors for $\boldsymbol{v}_2$ and raw correlation case, and in the utilities sector for $\boldsymbol{v}_2$ and the partial correlation case. The services and technology sectors are not detected in the case of $\boldsymbol{v}_2$ for either raw or partial correlations. Further, we find that the SDR for the Japanese stock market has a large value in the industrial goods and technology sectors for $\boldsymbol{v}_2$ and the raw correlation case, and in consumer goods sector for $\boldsymbol{v}_2$ for the partial correlation case.

Table B.3: The SDR from the second largest eigenvector $\boldsymbol{v}_2$ using raw correlation (R.C.) and partial correlation (P.C.) from January 2000 to December 2010. The threshold is $\tau = 1/\sqrt{N}$, where N is the number of stocks for each market.

	U.S.		U.K.		Germany		Japan	
Sector	R.C.	P.C.	R.C.	P.C.	R.C.	P.C.	R.C.	P.C.
Basic materials	-5.21%	-5.21%	-7.76%	-7.76%	15.5%	6.62%	-9.35%	-9.51%
Communications	-4.97%	-7.20%	6.28%	6.28%	0%	0%	6.61%	-1.89%
Consumer goods	-7.08%	-9.94%	-10.3%	-3.20%	-6.97%	6.37%	-21.3%	25.7%
Energy	-7.94%	-7.94%	0%	0%	0%	0%	-0.63%	-0.63%
Financial	31.3%	58.4%	-21.3%	-14.2%	-1.24%	-11.2%	-10.3%	6.85%
Health care	0%	0%	-3.45%	-3.45%	-10.1%	1.0%	0%	0%
Industrial goods	-10.7%	-10.5%	32.5%	-10.3%	37.6%	-1.25%	19.7%	-20.6%
Services	0%	0%	-6.16%	8.13%	-15.7%	-15.7%	0%	0%
Technology	11.1%	-11.2%	16.3%	30.5%	-14.6%	-14.6%	16.9%	-6.03%
Utilities	-6.45%	-6.45%	-6.03%	-6.03%	-4.49%	28.8%	-1.59%	6.11%

Comparing the values of SDR using different thresholds (Table B.1, Table B.2, Table B.3, and Table 6.3), one can observe that changing the threshold τ increases the difference in the SDR between the second largest eigenvector $\boldsymbol{v}_2$ and the largest eigenvector $\boldsymbol{v}_1$ for both raw and partial correlations. It is assumed that the SDR derived from components of the second largest eigenvector $\boldsymbol{v}_2$ are relatively more sensitive to noise than the SDR derived from the largest eigenvector $\boldsymbol{v}_1$. It is expected that the second largest eigenvalue for raw correlation and largest eigenvalue for partial correlation are similar to each other; however, the similarity of the second largest eigenvalue for raw correlation and the largest eigenvalue for partial correlation is not found in the analysis of SDR.

The yearly based and monthly based SDR from $\boldsymbol{v}_2$ with the threshold $\tau = 0$ for the U.S., U.K., German and Japanese stock markets are presented in Figure B.5. and Figure B.6, respectively, for both raw and partial correlations. The transitions of SDR on a yearly basis for the U.S., U.K., German, and Japanese stock markets using $\boldsymbol{v}_2$ for raw correlation and partial correlation with threshold $\tau = 1/\sqrt{N}$ are presented in Figure B.7. Unlike the SDR using $\boldsymbol{v}_1$ for raw and partial correlation, it is difficult to discern tendencies for the different sectors with respect to time. The transitions of SDR on a monthly basis for the U.S., U.K., German, and Japanese stock markets using $\boldsymbol{v}_2$ for raw correlation and partial correlation with threshold $\tau = 1/\sqrt{N}$ are presented in Figure B.8.

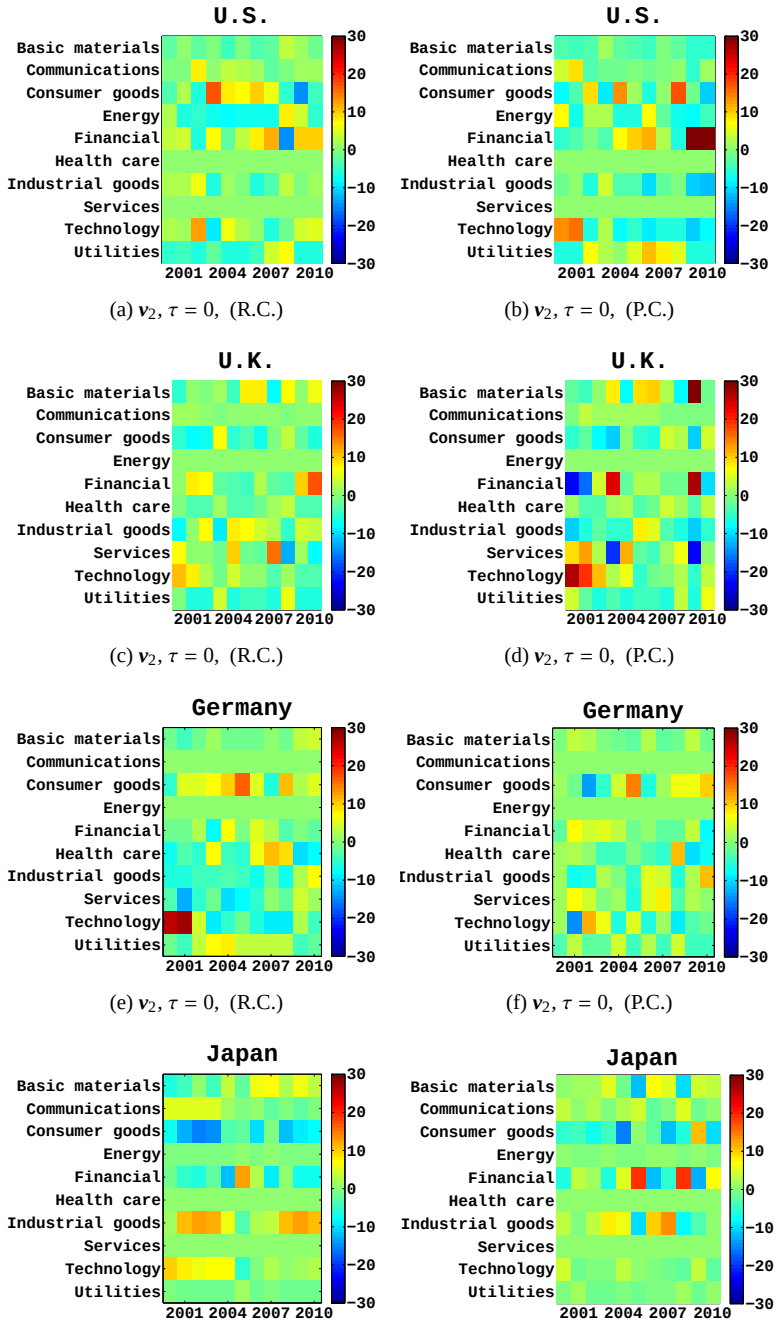

(a) $\boldsymbol{v}_2$, $\tau = 0$, (R.C.) (b) $\boldsymbol{v}_2$, $\tau = 0$, (P.C.)

(c) $\boldsymbol{v}_2$, $\tau = 0$, (R.C.) (d) $\boldsymbol{v}_2$, $\tau = 0$, (P.C.)

(e) $\boldsymbol{v}_2$, $\tau = 0$, (R.C.) (f) $\boldsymbol{v}_2$, $\tau = 0$, (P.C.)

(g) $\boldsymbol{v}_2$, $\tau = 0$,, (R.C.) (h) $\boldsymbol{v}_2$, $\tau = 0$, (P.C.)

Figure B.5: The yearly based SDR calculated from $\boldsymbol{v}_2$ with $\tau = 0$ for both raw and partial correlation for the U.S. (a,b), U.K. (c,d), Germany (e,f), and Japanese (g,h) stock markets.

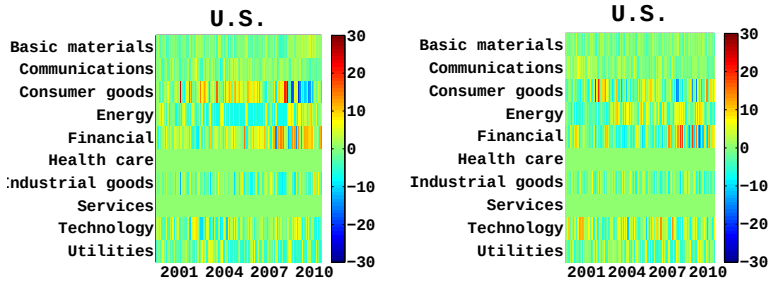

(a) $\boldsymbol{v}_2$, $\tau = 0$, (R.C.)

(b) $\boldsymbol{v}_2$, $\tau = 0$, (P.C.)

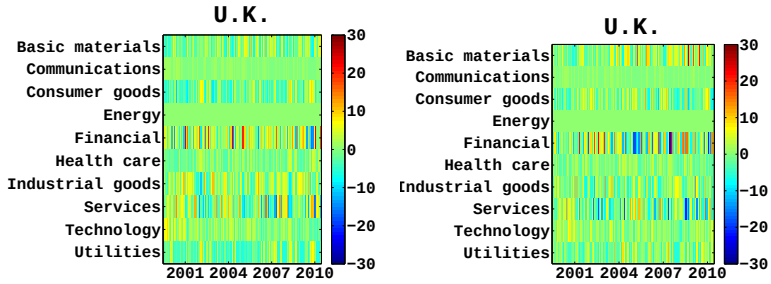

(c) $\boldsymbol{v}_2$, $\tau = 0$, (R.C.)

(d) $\boldsymbol{v}_2$, $\tau = 0$, (P.C.)

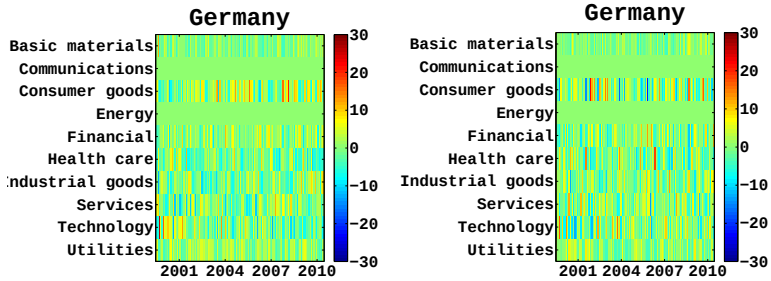

(e) $\boldsymbol{v}_2$, $\tau = 0$, (R.C.)

(f) $\boldsymbol{v}_2$, $\tau = 0$, (P.C.)

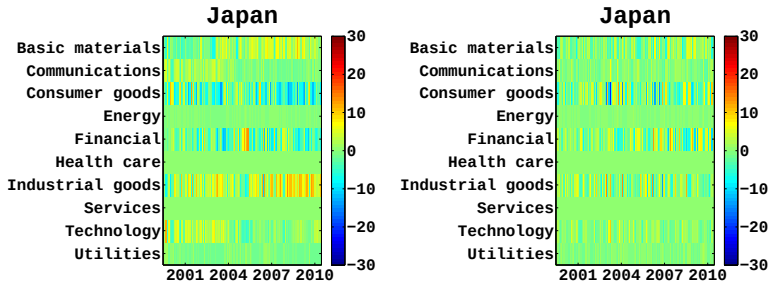

(g) $\boldsymbol{v}_2$, $\tau = 0$,, (R.C.)

(h) $\boldsymbol{v}_2$, $\tau = 0$, (P.C.)

Figure B.6: The monthly based SDR calculated from $\boldsymbol{v}_2$ with $\tau = 0$ for both raw and partial correlation for the U.S. (a,b), U.K. (c,d), Germany (e,f), and Japanese (g,h) stock markets.

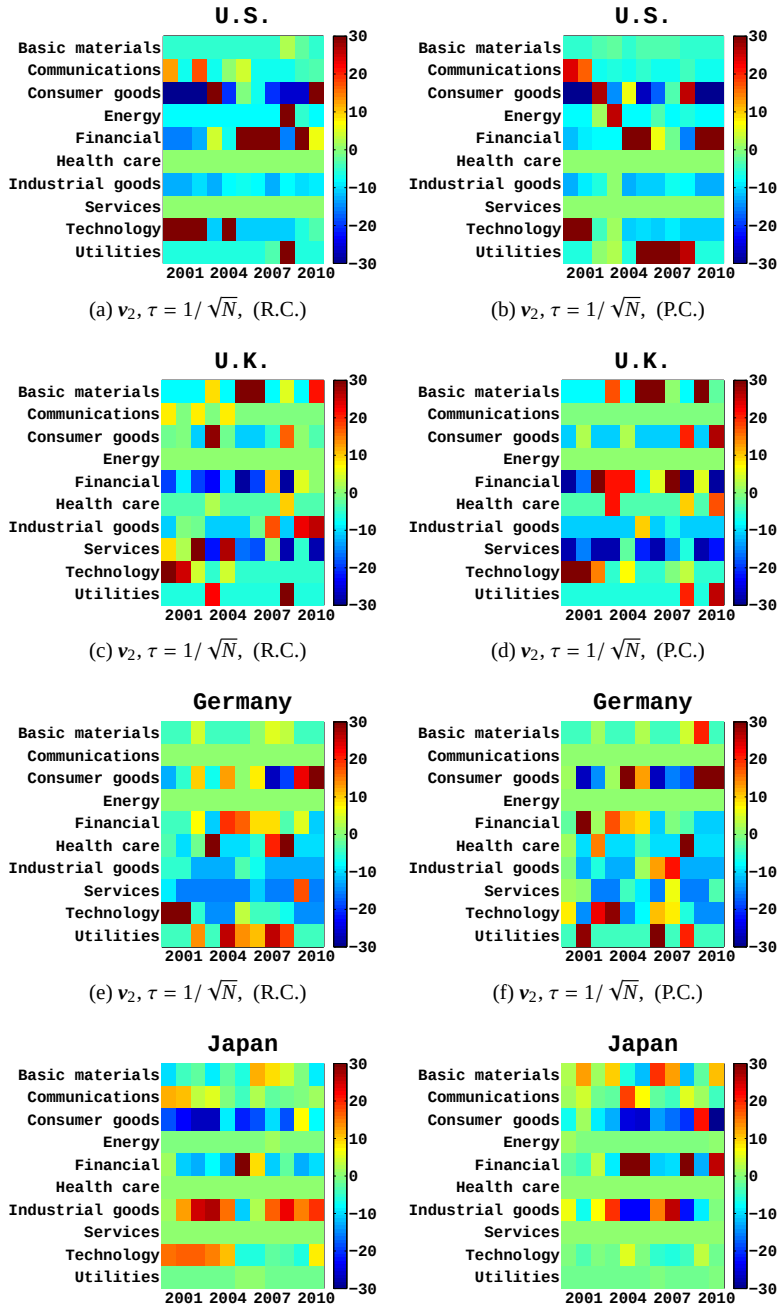

(a) $\boldsymbol{v}_2$, $\tau = 1/\sqrt{N}$, (R.C.) (b) $\boldsymbol{v}_2$, $\tau = 1/\sqrt{N}$, (P.C.)

(c) $\boldsymbol{v}_2$, $\tau = 1/\sqrt{N}$, (R.C.) (d) $\boldsymbol{v}_2$, $\tau = 1/\sqrt{N}$, (P.C.)

(e) $\boldsymbol{v}_2$, $\tau = 1/\sqrt{N}$, (R.C.) (f) $\boldsymbol{v}_2$, $\tau = 1/\sqrt{N}$, (P.C.)

(g) $\boldsymbol{v}_2$, $\tau = 1/\sqrt{N}$, (R.C.) (h) $\boldsymbol{v}_2$, $\tau = 1/\sqrt{N}$, (P.C.)

Figure B.7: The yearly based SDR calculated from $\boldsymbol{v}_2$ with $\tau = 1/\sqrt{N}$ for both raw and partial correlation for the U.S. (a,b), U.K. (c,d), Germany (e,f), and Japanese (g,h) stock markets.

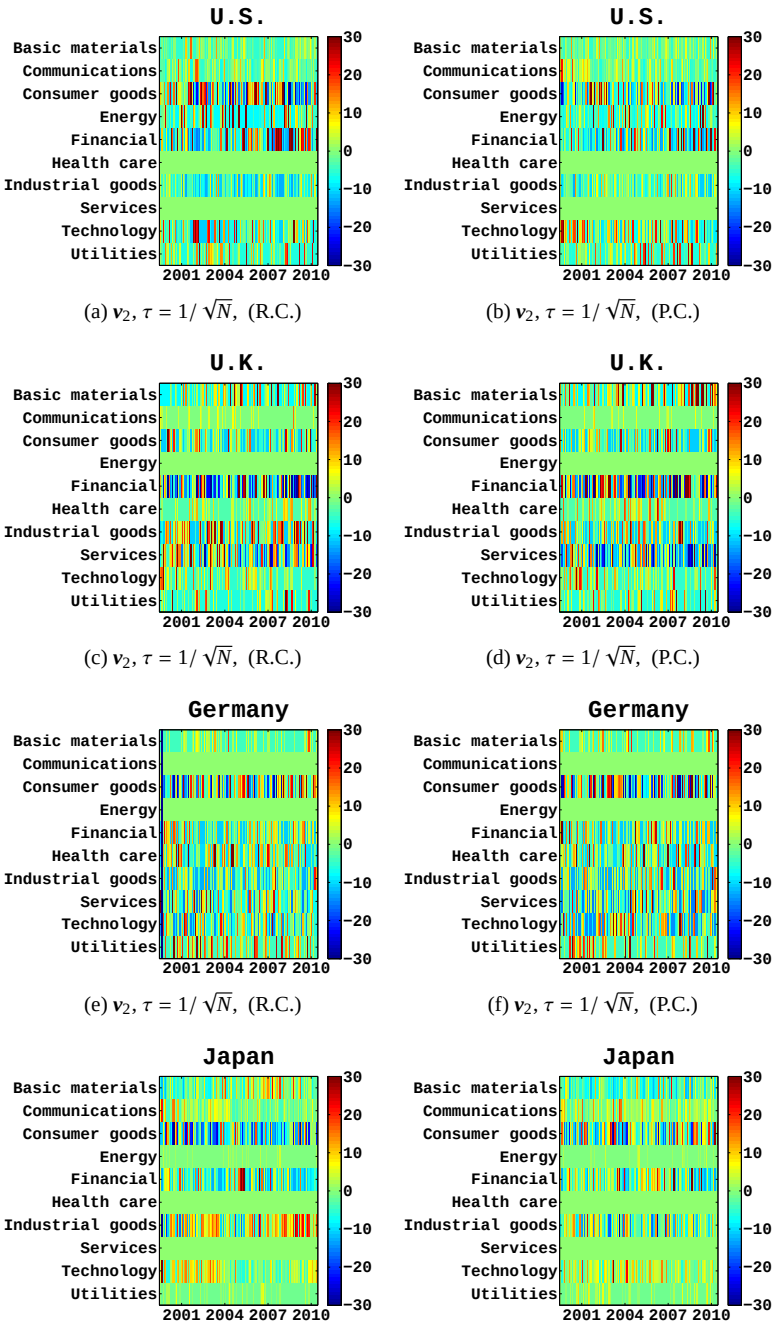

(a) $\boldsymbol{v}_2$, $\tau = 1/\sqrt{N}$, (R.C.)

(b) $\boldsymbol{v}_2$, $\tau = 1/\sqrt{N}$, (P.C.)

(c) $\boldsymbol{v}_2$, $\tau = 1/\sqrt{N}$, (R.C.)

(d) $\boldsymbol{v}_2$, $\tau = 1/\sqrt{N}$, (P.C.)

(e) $\boldsymbol{v}_2$, $\tau = 1/\sqrt{N}$, (R.C.)

(f) $\boldsymbol{v}_2$, $\tau = 1/\sqrt{N}$, (P.C.)

(g) $\boldsymbol{v}_2$, $\tau = 1/\sqrt{N}$, (R.C.)

(h) $\boldsymbol{v}_2$, $\tau = 1/\sqrt{N}$, (P.C.)

Figure B.8: The monthly based SDR calculated from $\boldsymbol{v}_2$ with $\tau = 1/\sqrt{N}$ for both raw and partial correlation for the U.S. (a,b), U.K. (c,d), Germany (e,f), and Japanese (g,h) stock markets.

Bibliography

[1] S. Allesina and S. Tang. Stability criteria for complex ecosystems. *Nature*, 483:205–208, 2012.

[2] R. Allez and J. P. Bouchaud. Individual and collective stock dynamics: intra-day seasonalities. *New Journal of Physics*, 13(2):025010, 2011.

[3] K. Baba, R. Shibata, and M. Sibuya. Partial correlation and conditional correlation as measures of conditional independence. *Australian & New Zealand Journal of Statistics*, 46(4):657–664, 2004.

[4] M. Basille, D. Fortin, C. Dussault, J. P. Ouellet, and R. Courtois. Ecologically based definition of seasons clarifies predator–prey interactions. *Ecography*, 36:220—229, 2011.

[5] T. Biancalani, T. Galla, and A. J. McKane. Stochastic waves in a brusselator model with nonlocal interaction. *Physical Review E*, 84:026201, 2011.

[6] M. Billio, M. Getmansky, A. W. Lo, and L. Pelizzon. Econometric measures of connectedness and systemic risk in the finance and insurance sectors. *Journal of Financial Economics*, 104(3):535–559, 2012.

[7] B. Blasius, A. Huppert, and L. Stone. Complex dynamics and phase synchronization in spatially extended ecological systems. *Nature*, 399:354–359, 1999.

[8] G. Bonanno, F. Lillo, and R. N. Mantegna. High-frequency cross-correlation in a set of stocks. *QUANTITATIVE FINANCE*, 1:96—104, 2001.

[9] J. P. Bouchaud. Power laws in economics and finance: some ideas from physics. *QUANTITATIVE FINANCE*, 1:105—112, 2001.

[10] J. P. Bouchaud and M. Potters. *Theory of financial risk and derivative pricing: from statistical physics to risk management*. Cambridge University Press, 2003.

[11] J. P. Bouchaud and M. Potters. Financial applications of random matrix theory: a short review. *arXiv preprint arXiv:0910.1205*, 2009.

[12] X. Chen and J. E. Cohen. Transient dynamics and food-web complexity in the lotka-volterra cascade model. *Proceedings of the Royal Society of London. Series B: Biological Sciences*, 268(1469):869–877, 2001.

[13] R. Cherniha and V. Davydovych. Conditional symmetries and exact solutions of the diffusive lotka–volterra system. *Mathematical and Computer Modelling*, 54(5):1238–1251, 2011.

[14] Y. Chou. *Statistical analysis: with business and economic applications*. Holt, Rinehart and Winston New York, 1975.

[15] A. Clauset, C. R. Shalizi, and M. E. J. Newman. Power-law distributions in empirical data. *SIAM review*, 51(4):661–703, 2009.

[16] J. E. Cohen and C. M. Newman. When will a large complex system be stable? *Journal of theoretical Biology*, 113(1):153–156, 1985.

[17] K. Constandinides and P. A. Damianou. Lotka-volterra equations in three dimensions satisfying the kowalevski-painlevé property. *Regular and Chaotic Dynamics*, 16(3-4):311–329, 2011.

[18] C. Coronnello, M. Tumminello, F. Lillo, S. Micciche, and R. N. Mantegna. Sector identification in a set of stock return time series traded at the london stock exchange. *arXiv preprint cond-mat/0508122*, 2005.

[19] J. Daniels and A. L. Mackay. The stability of connected linear systems. *Nature*, 251:49–50, 1974.

[20] J. J. Elser, I. Loladze, A. L. Peace, and Y. Kuang. Lotka re-loaded: Modeling trophic interactions under stoichiometric constraints. *Ecological Modelling*, 2012.

[21] C. Elton and M. Nicholson. The ten-year cycle in numbers of the lynx in canada. *The Journal of Animal Ecology*, pages 215–244, 1942.

[22] C. Eom, W.-S. Jung, T. Kaizoji, and S. Kim. Effect of changing data size on eigenvalues in the korean and japanese stock markets. *Physica A: Statistical Mechanics and its Applications*, 388(22):4780–4786, 2009.

[23] T. W. Epps. Comovements in stock prices in the very short run. *Journal of the American Statistical Association*, 74(366a):291–298, 1979.

[24] E. F. Fama and K. R. French. Common risk factors in the returns on stocks and bonds. *Journal of financial economics*, 33(1):3–56, 1993.

[25] J. Fernandez-Nunez. Lagrangian structure of the two-dimensional lotka–volterra system. *International journal of theoretical physics*, 37(9):2457–2462, 1998.

[26] R. Fujie and T. Odagaki. Self organization of social hierarchy and clusters in a challenging society with free random walks. *Physica A: Statistical Mechanics and its Applications*, 389(7):1471–1479, 2010.

[27] A. Garas and P. Argyrakis. Correlation study of the athens stock exchange. *Physica A: Statistical Mechanics and its Applications*, 380:399–410, 2007.

[28] N. H. Gazi. Dynamics of a marine plankton system: Diffusive instability and pattern formation. *Applied Mathematics and Computation*, 218:8895–8905, 2012.

[29] J. F. Geweke. Measures of conditional linear dependence and feedback between time series. *Journal of the American Statistical Association*, pages 907–915, 1984.

[30] A. Gierer and H. Meinhardt. A theory of biological pattern formation. *Biological Cybernetics*, 12(1):30–39, 1972.

[31] H. Goldstein, C. P. Poole, and J. L. Safko. *Classical Mechanics*. Addison-Wesley, 3rd edition.

[32] E. González and M. Villena. Spatial lanchester models. *European Journal of Operational Research*, 210(3):706–715, 2011.

[33] E. González and M. Vollena. Business cycle and conserved quantity in economics. *Journal of the Physical Society of Japan*, 210:707–715, 2011.

[34] P. Gopikrishnan, B. Rosenow, V. Plerou, and H. E. Stanley. Quantifying and interpreting collective behavior in financial markets. *Physical Review E*, 64(3):035106, 2001.

[35] C. W. J. Granger. Investigating causal relations by econometric models and cross-spectral methods. *Econometrica: Journal of the Econometric Society*, pages 424–438, 1969.

[36] C. W. J. Granger. Testing for causality: a personal viewpoint. *Journal of Economic Dynamics and control*, 2:329–352, 1980.

[37] D. Helbing and S. Balietti. From social data mining to forecasting socio-economic crises. *The European Physical Journal Special Topics*, 195(1):3–68, 2011.

[38] N. H. Ibragimov and T. Kolsrud. Lagrangian approach to evolution equations: symmetries and conservation laws. *Nonlinear dynamics*, 36(1):29–40, 2004.

[39] L. Ironi, L. Panzeri, E. Plahte, and V. Simoncini. Dynamics of actively regulated gene networks. *Physica D: Nonlinear Phenomena*, 240(8):779–794, 2011.

[40] I. Ispolatov and M. Doebeli. Omnivory can both enhance and dampen perturbations in food webs. *Theoretical Ecology*, 4(1):55–67, 2011.

[41] S. Ito. Chizuko ueno, patriarchy and capitalism: The horizon of marxist feminism. *Economic Review*, 43(1):87–89, 1992.

[42] N. M. Ivanova. Conservation laws of multidimensional diffusion–convection equations. *Nonlinear Dynamics*, 49(1-2):71–81, 2007.

[43] A. R. Ives and S. R. Carpenter. Stability and diversity of ecosystems. *Science*, 317(5834):58–62, 2007.

[44] A. G. Johnpillai, A. H. Kara, and F. M. Mahomed. Approximate noether-type symmetries and conservation laws via partial lagrangians for pdes with a small parameter. *Journal of Computational and Applied Mathematics*, 223(1):508–518, 2009.

[45] L. Kadanoff, S. Coppersmith, and M. Aldana. Boolean dynamics with random couplings. *arXiv preprint nlin/0204062*, 2002.

[46] A. H. Kara and F. M. Mahomed. Noether-type symmetries and conservation laws via partial lagrangians. *Nonlinear Dynamics*, 45(3-4):367–383, 2006.

[47] S. A. Kauffman. *The origins of order: Self-organization and selection in evolution*. Oxford university press, 1993.

[48] D. Y. Kenett, E. Ben-Jacob, H. E. Stanley, and G. Gur-Gershgoren. How high frequency trading affects a market index. *Scientific reports*, 3, 2013.

[49] D. Y. Kenett, X. Huang, I. Vodenska, S. Havlin, and H. E. Stanley. Partial correlation analysis: Applications for financial markets. *arXiv preprint arXiv:1402.1405*, 2014.

[50] D. Y. Kenett, T. Preis, G. Gur-Gershgoren, and E. Ben-Jacob. Dependency network and node influence: Application to the study of financial markets. *International Journal of Bifurcation and Chaos*, 22(7):1250181, 2012.

[51] D. Y. Kenett, T. Preis, G. Gur-Gershgoren, and E. Ben-Jacob. Quantifying meta-correlations in financial markets. *EPL (Europhysics Letters)*, 99(3):38001, 2012.

[52] D. Y. Kenett, M. Raddant, T. Lux, and E. Ben-Jacob. Evolvement of uniformity and volatility in the stressed global financial village. *PLoS One*, 7(2):e31144, 2012.

[53] D. Y. Kenett, M. Raddant, L. Zatlavi, T. Lux, and E. Ben-Jacob. Correlations and dependencies in the global financial village. In *International Journal of Modern Physics: Conference Series*, volume 16, pages 13–28. World Scientific, 2012.

[54] D. Y. Kenett, Y. Shapira, and E. Ben-Jacob. Rmt assessments of the market latent information embedded in the stocks' raw, normalized, and partial correlations. *Journal of Probability and Statistics*, 2009, 2010.

[55] D. Y. Kenett, M. Tumminello, A. Madi, G. Gur-Gershgoren, R. N. Mantegna, and E. Ben-Jacob. Dominating clasp of the financial sector revealed by partial correlation analysis of the stock market. *PLoS one*, 5(12):e15032, 2010.

[56] Y. N. Kenett, D. Y. Kenett, E. Ben-Jacob, and M. Faust. Global and local features of semantic networks: Evidence from the hebrew mental lexicon. *PloS one*, 6(8):e23912, 2011.

[57] E. H. Kerner. A statistical mechanics of interacting biological species. *The bulletin of mathematical biophysics*, 19(2):121–146, 1957.

[58] E. H. Kerner. Further considerations on the statistical mechanics of biological associations. *The bulletin of mathematical biophysics*, 21(2):217–255, 1959.

[59] R. Z. Khaminskii, F. C. Klebaner, and R. Liptser. Some results on the lotka-volterra model and its small random perturbations. *Acta Applicandae Mathematicae*, 78(1):201–206, 2003.

[60] W. B. Kinlaw, M. Kritzman, and D. Turkington. Toward determining systemic importance. *The Journal of Portfolio Management*, 38(4):100–111.

[61] P. E. Kloeden and C. Pötzsche. Dynamics of modified predator-prey models. *International Journal of Bifurcation and Chaos*, 20(09):2657–2669, 2010.

[62] S. Kondo and R. Asai. A reaction-diffusion wave on the skin of the marine angelfish pomacanthus. *Nature*, 376(6543):765–768, 1995.

[63] C. J. Krebs, R. Boonstra, S. Boutin, and A. R. E. Sinclair. What drives the 10-year cycle of snowshoe hares? *BioScience*, 51(1):25–35, 2001.

[64] M. Kritzman, Y. Li, S. Page, and R. Rigobon. Principal components as a measure of systemic risk. *The Journal of Portfolio Management*, 37(4):112–126, 2011.

[65] N. Kumar and W. Horsthemke. Effects of cross diffusion on turing bifurcations in two-species reaction-transport systems. *Physical Review E*, 83:036105, 2011.

[66] O. Kwon and J.-S. Yang. Information flow between composite stock index and individual stocks. *Physica A: Statistical Mechanics and its Applications*, 387(12):2851–2856, 2008.

[67] L. Laloux, P. Cizeau, J. P. Bouchaud, and M. Potters. Noise dressing of financial correlation matrices. *Physical Review Letters*, 83(7):1467–1470, 1999.

[68] L. Laloux, P. Cizeau, M. Potters, and J. P. Bouchaud. Random matrix theory and financial correlations. *International Journal of Theoretical and Applied Finance*, 3(03):391–397, 2000.

[69] O. Ledoit and M. Wolf. Improved estimation of the covariance matrix of stock returns with an application to portfolio selection. *Journal of Empirical Finance*, 10(5):603–621, 2003.

[70] D. Lee, K.-I. Goh, and B. Kahng. Branching process approach for boolean bipartite networks of metabolic reactions. *Physical Review E*, 86(2):027101, 2012.

[71] I. Lengyel and I. R. Epstein. Modeling of turing structures in the chlorite-iodide-malonic acid-starch reaction system. *Science*, 251(4994):650–652, 1991.

[72] J. D. Logan. First integrals in the discrete variational calculus. *Aequationes Mathematicae*, 9(2-3):210–220, 1973.

[73] J. D. Logan. *Invariant Variational Principles*, volume MATHEMATICS IN SCIENCE AND ENGINEERING *Volume 138*. ACADEMIC PRESS, 1977.

[74] A. J. Lotka. Elements of mathematical biology, 1956.

[75] T. Lux. Herd behaviour, bubbles and crashes. *The economic journal*, pages 881–896, 1995.

[76] D. A. Mac Lulich. *Fluctuations in the numbers of varying hare*. Number 43. The University of Toronto press, 1937.

[77] A. Madi, D. Y. Kenett, S. Bransburg-Zabary, Y. Merbl, F. J. Quintana, S. Boccaletti, A. I. Tauber, I. R. Cohen, and E. Ben-Jacob. Analyses of antigen dependency networks unveil immune system reorganization between birth and adulthood. *Chaos: An Interdisciplinary Journal of Nonlinear Science*, 21(1):016109–016109, 2011.

[78] R. N. Mantegna and H. E. Stanley. *Introduction to econophysics: correlations and complexity in finance*. Cambridge university press, 2000.

[79] J. Maquet, C. Letellier, and L. A. Aguirre. Global models from the canadian lynx cycles as a direct evidence for chaos in real ecosystems. *Journal of Mathematical Biology*, 55:21–39, 2007.

[80] I. Martinez, C. Juarez, and P. M. Nancy J. Predator-prey analytical dynamics behavior using normal form method. In *Electrical Engineering Computing Science and Automatic Control (CCE), 2011 8th International Conference on*, pages 1–6. IEEE, 2011.

[81] R. D. Mattuck. *A guide to Feynman diagrams in the many-body problem*. Courier Dover Publications, 1976.

[82] M. J. Mauboussin. Revisiting market efficiency: the stock market as a complex adaptive system. *Journal of Applied Corporate Finance*, 14(4):47–55, 2002.

[83] R. M. May. Will a large complex system be stable? *Nature*, 238:413–414, 1972.

[84] F. Mazenc and M. Malisoff. Strict lyapunov function constructions under lasalle conditions with an application to lotka-volterra systems. *IEEE Transactions on Automatic Control*, 55(4):841, 2010.

[85] F. X. Mei. Lie symmetries and conserved quantities of constrained mechanical systems. *Acta Mechanica*, 141(3-4):135–148, 2000.

[86] H. Meinhardt and H. Meinhardt. *Models of biological pattern formation*, volume 6. Academic Press London, 1982.

[87] R. C. Merton. An intertemporal capital asset pricing model. *Econometrica: Journal of the Econometric Society*, pages 867–887, 1973.

[88] A. Mochizuki. Structure of regulatory networks and diversity of gene expression patterns. *Journal of theoretical biology*, 250(2):307–321, 2008.

[89] D. Mollison. Dependence of epidemic and population velocities on basic parameters. *Mathematical biosciences*, 107(2):255–287, 1991.

[90] G.-H. Mu, W.-X. Zhou, W. Chen, and J. Kertész. Order flow dynamics around extreme price changes on an emerging stock market. *New Journal of Physics*, 12(7):075037, 2010.

[91] M. C. Münnix, T. Shimada, R. Schäfer, F. Leyvraz, T. H. Seligman, T. Guhr, and H. E. Stanley. Identifying states of a financial market. *Scientific Reports*, 2:644, 2012.

[92] Y. Murase, T. Shimada, and N. Ito. A simple model for skewed species-lifetime distributions. *New Journal of Physics*, 12(6):063021, 2010.

[93] J. C. Nacher and T. Akutsu. On the degree distribution of projected networks mapped from bipartite networks. *Physica A: Statistical Mechanics and its Applications*, 390(23):4636–4651, 2011.

[94] Y. Nakayama and H. Iyetomi. Random matrix theory of dynamical cross correlations in financial data. *Progress of Theoretical Physics Supplement*, 179:60–70, 2009.

[95] M. E. J. Newman, S. H. Strogatz, and D. J. Watts. Random graphs with arbitrary degree distributions and their applications. *Physical Review E*, 64(2):026118, 2001.

[96] G. Nicolis and I. Prigogine. Self-organization in nonequilibrium systems. 191977, 1977.

[97] E. Noether. Invariant variational problems. In *The Noether Theorems*, pages 3–22. Springer, 2011.

[98] K. Pearson. Contributions to the mathematical theory of evolution ii: skew variations in homogeneous material. *Phil. Trans. R. Soc. Lond. A*, 186:343–414, 1895.

[99] V. Plerou, P. Gopikrishnan, B. Rosenow, L. A. N. Amaral, T. Guhr, and H. E. Stanley. Random matrix approach to cross correlations in financial data. *Physical Review E*, 65(6):066126, 2002.

[100] B. Podobnik, D. Horvatić, D. Y. Kenett, and H. E. Stanley. The competitiveness versus the wealth of a country. *Scientific reports*, 2, 2012.

[101] B. Podobnik and H. E. Stanley. Detrended cross-correlation analysis: a new method for analyzing two nonstationary time series. *Physical review letters*, 100(8):84102, 2008.

[102] R. Pool. Did turing discover how the leopard got its spots? *Science*, 251(4994):627, 1991.

[103] M. Potters, J. P. Bouchaud, and L. Laloux. Financial applications of random matrix theory: Old laces and new pieces. *arXiv preprint physics/0507111*, 2005.

[104] I. Prigogine and I. Stengers. Order out of chaos. 1984. *New York*, 1984.

[105] L. Qian, E. Winfree, and J. Bruck. Neural network computation with dna strand displacement cascades. *Nature*, 475(7356):368–372, 2011.

[106] K. Raghuraj Rao and S. Lakshminarayanan. Partial correlation based variable selection approach for multivariate data classification methods. *Chemometrics and intelligent laboratory systems*, 86(1):68–81, 2007.

[107] P.-A. Reigneron, R. Allez, and J. P. Bouchaud. Principal regression analysis and the index leverage effect. *Physica A: Statistical Mechanics and its Applications*, 390(17):3026–3035, 2011.

[108] F. Ren and W.-X. Zhou. Random matrix approach to dynamic evolution of cross-correlations in the chinese stock market. *arXiv preprint arXiv:1308.1154*, 2013.

[109] S. A. Ross. The arbitrage theory of capital asset pricing. *Journal of economic theory*, 13(3):341–360, 1976.

[110] C. Schinckus. Economic uncertainty and econophysics. *Physica A: Statistical Mechanics and its Applications*, 388(20):4415–4423, 2009.

[111] D. E. Schindler, J. L. Carter, T. B. Francis, P. J. Lisi, P. J. Askey, and D. C. Sebastian. *Mysis* in the okanagan lake food web: a time-series analysis of interaction strengths in an invaded plankton community. *Aquatic Ecology*, 46:1–13, 2012.

[112] H. G. Schuster and W. Just. *Deterministic chaos: an introduction*. John Wiley & Sons, 2006.

[113] Y. Shapira, D. Y. Kenett, and E. Ben-Jacob. The index cohesive effect on stock market correlations. *The European Physical Journal B - Condensed Matter and Complex Systems*, 72(4):657–669, 2009.

[114] K. D. Shiang. A perturbation-based estimate algorithm for parameters of coupled ordinary differential equations, applications from chemical reactions to metabolic dynamics. *Computer methods and programs in biomedicine*, 94(2):118–142, 2009.

[115] T. Shimada, S. Yukawa, and N. Ito. Self-organization in an ecosystem. *Artificial Life and Robotics*, 6(1-2):78–81, 2002.

[116] A. G. Smart, L. A. N. Amaral, and J. M. Ottino. Cascading failure and robustness in metabolic networks. *Proceedings of the National Academy of Sciences*, 105(36):13223–13228, 2008.

[117] D. Sornette. *Why stock markets crash: critical events in complex financial systems*. Princeton University Press, 2004.

[118] S. Squires, E. Ott, and M. Girvan. Dynamical instability in boolean networks as a percolation problem. *Physical Review Letters*, 109(8):85701, 2012.

[119] H. E. Stanley. Introduction to phase transitions and critical phenomena. *Introduction to Phase Transitions and Critical Phenomena, by H Eugene Stanley, pp. 336. Foreword by H Eugene Stanley. Oxford University Press, Jul 1987. ISBN-10: 0195053168. ISBN-13: 9780195053166*, 1, 1987.

[120] H. E. Stanley, V. Afanasyev, L. A. N. Amaral, S. V. Buldyrev, A. L. Goldberger, S. Havlin, H. Leschhorn, P. Maass, R. N. Mantegna, C.-K. Peng, P. A. Prince, M. A. Salingerg, M. H. R. Stanley, and G. M. Viswanathana. Anomalous fluctuations in the dynamics of complex systems: from dna and physiology to econophysics. *Physica A: Statistical Mechanics and its Applications*, 224(1):302–321, 1996.

[121] N. C. Stenseth, W. Falck, O. N. Bjørnstad, and C. J. Krebs. Population regulation in snowshoe hare and canadian lynx: asymmetric food web configurations between hare and lynx. *Proceedings of the National Academy of Sciences*, 94(10):5147, 1997.

[122] N. C. Stenseth, W. Falck, K. S. Chan, O. N. Bjornstad, M. O'Donoghue, H. Tong, R. Boonstra, S. Boutin, C. J. Krebs, and N. G. Yoccoz. From patterns to processes: phase and density dependencies in the canadian lynx cycle. *Proceedings of the National Academy of Sciences*, 95(26):15430, 1998.

[123] K. Takemoto, T. Tamura, Y. Cong, W. K. Ching, J. P. Vert, and T. Akutsu. Analysis of the impact degree distribution in metabolic networks using branching process approximation. *Physica A: Statistical Mechanics and its Applications*, 391(1):379–387, 2012.

[124] T. Tamura, C. Yang, T. Akutsu, and W. K. Ching. An efficient method of computing impact degrees for multiple reactions in metabolic networks with cycles. *IEICE TRANSACTIONS on Information and Systems*, 94(12):2393–2399, 2011.

[125] M. Taniguchi, M. Bando, and A. Nakayama. Business cycle and conserved quantity in economics. *Journal of the Physical Society of Japan*, 77(11), 2008.

[126] K. Tokita. Species abundance patterns in complex evolutionary dynamics. *Physical review letters*, 93(17):178102, 2004.

[127] M. Tumminello, F. Lillo, and R. N. Mantegna. Correlation, hierarchies, and networks in financial markets. *Journal of Economic Behavior & Organization*, 75(1):40–58, 2010.

[128] M. Tumminello, S. Micciché, F. Lillo, J. Piilo, and R. N. Mantegna. Statistically validated networks in bipartite complex systems. *PloS one*, 6(3):e17994, 2011.

[129] A. M. Turing. The chemical basis of morphogenesis. *Philosophical Transactions of the Royal Society of London. Series B, Biological Sciences*, 237:37–72, 1952.

[130] L. Uechi and T. Akutsu. Conservation laws and symmetries in competitive systems. *Progress of Theoretical Physics Supplement*, 194:210–222, 2012.

[131] L. Uechi and T. Akutsu. Stability and restoration phenomena in competitive systems. *arXiv preprint arXiv:1209.1178*, 2012.

[132] C. Ueno. *The modern family in Japan: Its rise and fall*. Trans Pacific Press, 2009.

[133] J. Voit. *The statistical mechanics of financial markets*. Springer, 2005.

[134] V. Volterra. *Variazioni e fluttuazioni del numero d'individui in specie animali conviventi*. C. Ferrari, 1927.

[135] H. S. Wilf. *Generatingfunctionology*. Citeseer, 1990.

[136] Y. Yoshino, T. Galla, and K. Tokita. Statistical mechanics and stability of a model eco-system. *Journal of Statistical Mechanics: Theory and Experiment*, 2007:P09003, 2007.